UNIVERSIDAD DE BURGOS

ESCUELA DE DOCTORADO

TESIS

ESTUDIO DE LA FILTRACIÓN DE FANGOS ANAEROBIOS CON MEMBRANAS SUMERGIDAS DE FIBRAS HUECAS Y TUBULARES EXTERNAS EMPLEADAS EN BIORREACTORES DE MEMBRANAS

Departamento de Biotecnología y Ciencia de los Alimentos.

Área de Ingeniería Química

Raquel Martínez Díaz

Burgos, 2020

Departamento de Biotecnología y Ciencia de los Alimentos
Área de Ingeniería Química
Universidad de Burgos

Memoria para optar al grado de Doctor por la Universidad de Burgos presentada por

RAQUEL MARTÍNEZ DÍAZ

Burgos, julio 2020

Departamento de Biotecnología y Ciencia de los Alimentos
Área de Ingeniería Química
Universidad de Burgos

DOCTOR VICTORINO DIEZ BLANCO Y DOCTORA MARIA OLGA RUIZ PEREZ, PROFESORES TITULARES DE UNIVERSIDAD DEL ÁREA DE INGENIARÍA QUIMICA DEL DEPARTAMENTO DE BIOTECNOLOGÍA Y CIENCIA DE LOS ALIMENTOS DE LA UNIVERSIDAD DE BURGOS,

INFORMAN:

Que la memoria titulada "ESTUDIO DE LA FILTRACIÓN DE FANGOS ANAEROBIOS CON MEMBRANAS SUMERGIDAS DE FIBRAS HUECAS Y TUBULARES EXTERNAS EMPLEADAS EN BIORREACTORES DE MEMBRANAS", ha sido realizada bajo nuestra dirección, en el Área de Ingeniería Química del Departamento de Biotecnología y Ciencia de los Alimentos de la Universidad de Burgos.

En Burgos, julio de 2020.

DIEZ BLANCO VICTORINO - 12740777L

Firmado digitalmente por DIEZ BLANCO VICTORINO - 12740777L
Nombre de reconocimiento (DN): c=ES, serialNumber=IDCES-12740777L, givenName=VICTORINO, sn=DIEZ BLANCO, cn=DIEZ BLANCO VICTORINO - 12740777L
Fecha: 2020.07.29 17:47:06 +02'00'

Firmado digitalmente por RUIZ PEREZ MARIA OLGA - 13130364D
Fecha: 2020.07.29 18:16:13 +02'00'

Fdo. Dr. D. Victorino Diez Blanco

Fdo. Dra. Dña. Mª Olga Ruiz Pérez

Agradecimientos

A mis directores de tesis,

Gracias Victor por haberme dado la oportunidad de trabajar contigo, por tu dedicación, compromiso y paciencia conmigo. Nunca olvidaré la que para mí fue una de las mejores lecciones que me pudiste dar: "Los resultados de un buen trabajo no siempre son los perseguidos o deseados. Un buen trabajo culmina con una discusión sincera de los resultados obtenidos". Gracias por todo lo que me has enseñado, no solo a nivel académico sino también a nivel personal. A partir de ahora siempre escucharé Radio3.

Gracias Olga por tu apoyo incondicional durante todos estos años, por tus consejos y dirección que tan útiles y necesarios han sido para mí. Porque las lecciones con cariño se aprenden mejor y en eso eres una experta.

Sois unos profesores extraordinarios y unas personas maravillosas.

A los miembros de la universidad,

Gracias Chema por tu compromiso y colaboración con este trabajo que ha sido de vital importancia para mí.

Gracias a Cipri y a Beti por ayudarme tanto. He tenido mucha suerte de coincidir con vosotros.

A mi familia,

Gracias a mis padres por la educación y valores que me habéis transmitido, por vuestro apoyo incondicional, por impulsarme… en definitiva, por absolutamente TODO. Este trabajo es por y para vosotros. Os quiero.

Gracias a mis hermanos, Esther y Miguel, con quienes he compartido los mejores momentos de mi vida. Pese a la distancia siempre os he sentido a mi lado.

Gracias Toño por haber confiado siempre en mí y por tus palabras de aliento animándome a seguir adelante en los peores momentos.

Gracias Concha por haber sido para mí un ejemplo de trabajo y superación. Gracias por haber creído siempre en mí.

Gracias a Javier y Fernanda por ser tan buenos conmigo y haberos preocupado por mi como si fuese vuestra propia hija.

A mis amigas,

A las de siempre y las que se han ido incorporado a mi vida más recientemente. Gracias por preocuparos siempre por mí y darme fuerza cuando los ánimos estaban más bajos. (En este apartado incluyo a Jan Koum por haber creado whatsapp, ☺, que nos ha mantenido unidas en la distancia).

A Javi,

Gracias por tu comprensión y paciencia, gracias por tu apoyo incondicional, gracias por tu amor que me dio tanta fuerza para seguir adelante. Te quiero.

Gracias a todos de corazón

Ya está hecho.

Resumen y objetivos

Los biorreactores anaerobios de membrana son una tecnología muy eficiente para el tratamiento de aguas residuales. Presentan numerosas ventajas frente a los sistemas de tratamiento convencionales. Sin embargo, su desarrollo se ve limitado por los costes de instalación y mantenimiento, especialmente aquellos costes derivados del ensuciamiento de las membranas.

Dada la importancia que el ensuciamiento de las membranas tiene en el desarrollo e implementación de los reactores de membrana, en esta tesis se ha estudiado detalladamente este fenómeno con el fin de comprenderlo mejor y así poder operar los sistemas de filtración de un modo más eficaz.

Se ha comprobado cómo la configuración de membrana, la naturaleza química del fango o las condiciones de operación pueden afectar al proceso de filtración. Además, dada la implicación de la composición química del fango sobre el ensuciamiento de las membranas, se ha hecho un estudio sobre la extracción de los compuestos que más afecta al ensuciamiento de la membrana, las sustancias poliméricas extracelulares (EPS), de fango anaerobio y se ha estudiado su efecto sobre el ensuciamiento en una fibra hueca en un ensayo de laboratorio.

Por un lado, se ha estudiado cómo 2 configuraciones de membrana, tubular externa y sumergida de fibras huecas, pueden comportarse frente a diferentes condiciones hidrodinámicas que pueden provocar cambios en las características del fango, alterando el comportamiento biológico, y dando lugar a diferencias en la retención de materiales y en las velocidades de ensuciamiento de la membrana.

Posteriormente, se presenta un estudio detallado del proceso de filtración de 3 fangos anaerobios de tres industrias alimentarias (fábrica de snack, matadero y cervecera) empleando las dos configuraciones de membranas nombradas anteriormente. Se ha estudiado cómo vertidos de distinta naturaleza química afectan a las distintas componentes del ensuciamiento de las membranas y su capacidad de retención de materiales.

Por otro lado, se ha estudiado el efecto de las condiciones de operación sobre el ensuciamiento reversible e irreversible de las membranas. Las condiciones estudiadas fueron: duración del ciclo, duración del contralavado, flujo de filtración y contralavado, flujo de gas y en el caso de la membrana tubular externa también se estudió la velocidad de contralavado. Se ha observado que los parámetros que influyen sobre el ensuciamiento de cada tipo de membrana no son los mismos en cada una, siendo necesaria una optimización individual de cada sistema para determinar sus condiciones de operación más adecuadas.

Además, dada la implicación de los EPS en el ensuciamiento de las membranas también se presenta un estudio de cómo el modo y el tiempo de contacto, la temperatura y la salinidad afectan a la extracción de EPS en una muestra de fango anaerobio. Se determinó la cinética de extracción y se estudió el efecto de la salinidad y la concentración de EPS sobre el aumento de resistencia específica a la filtración en una membrana sumergida de fibra hueca, el grado de retención y la compresibilidad de la capa de ensuciamiento correspondiente.

Lista de figuras

Lista de tablas

Índice

Capítulo 1: Introducción

1.1 Introducción

La escasez de agua y los problemas derivados del vertido de aguas residuales al medio hacen del tratamiento de las aguas residuales un proceso imprescindible para la conservación de este recurso y del medio ambiente.

Los biorreactores anaerobios de membrana, AnMBR, son una tecnología muy eficiente que combina la degradación anaerobia de materia orgánica con una etapa de filtración con membranas. El tratamiento anaerobio del agua residual es capaz de degradar eficientemente vertidos con elevadas concentraciones de materia orgánica, producen poco fango, son estables frente a cambios y producen energía en forma de biogás [1]. Al combinar el proceso biológico anaerobio con una etapa de separación con membranas se obtiene un efluente de elevada calidad libre de sólidos y patógenos [2].

Dadas sus ventajas, la tecnología AnMBR ha generado un gran interés por parte de investigadores e industria en su aplicación para el tratamiento de una gran variedad de vertidos residuales urbanos y de distintas industrias. Se ha aplicado la tecnología AnMBR en el tratamiento de vertidos sintéticos a base de glucosa, peptona, extracto de levaduras, ácidos grasos volátiles, melaza, suero, extracto de carne, etc. [3–9]. A nivel industrial se puede encontrar esta tecnología aplicada al tratamiento de vertidos de industria alimentaria como pueden ser el suero lácteo, vertidos del procesado de tofu, aguas residuales de cervecera, vertidos de almazara, vertidos de matadero, [10–14]. También se aplica para el tratamiento de vertidos de industrias no alimentarias como por ejemplo para vertidos de industria textil [15] o en tratamiento de vertidos municipales, [16,17]. Sin embargo, el ensuciamiento de las membranas provocado por la acumulación de materiales sobre la superficie de la membrana sigue siendo el principal cuello de botella para la expansión de esta tecnología.

El tratamiento biológico aerobio de vertidos comenzó a finales del siglo XIX, llegando a ser habituales en los años 30 del siglo XX [18]. Los sistemas convencionales de tratamiento de

vertidos combinan un tratamiento biológico aerobio con una etapa de decantación para la separación de sólidos donde se obtiene un sobrenadante libre de sólidos.

Fueron Smith y col. [19] quienes en el año 1969 sustituyeron por primera vez la etapa de decantación de los sistemas de fangos activados convencionales (CAS) por una etapa de filtración con membranas que mejora notablemente la eficiencia del tratamiento biológico y la calidad del vertido. A continuación, la empresa canadiense Dorr-Oliver, desarrolló un sistema denominado Membrane Sewage Treatment (MST) [20] en el que incorporaron membranas externas planas de ultrafiltración para el tratamiento biológico de aguas residuales de embarcaciones [21]. Pese a operar en unas condiciones que daban lugar a bajos rendimientos, con una permeabilidad de 10 $L/m^2h \cdot bar$, el sistema era capaz de alcanzar su objetivo principal: concentrar la biomasa y obtener un efluente de alta calidad.

Los reactores con membrana externa dieron lugar a la aparición de los primeros biorreactores anaerobios de membrana, AnMBR. En 1978, H. E. Grethlein [22] empleó un AnMBR con membrana externa para el tratamiento de vertido doméstico alcanzando una reducción de la materia orgánica entre el 85 y 95% en DBO. Posteriormente, en 1989, Yamamoto y col. [23] simplificaron el sistema al sumergir la membrana directamente en el fango, dando lugar a los biorreactores de membrana sumergidos. Las compañías Zenon (Canadá) y Mitsubishi Rayon (Japón) desarrollaron estos reactores durante la década de los 90 empleando membranas de fibras huecas.

A principios de los 90 el gobierno de Japón dio comienzo al proyecto nacional "Aqua-Renaissance‘90" que permitió el desarrollo de distintos AnMBR, principalmente en configuración externa [24–26]. Simultáneamente la empresa Japonesa Kubota desarrolló membranas planas de microfiltración para MBRs aerobios que operaban en configuración sumergida [27].

En la industria alimentaria, la aplicación de biorreactores de membrana tuvo lugar por primera vez en 1982 llevado a cabo por la empresa Dorr-Oliver [28] que instaló un reactor anaerobio con

membrana externa para el tratamiento de suero lácteo denominado “Membrane Anaerobic Reactor System” MARS.

A nivel académico, desde los años 90, el número de publicaciones sobre esta tecnología ha aumentado exponencialmente. En la Fig. 1 se recoge el número de publicaciones que aparecen en la base de datos Scopus sobre MBR y AnMBR, cada año, desde el año 1981 hasta diciembre de 2019. En total y hasta la fecha (julio, 2020) se han publicado 8587 artículos sobre MBR y tan solo 749 sobre AnMBR.

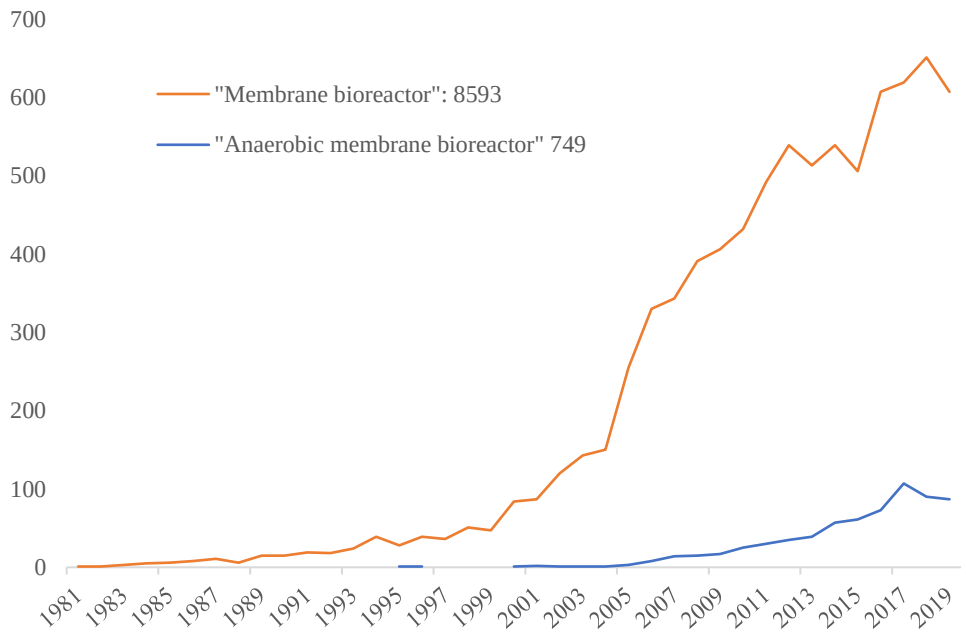

Fig. 1. Número de publicaciones sobre biorreactores de membrana desde el año 1981 hasta diciembre de 2019, recogidas en la base de datos Scopus.

Los costes de instalación derivados del precio de las membranas y el mantenimiento de las mismas hacen que el tratamiento de vertidos con MBR no sea la primera opción elegida por los responsables del tratamiento de vertidos. En la actualidad, pese al gran desarrollo y las ventajas que presenta la tecnología MBR tan solo un 5% de los vertidos tratados en todo el mundo se hace mediante esta tecnología [29].

1.2 Aguas residuales

Según el Diccionario del español jurídico de la Real Academia Española, un vertido es una *evacuación deliberada al medio de productos, sustancias o compuestos que pueden tener una incidencia o impacto ambiental*. Determinadas actividades humanas provocan un grave deterioro en la calidad natural de las aguas fluviales dando lugar a vertidos que no pueden ser asimilados por la naturaleza al ritmo que se producen. Estas aguas residuales se caracterizan por tener una elevada cantidad de sustancias minerales, materia orgánica y/o microorganismos que se encuentran suspendidas, en estado coloidal o disueltas.

Atendiendo al origen del vertido, las aguas residuales se pueden clasificar en 4 grupos [30,31]:

- Aguas residuales domésticas: vertidos procedentes de la actividad doméstica diaria que incorpora restos de materia fisiológica humana, jabones, detergentes, etc. Son aguas residuales con una elevada concentración de materia orgánica y microorganismos.
- Aguas residuales industriales: aguas de procesos de fabricación, limpieza, refrigeración, etc. que dan lugar a vertidos de una naturaleza físico-química muy diversa.
- Aguas residuales agrícolas y ganaderas: procedentes de la lluvia o riego, pueden arrastrar fertilizantes (químicos o naturales) y plaguicidas. Su tratamiento previo a vertido no es posible ya que se filtran directamente en el subsuelo, donde pueden contaminar aguas subterráneas, o se vierten directamente a cauce.
- Aguas residuales indeterminadas: son vertidos procedentes de precipitaciones, riego de jardines o limpieza de zonas urbanas. Dependiendo de los niveles de precipitación local pueden ser evacuados al colector municipal o directamente a cauce.

Los compuestos orgánicos más comunes presenten en los vertidos son carbohidratos, grasas y aceites, proteínas, fenoles, tensioactivos, compuestos orgánicos volátiles y pesticidas. En el caso

de vertidos de naturaleza inorgánica, se pueden encontrar cloruros, metales pesados, nitrógeno, fósforo o azufre y/o problemas de alcalinidad o acidez. También es posible que determinadas actividades industriales den lugar a vertidos de elevada temperatura.

Los vertidos incontrolados pueden provocar malos olores y sabores, facilitan la dispersión de tóxicos favoreciendo así su incorporación en organismos vivos, dan lugar a la proliferación de microorganismos patógenos, también pueden causar alteraciones físico-químicas (temperatura, pH, turbulencia, etc.), eutrofización o el agotamiento del oxígeno disuelto, por lo que es imprescindible el tratamiento de estas aguas contaminadas para reducir o incluso eliminar los contaminantes presentes en el vertido previamente a su evacuación al medio.

1.3 Aguas residuales de Industria Alimentaria

La producción de alimentos a escala industrial consume una gran cantidad agua potable y energía, no solo para el procesado de los alimentos sino también para la limpieza de materias primas y superficies de producción. Tras su utilización, este agua se transforma en un vertido de elevada carga orgánica que ha de ser tratado con el fin de evitar problemas de salud y medioambientales.

Los vertidos de industria alimentaria presentan una composición físico-química muy heterogénea que depende, entre otros factores, del tipo de producto que elaboren, la estacionalidad y la demanda, incluso, una misma empresa puede dar lugar a vertidos con diferente composición de acuerdo con las especificaciones de cada uno de sus productos. En general, los vertidos de la industria alimentaria suelen ser biodegradables y no tóxicos, con una elevada concentración de materia orgánica y sólidos suspendidos [32]. En la Tabla 1 se muestra algunos ejemplos de la composición química de los vertidos de varias industrias alimentarias.

Tabla 1. Composición química de distintos vertidos de industria alimentaria.

Muestra	ST (g/L)	SV (g/L)	SST (g/L)	SSV (g/L)	DQO_T (g/L)	DQO_S (g/L)	AyG (g/L)	NKT (mg/L)	pH	Ref.
Aperitivos (a)			2.2 – 4.9	2.4 – 4.5	8.6 – 14.8		0.1 – 0.4	140 – 299	4.4 – 5.9	[1]
Aperitivos (b)					8.2 – 22		4.4 – 6.0	75 – 380		[33]
Matadero (a)	1.2 – 7.0	0.9 – 6.2			2.1 – 13.4	0.47 – 2.8	0.3 – 5.9	108 – 295		[34]
Matadero (b)	2.0 – 15.5	1.8 – 14.4			3.2 – 31.6	0.16 – 4.5	0.01 – 5.5	130 – 1160		[34]
Cervecera			0.5 – 1.4	0.4 – 1.2	8.7 – 13.8	7.9 – 12.5				[35]
Cervecera			0.10 – 0.15		80 – 90			110 – 210	3.4 – 4.5	[36]
I. Láctea			0.4 – 1.2	0.5 – 1.0	2.0 – 4.7		240 – 286	45.3 – 56.7	6.7 – 9.1	[37]
I. Láctea	3.9	1.5			5			16.5	7.1	[38]
Suero Lácteo			20 – 22	8.5 - 13.2	73 – 86	59 – 71		897 – 1200	4.5 – 5.0	[39]
Suero Lácteo			1.3 – 1.4		65 – 72		8.3 – 10.6	1110 – 1130	4.6 – 5.2	[10]
Bodega/arroz			0.3 – 0.7		29.5 – 35.4			70 – 140	4.8 – 5.9	[40]
Mascotas			17.3 – 61.7	15.2 - 59.8	74.9 – 154		38.8		5 – 6	[41]
I. pesquera (a)			1.9		0.94			162	5.7	[42]
I. pesquera (b)			0.56		1.47			19	5.9	[42]
I. pesquera (c)			0.55		1.92			138	6.3	[42]

ST: sólidos totales, SV: sólidos volátiles, SST: sólidos suspendidos totales, SSV: sólidos suspendidos volátiles, DQO_T: demanda química de oxígeno total, DQO_S: demanda química de oxígeno soluble, AyG: aceites y grasas, NKT: nitrógeno total.

Los vertidos procedentes de la fabricación de aperitivos (a) y (b), y de matadero (a) y (b), siendo de las mismas empresas, presentan una composición distinta. El contenido en aceites y grasas de las aguas residuales tipo (b) de fábrica de aperitivos es muy superior a las de tipo (a) debido a que las muestras se tomaron cuando los picos de producción eran distintos. En el caso de los vertidos de matadero (a) y (b) difieren en que la muestra (a) fue sometida a un tratamiento previo para forzar la flotación con aire disuelto y eliminar así la mayoría de los sólidos y grasas por lo que la concentración de los parámetros analizados en la amuestra (a) es menor que la muestra (b).

Según datos de la Organización de las Naciones Unidas se estima que la población mundial aumentará en 2.000 millones de personas en los próximos 30 años. Esto hará que la demanda de alimentos aumente por lo que la industria alimentaria debe prepararse para afrontar este reto. Es prioritario desarrollar una industria alimentaria sostenible y segura, capaz de satisfacer las

necesidades de una población mundial en aumento sin perjuicio de los recursos naturales existentes que han de quedar disponibles para las generaciones futuras.

1.4 Legislación

Desde el año 1991 la Directiva 1991/271/CEE regula la recogida, tratamiento y vertido de las aguas residuales urbanas que incluye los vertidos de determinados sectores industriales con aguas biodegradables, entre los que se encuentra la práctica totalidad de la industria alimentaria. Esta Directiva fue traspuesta a la legislación española en el Real Decreto-ley 11/1995 que establece las normas aplicables al tratamiento de las aguas residuales urbanas.

En el artículo 8 del Real Decreto 509/1996 que desarrolla el Real Decreto-ley 11/1995, se establece la necesidad de tratamiento previo del vertido de las aguas residuales industriales que vierten a colectores por diversos motivos, entre otros: proteger la salud de los trabajadores de los sistemas colectores y plantas de tratamiento, evitar el deterioro de las instalaciones de tratamiento así como evitar que se obstaculice su correcto funcionamiento, evitar efectos nocivos sobre el medio ambiente y no impidan que las aguas receptoras cumplan los objetivos de calidad de la normativa vigente, y por último, garantizar que los fangos puedan ser evacuados de forma segura desde el punto de vista medioambiental.

Además, desde el año 2000 la Directiva Marco Europea del Agua (DMA), Directiva 2000/60/CE, regula las actuaciones en materia de gestión del agua con el fin de proteger las aguas superficiales continentales, las aguas de transición, las aguas costeras y las aguas subterráneas. Esta directiva trata de reducir los vertidos de sustancias peligrosas en el agua. Las decisiones sobre la planificación y ejecución de las medidas destinadas a garantizar la protección y el uso sostenible del agua deben tomarse al nivel más cercano posible donde tiene lugar el uso o degradación del agua mediante programas ajustados a las condiciones regionales o locales.

De este modo, con el fin de optimizar el consumo de agua, la industria alimentaria asume la responsabilidad de aplicar estrategias tanto de carácter preventivo, reduciendo al máximo el

consumo de agua potable, como de carácter correctivo, orientados a la reducción de contaminantes en el agua.

1.5 Tratamiento de vertidos

A través del tratamiento de vertidos se pretende reducir la contaminación, proteger el medio ambiente, ahorrar recursos y energía y dar valor a los desechos generados.

Actualmente se emplean distintos tratamientos que mejoran notablemente la calidad de los vertidos permitiendo su reincorporación al medio ambiente y/o reutilización sin perjuicio del ecosistema ni de la salud humana. Estos tratamientos pueden ser de naturaleza físico-química o biológicos, en ocasiones, y con el fin de mejorar la eficacia del tratamiento, se combinan ambos.

- ***Tratamiento físico-químico***

Los tratamientos físico-químicos permiten la separación de la materia suspendida y coloidal del agua mediante procesos de sedimentación, flotación, coagulación-floculación, precipitación, filtración, centrifugación y desinfección, dando lugar a la formación de lodos que, en el mejor de los casos, se reutilizan para compostaje y producción de biogás. Estos tratamientos alcanzan los requisitos de calidad para el vertido indirecto, pero tratándose de procesos de separación, generan fangos y en ocasiones requieren de la utilización de reactivos químicos y/o tienen un elevado consumo energético.

- ***Tratamiento biológico***

Los tratamientos biológicos consisten en la degradación de compuestos orgánicos y nutrientes disueltos, o en estado coloidal, mediante la actividad propia de los microorganismos. Estos procesos presentan numerosas ventajas frente a los tratamientos físico-químicos convencionales. Su alta eficacia en el tratamiento del vertido, con unas reducciones de DQO de más del 90% y un menor coste de operación y mantenimiento, hacen del tratamiento biológico de los vertidos una opción muy atractiva tanto para el tratamiento de vertidos municipales como industriales.

Existen múltiples configuraciones de reactores de modo que pueden adaptarse a cada tipo de vertido. En función del modo de operación pueden ser en continuo o discontinuo. Dependiendo del tipo de cultivo pueden ser de cultivo suspendido o de cultivo adherido. Los reactores de cultivo adherido pueden ser de lecho fijo o lecho móvil.

Atendiendo a la relación con el oxígeno estos tratamientos biológicos pueden ser aerobios Eq.(1) o anaerobios Eq.(2):

$$\text{Materia Orgánica} + O_2 \xrightarrow{\text{Microorganismos aerobios}} CO_2 + H_2O + \text{biomasa} \quad (1)$$

$$\text{Materia Orgánica} \xrightarrow{\text{Microorganismos anaeriobios}} CH_4 + CO_2 + H_2 + NH_3 + H_2S + \text{biomasa} \quad (2)$$

Los tratamientos anaerobios presentan numerosas ventajas frente a los tratamientos aerobios. Los sistemas aerobios convencionales conllevan un mayor consumo de energía, producen una elevada cantidad de fango, requieren de un mayor espacio y los costes de mantenimiento son mayores. Sin embargo, los reactores anaerobios son más sensibles a la inhibición por tóxicos y su puesta en marcha es más lenta [16,43].

La

Fig. 2 muestra un esquema de las principales vías metabólicas implicadas en proceso de degradación de materia orgánica en ausencia de oxígeno:

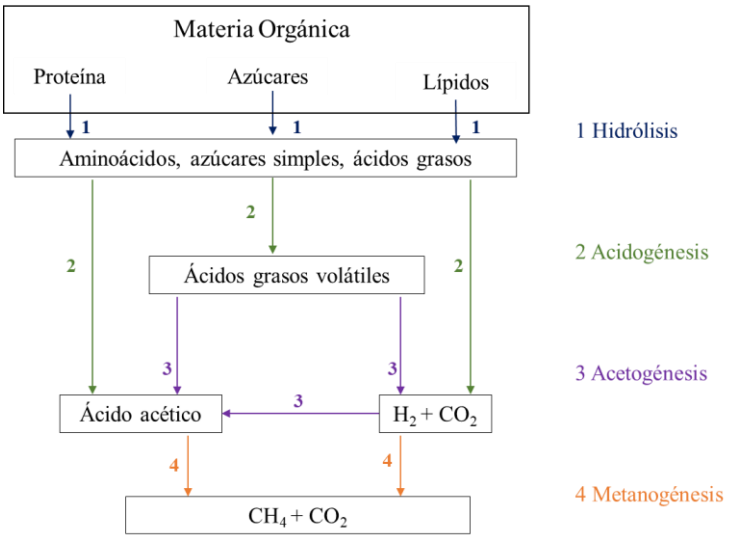

Fig. 2. Reacciones propias de la digestión anaerobia de materia orgánica (adaptado de Pavlostathis [44]).

La secuencia de las reacciones de degradación de materia orgánica en ausencia de oxígeno comienza con la hidrólisis de compuestos solubles formados por macromoléculas complejas de proteínas, lípidos e hidratos de carbono (

Fig. 2 (1)). Las bacterias anaerobias hidrolíticas transforman las proteínas, lípidos y azúcares en aminoácidos, azúcares simples y ácidos grasos. Estas reacciones de hidrólisis se ven limitadas por la temperatura, pH, concentración microbiana y complejidad de las macromoléculas de materia orgánica [45]

A continuación, tiene lugar la acidogénesis (

Fig. 2 (2)), en la que las proteínas, azúcares y lípidos se transforman en ácidos grasos volátiles de cadena corta (ácido fórmico, ácido butírico. ácido propiónico y ácido acético) alcoholes, aldehídos, hidrógeno y CO_2. Las bacterias acidogénicas crecen rápidamente y pueden dar lugar a la acumulación de ácidos grasos volátiles que disminuyen el pH en el medio y limitan el crecimiento de bacterias metanogénicas[46].

Posteriormente tiene lugar la acetogénesis (

Fig. 2 (3)). En este proceso las bacterias acetogénicas transforman los productos intermedios y el hidrógeno en acetato. Dos grupos de baterías llevan a cabo este proceso. Por un lado, bacterias

productoras de H_2 que oxidan ácidos grasos volátiles y por otro lado bacterias homoacetogénicas que consumen H_2 y CO_2 para producir ácido acético. Estas bacterias son de los géneros *Clostridium, Acetobacterium* y *Sporomusa* [47].

Finalmente tiene lugar la metanogénesis (

Fig. 2 (4)). La producción de metano tiene lugar por dos vías. En primer lugar se produce metano a partir de acetato por la vía aceticlástica mediante bacterias de los géneros *Methanosarcina* y *Methanosaeta* [47]. Aproximadamente un 70% del metano se produce por esta vía. El 30% restante tiene lugar por conversión de CO_2 y H_2 en metano y CO_2 mediante bacterias metanógenas hidrogenotróficas [48].

- ***Tratamiento combinado***

Cuando al tratamiento biológico de vertidos se le acopla una etapa de filtración con membranas se les denomina biorreactores de membrana, MBR.

Esta etapa de filtración permite que el tiempo de retención de sólidos, SRT, pueda ser controlado independientemente del tiempo de retención hidráulico, HRT, mejorando el desarrollo de los microorganismos y la eficiencia del tratamiento biológico, especialmente aquellos de crecimiento lento implicados en procesos anaerobios y en los procesos de eliminación de nutrientes.

Por otro lado, debido a las elevadas edades del fango a las que operan estos reactores se ve favorecido el desarrollo de biomasa especializada en degradar compuestos que requieren más tiempo para su completa eliminación. Además, gracias a la gran concentración de biomasa, estos reactores presentan una mayor estabilidad.

Cuando se combina el tratamiento anaerobio de vertidos con una etapa de filtración por membranas se denomina biorreactor anaerobio de membranas, AnMBR. Se trata de una prometedora alternativa a los MBR aerobios ya que requiere de un menor consumo energético, dan lugar a una menor producción de fangos y ocupan poco espacio. Mediante el tratamiento de vertidos con la tecnología AnMBR es posible recuperar recursos en forma de energía (metano), nutrientes que pueden ser empleados como fertilizantes o reutilización del efluente [49].

Capítulo 2: Filtración con membranas

2.1 Proceso de filtración

El proceso de filtración consiste en la separación de partícula y material coloidal presente en un líquido por medio de un material poroso denominado filtro que retiene la fracción sólida de tamaño superior al tamaño del poro del filtro.

La filtración se puede llevar a cabo bien por gravedad, donde la única fuerza impulsora que hace que el líquido atraviese el filtro es la hidrostática, a vacío donde la fuerza impulsora es la diferencia entre la presión atmosférica y presión relativa negativa, generada por succión o vasos comunicantes, o bien a presión donde el fluido ejerce una presión relativa positiva sobre el filtro forzando al líquido a atravesarlo. Estos dos últimos son los métodos más empleados en los procesos de filtración con membranas en reactores biológicos.

2.2 Tipos de membrana

Una membrana semipermeable consiste en un filtro cuya composición y tamaño de poro permite, bajo la acción de una diferencia de presión transmembranal adecuada, separar sólidos, coloides y diferentes sustancias disueltas en función de sus propiedades físicas y/o químicas. La membrana permite separar la alimentación en dos corrientes, un filtrado o permeado que es la fracción que atraviesa la membrana y un retenido con los materiales que no pueden atravesarla.

Según las características de la alimentación, de la membrana y de los parámetros de proceso seleccionados es posible mejorar el grado de retención para conseguir un efluente de mayor calidad, siendo esto último imprescindible en el tratamiento de aguas residuales.

El tipo de membrana, el material con que esté fabricada, la configuración de la membrana, el diseño del módulo de membrana y los parámetros de proceso influyen directamente en la retención de biomasa y compuestos solubles presentes en el licor de mezcla.

2.2.1 Tamaño de poro y material

Atendiendo al tamaño de poro existen 4 tipos de operaciones de separación con membrana: microfiltración (MF), ultrafiltración (UF), nanofiltración (NF) u osmosis inversa (OI). En la Fig. 3. Guía de aplicación de los procesos de filtración con membranas (adaptado del *Water treatment plant design* de AWWA y ASCE, Capítulo 13 se muestra de forma esquemática la capacidad de filtración de cada tipo de membrana dependiendo de su tamaño de poro y del tipo de moléculas que son capaces de atravesarla o retener.

Las membranas de MF presentan el mayor tamaño de poro, entre 0.1 y 10 µm impidiendo el paso de partículas, sólidos suspendidos y bacterias. Las membranas de UF, que tienen un tamaño de poro entre 0.05 y 0.005 µm, son capaces de retener macromoléculas y/o coloides. Las membranas NF son más selectivas, tan solo permiten el paso de moléculas de bajo peso molecular, iones polivalentes. Por último, la más selectiva de todas es la membrana de osmosis inversa (OI) que produce retenciones elevadas, incluso de sales monovalentes, mientras que las moléculas de agua pueden pasar libremente a través de la membrana.

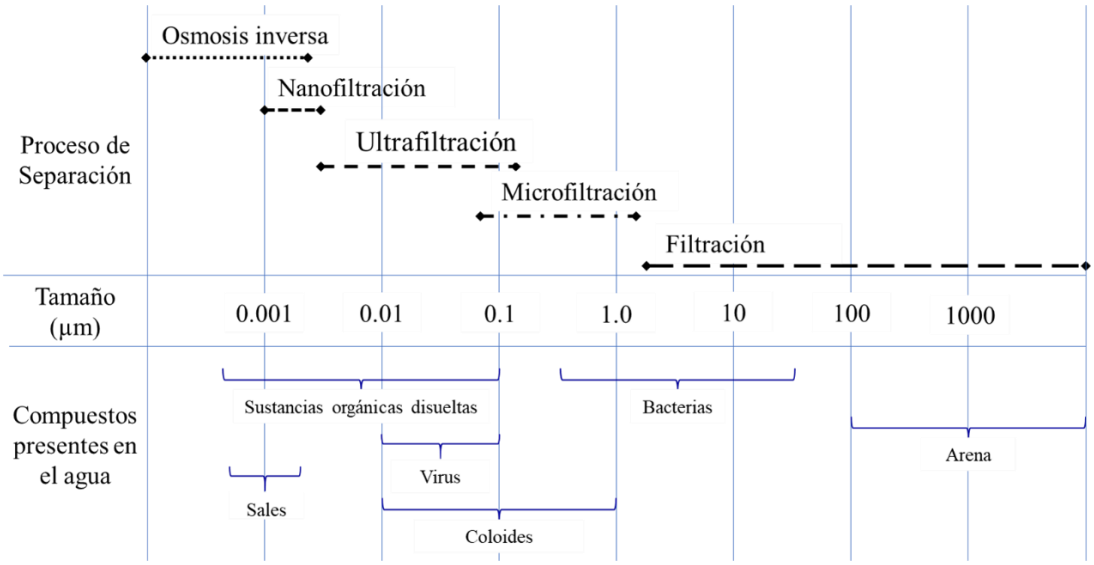

Fig. 3. Guía de aplicación de los procesos de filtración con membranas (adaptado del *Water treatment plant design* de AWWA y ASCE, Capítulo 13 [50]).

Las membranas más empleadas en el proceso de filtración de fangos en MBR son las de MF o UF debido a que su corte molecular es suficientemente pequeño como para conseguir una buena retención de microorganismos y coloides, lo que repercute en una mejora considerable en la calidad del agua tratada o corriente permeado. En el caso MF o UF es posible alcanzar la retención total de sólidos y en ocasiones la reducción en más de un 90% la concentración de DQO respecto al vertido original [51]. Debido a ello y a su menor precio hacen que las membranas de MF o UF sean la opción más atractiva a la hora de seleccionar el tipo de membrana para la filtración de fangos [32].

Sin embargo, existen estudios en los que con el fin de obtener un efluente de mejor calidad ese han combinado procesos de UF o MF con NF u OI [52] como tratamiento terciario capaz de eliminar las sales y contaminantes de menor tamaño, permitiendo así la reutilización del efluente.

Las membranas para MBR están fabricadas habitualmente con materiales poliméricos sintéticos (fluoruro de polivinilideno, PVDF, polieter-sulfona, PES, polietileno, PE, polipropileno, PP o polisulfona, PSF, politetrafluoroetileno, PTFE, o acrilonitrilo), o materiales inorgánicos (metálicas, cerámicas o de zeolita).

Las membranas poliméricas son más baratas en comparación con las inorgánicas de modo que suelen ser más empleadas en multitud tratamientos pese a que son menos estables a temperaturas altas, no permiten trabajar en todo el intervalo de pH, tienen menor resistencia mecánica y no soportan ciclos de limpieza agresivos que reducen su vida útil. Las membranas cerámicas o metálicas se emplean en tratamientos específicos, como por ejemplo para vertidos de temperatura elevada. Es por esto que las membranas de microfiltración o ultrafiltración de PVDF son las más empleadas en AnMBR. [53]

2.2.2 *Configuración y diseño*

En la Fig. 4. se muestran imágenes de las 3 configuraciones de membrana empleadas habitualmente en los MBR o AnMBR: membrana tubular (a), membrana de fibras huecas (b) y membrana plana (c).

(a) (b) (c)

Fig. 4. Membranas tubulares (a), membrana de fibras huecas (b) y membrana plana (c).

Las distintas configuraciones de membrana emplean modos de filtración distintos: in – out o out – in. En la Fig. 5 (a) se muestra de forma esquemática el proceso filtración en membranas tubulares, donde gracias a una fuerza impulsora que genera una presión relativa positiva, P(+), hace que el alimento pase por el interior de los canales o túbulos y el efluente salga por las paredes del canal atravesando la membrana. En la Fig. 5 (b) se muestra cómo el efluente atraviesa las membranas de fibras huecas o planas desde la parte exterior donde la membrana está en contacto con la mezcla solido-líquido a presión atmosférica, hacia el interior, donde una presión relativa negativa (vacío), P (-), ejerce la fuerza impulsora que permite al efluente atravesar la membrana.

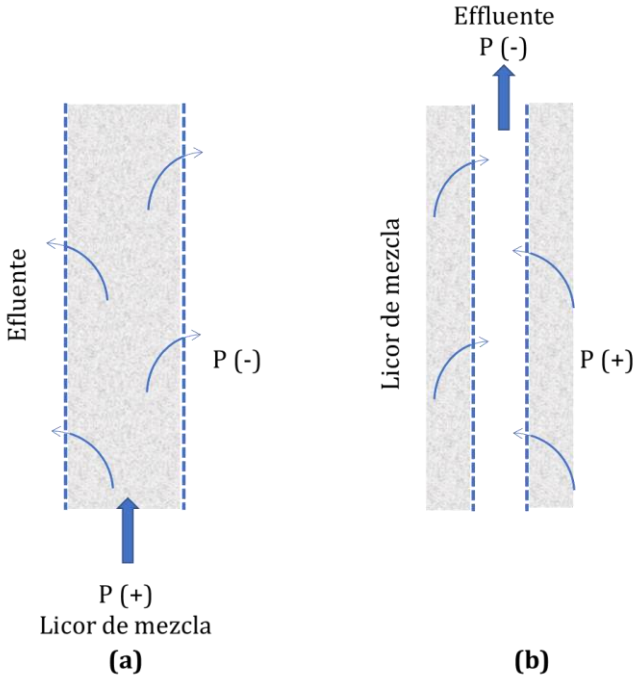

Fig. 5. Régimen de flujo a través de (a) membranas tubulares y (b) membranas sumergidas.

Atendiendo a la configuración de la membrana, según como la membrana se acople al reactor, los AnMBR se pueden clasificar en 2 tipos:

- Reactores biológicos anaerobios de membrana externa, eAnMBR, Fig. 6 (a).
- Reactores biológicos anaerobios de membrana sumergida, sAnMBR, que pueden ser de membrana sumergida directamente en el reactor biológico, Fig. 6 (b), o sumergida en un tanque de filtración externo, Fig. 6 (c).

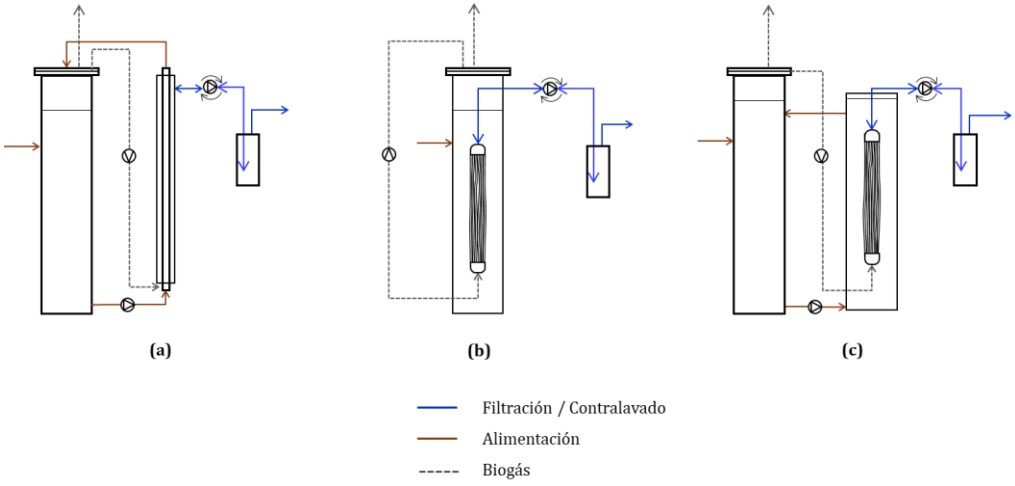

Fig. 6. Configuraciones de membrana según su acoplamiento al reactor biológico siendo (a) membrana externa, (b) membrana sumergida y (c) membrana sumergida en tanque externo.

Los eAnMBR, Fig. 6 (a), suelen emplear membranas tubulares (Fig. 4 (a)) en modo de filtración in-out, (Fig. 5 (a)). La membrana es alimentada por una bomba de recirculación que asegura un gradiente de presión desde el interior de los canales/túbulos hacia la parte exterior atravesando la membrana. La recirculación continua de fango dificulta la formación de torta sobre la superficie de la membrana y mejora la mezcla en el reactor. Para evitar la formación de la torta, además de la recirculación, también puede inyectarse un gas en el interior de los canales, lo que se conoce como "gas-lift". La configuración de membrana externa facilita la limpieza y el reemplazo de las membranas sin interrumpir el proceso biológico.

Los sAnMBR, descrito en la Fig. 6 (b), introducen la membrana en el reactor, en contacto directo con el fango. Se suelen emplear membranas sumergidas de fibras huecas (Fig. 4 (b)) en modo de filtración out-in (Fig. 5 (b)), y no requieren de una bomba de recirculación ya que el régimen de flujo depende de la presión de vacío generada en el interior de las fibras por la succión de la bomba de filtración. La ausencia de recirculación reduce el consumo energético del sistema y el estrés mecánico provocado sobre el fango. En estos reactores, para reducir la acumulación de fango sobre la superficie de la membrana, las fibras se agitan mediante el burbujeo de un gas. Para la limpieza y reposición de las membranas es necesario detener el sistema.

Los sAnMBR, descrito en la Fig. 6 (c), combinan propiedades de los dos diseños anteriores: emplean membranas sumergidas en un tanque de filtración exterior (Fig. 4 (c)). Una membrana de fibras huecas o plana se encuentra sumergida en un tanque externo con recirculación y opera en régimen out-in (Fig. 5 (b)). La relación de recirculación es mucho menor que en la membrana tubular ya que la única función de la recirculación es alimentar el tanque donde se encuentra sumergida la membrana, no eliminar la torta de la superficie de la membrana, de modo que el estrés mecánico es notablemente menor. Para el mantenimiento en continuo durante la operación se emplea burbujeo para hacer vibrar las fibras y/o barrer la superficie de las membranas y retirar parte de la torta. Para la limpieza intensiva o sustitución de las membranas no es necesario detener el proceso biológico.

2.3 Ensuciamiento de las membranas

La filtración con membranas de los MBR ofrece numerosas ventajas derivadas de la retención de materiales presentes en el fango frente a los tratamientos convencionales en lo que se emplean un sedimentador para separar la biomasa. Sin embargo, esta acumulación de materiales sobre la superficie de filtración minimiza la permeabilidad de la membrana, lo que incrementa los costes de mantenimiento derivados de la limpieza de la membrana afectando negativamente a la expansión y desarrollo la tecnología MBR.

2.3.1 Evolución de la filtración de fangos

El ensuciamiento de las membranas tiene lugar cuando los materiales que forman el fango, partículas, coloides y solutos, bloquean los poros y se depositan sobre la membrana formando una capa de gel superficial o torta que reduce la permeabilidad de la membrana [46]. Comprender detalladamente el proceso de ensuciamiento es fundamental a la hora de establecer un sistema de control adecuado a cada tratamiento.

En la Fig. 7 se muestran los dos mecanismos principales de ensuciamiento de las membranas regido por el tamaño de los materiales implicados. Mientras que coloides y solutos de diámetro

igual o inferior al tamaño de poro quedan retenidos en los poros de la membrana, las partículas que tienen un diámetro superior se depositan superficialmente formando un conglomerado de partículas, coloides y solutos que se acumulan e interaccionan entre sí.

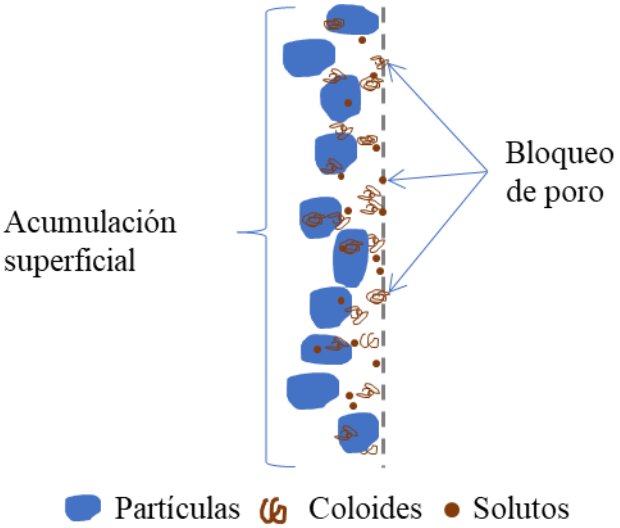

Fig. 7. Mecanismos de ensuciamiento de la membrana: acumulación superficial y bloqueo de poro.

El proceso de ensuciamiento tiene lugar durante la filtración y comienza con la adsorción de partículas de menor tamaño como solutos y coloides sobre la superficie de la membrana limpia, Fig. 9 (a). Seguidamente las interacciones entre compuestos dan lugar a la formación de flóculos de mayor tamaño que se depositan sobre la membrana formando una torta o gel que se comprime a medida que avanza la filtración, provocado por la presión del flujo tangencial, Fig. 9 (b).

La filtración no puede realizarse de forma continua dado que la acumulación de materiales sobre la membrana sería tal que la obstrucción de los poros haría inviable continuar operando tras un breve periodo de tiempo. Es por ello que el proceso de filtración se combina con paradas para la relajación y contralavado que facilitan el desprendimiento de los materiales acumulados.

En la Fig. 8 se muestra cómo varía la presión transmembranal, TMP, en un ciclo típico de filtración con una parada para la relajación, una etapa de contralavado, seguidamente otra para de relajación y por último, la etapa de filtración.

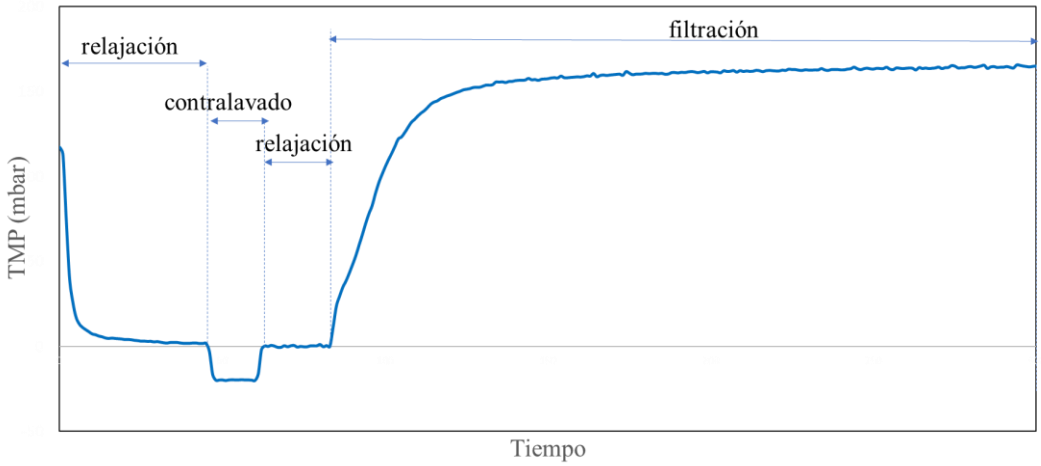

Fig. 8. Perfil de presión de un ciclo de operación con una etapa de relajación, una etapa de contralavado, una segunda etapa de relajación y una etapa de filtración.

Cuando tiene lugar la relajación o el contralavado Fig. 9 (c) la torta se afloja y se desprenden parte de los materiales adheridos. La inyección de gas, representada por las líneas inferiores de color marrón, empleada para el barrido de la membrana, *scouring*, favorece el desprendimiento de materiales, lo que permite reducir parcialmente la resistencia a la filtración aumentando la eficacia del sistema. Parte de estos materiales desprendidos vuelven a depositarse de nuevo en el siguiente ciclo de filtración de forma reversible [54].

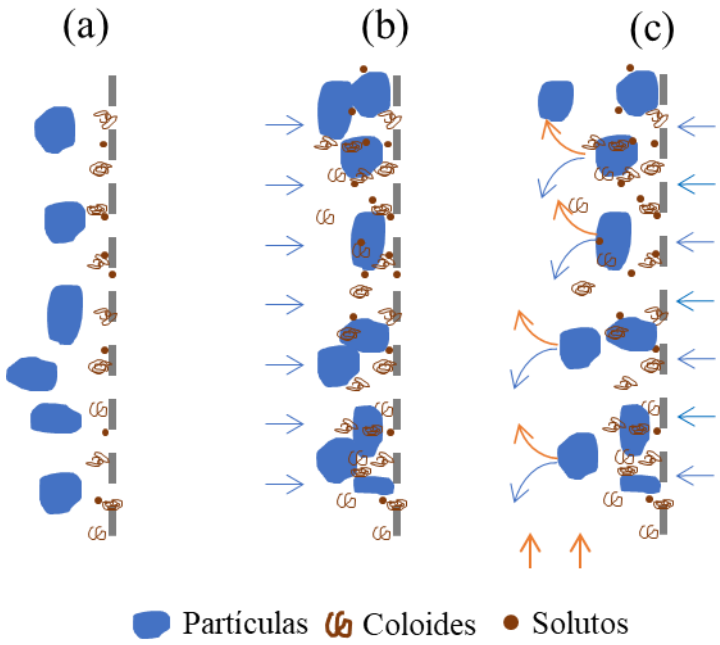

Fig. 9. Acumulación y desprendimiento de partículas, coloides y solutos sobre la membrana. (a) adhesión inicial de coloides y solutos sobre la membrana limpia, (b) formación de torta por acumulación y presión de flujo y (c) relajación de la torta y desprendimiento de materiales por contralavado, relajación, scouring o recirculación en el caso de las membranas tubulares externas.

Operacionalmente, a largo plazo, esto se traduce en un proceso de filtración donde la TMP es cada vez mayor en cada ciclo. La evolución global de la TMP a largo plazo se puede dividir en 3 fases que vienen representadas en la Fig. 10:

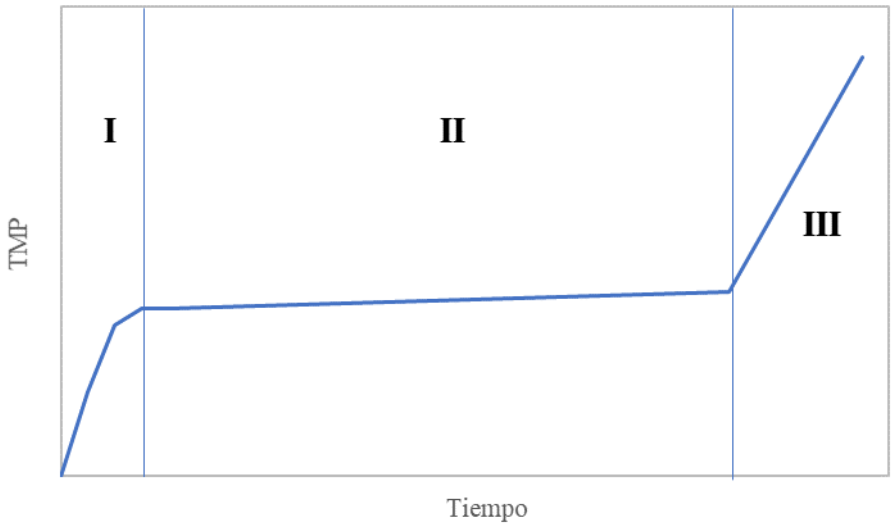

Fig. 10. Perfil de presión a lo largo del tiempo operando en condiciones constantes. Etapas I de ensuciamiento rápido inicial, etapa II, de ensuciamiento creciente estable y etapa III de salto de presión.

En la fase inicial (I) tiene lugar un crecimiento rápido de la TMP en cada ciclo que corresponde a la adhesión de los materiales sobre la membrana limpia y la formación de la torta. Posteriormente en la etapa (II) tienen lugar procesos de desprendimiento y deposición de materiales provocados por la filtración cíclica con periodos de contralavado y filtración que inevitablemente se van acumulando y provocan un crecimiento lento de TMP en cada ciclo hasta que llega un punto en que el ensuciamiento es tal que da comienzo a la fase (III) donde TMP experimenta un gran salto en un breve periodo de tiempo [55,56].

Ajustando correctamente las condiciones de operación se puede disminuir el ensuciamiento, a pesar de ello, la acumulación irreversible de materiales llega a un punto que no permite continuar operando correctamente y obliga a realizar paradas para la limpieza intensiva.

2.3.2 Composición química del ensuciamiento

La caracterización química de la biocapa el ensuciamiento de la membrana permite conocer cómo tiene lugar el ensuciamiento y permite mejorar las condiciones de operación del sistema. El análisis de la composición de la fase líquida y la fase sólida pueden dar información acerca de las interacciones entre los biopolímeros y la biomasa que forma los flóculos y relacionarlo así con la elevada resistencia a la filtración del fango que forma la torta alrededor de la membrana [57].

La biomasa es un medio complejo y heterogéneo compuesto por microorganismos, materia orgánica y en menor medida materia inorgánica

Los microorganismos, bien sean células libres o agrupados en fóculos, se depositan sobre la superficie de la membrana formando parte de la torta donde continúan con su metabolismo habitual [58,59], multiplicándose y liberando sustancias como EPS y SMP (productos microbianos solubles) que también contribuye al crecimiento de la torta y aumentar la resistencia a la filtración. [60,61]. Debido a su capacidad de deformación y adhesión, contribuyen de manera importante a aumentar la resistencia a la filtración.

La materia orgánica presente en la biomasa corresponde a compuestos de menor tamaño, como pueden ser polisacáridos, proteínas o sustancias húmicas presentes en aguas residuales o pueden ser sustancias origen microbiano EPS o SMP.

Los polisacáridos son considerados los principales responsables del ensuciamiento de la membrana [62] y el principal componente presente en los biopolímeros causantes del ensuciamiento. Su gran tamaño, su capacidad gelificante y su baja biodegradabilidad, hace que los polisacáridos tengan mayor capacidad de ensuciamiento que otros compuestos como sustancias húmicas o proteínas [63]. Estos geles están formados por redes de cadenas de polisacáridos cuya unión se ve favorecida por la presencia de cationes di/multivalentes, como el calcio, que actúan como puentes entre los grupos carboxilo de los polisacáridos [64]. Estos geles mantienen su estructura en condiciones ácidas o neutras y pueden desestabilizarse cuando el pH es más elevado [65].

Las sustancias húmicas, de naturaleza hidrofóbica, se adhieren a la membrana y pueden establecer interacciones hidrofóbicas o electrostáticas con polisacáridos o proteínas [64,66]. Jermann y col. [64] observaron que, mientras que las sustancias húmicas están implicadas en el ensuciamiento irreversible, la acumulación de polisacáridos es más bien reversible.

Los EPS y los SMP, EPS solubles, están formados por una gran variedad de moléculas y compuestos entre los que se encuentran proteínas, polisacáridos, ácidos nucleicos o sustancias húmicas que derivan de la actividad metabólica de los microorganismos [67,68]. Su contribución al ensuciamiento de las membranas es muy importante ya que se depositan fácilmente sobre la membrana durante la filtración y se adhieren más firmemente a la membrana que otras partículas de mayor tamaño [69]. Aunque no existe un mecanismo de control directo que minimice la presencia de estas sustancias en el medio, sí que se ha podido observar cómo distintos SRT, HRT y OLR (organic loading rate, velocidad de carga orgánica) son capaces de modificar la presencia de EPS en el medio ya que estos parámetros influyen directamente en el crecimiento o muerte celular. [69]. También es posible controlar la presencia de estas sustancias mediante la adición de

adsorbentes o coagulantes que favorecen la floculación. Por ejemplo, el carbón activo ayuda a la formación de estructuras más estables que facilitan el crecimiento de microorganismos y la captación de SMP que de otro modo terminarían directamente sobre la membrana [70,71]. Por otro lado, los coagulantes actúan neutralizando las cargas negativas de la superficie de los fóculos facilitando su agregación dando lugar a partículas de mayor tamaño minimizando el bloqueo de los poros. Algunas de las sustancias empleadas habitualmente como coagulantes suelen calcio, sales de aluminio (sulfato de aluminio y policloruro de aluminio, PAC) o sales de hierro (cloruro férrico), polisacáridos como quitosano, PAM (poliacrilamida), entre otros.

Junto a la materia orgánica que forma la capa de ensuciamiento de la membrana, también pueden encontrarse, en menor medida, elementos inorgánicos como Si, Ca, Mg, Al o Fe, entre otros, que contribuyen simultáneamente al ensuciamiento de la membrana[72]. El ensuciamiento por elementos inorgánicos puede formarse por precipitación química o precipitación biológica [69] Kang y col. [73] observaron que el empleo de membranas inorgánicas favorece la aparición de estos compuestos en la biomasa. Es posible reducir la presencia de elementos inorgánicos en el ensuciamiento de la membrana mediante el pretratamiento del filtrado. Sin embargo, la presencia de una pequeña cantidad de calcio puede ser beneficioso a la hora de mejorar la permeabilidad de la membrana [74]. La limpieza química es la forma más eficaz de eliminar los compuestos inorgánicos que ensucian la membrana[69].

2.3.3 Caracterización del ensuciamiento

La caracterización del ensuciamiento permite describir de qué manera tiene lugar el ensuciamiento de la membrana siendo clave a la hora de seleccionar las condiciones de operación que mejoren las condiciones de filtración. El estudio del ensuciamiento nos ofrece una idea del modo en el que tiene lugar la deposición de sólidos sobre la membrana durante la filtración.

Atendiendo a la fuerza con la que los materiales se adhieren tanto a la membrana como entre sí y al proceso de limpieza requerido para eliminarlo, se puede diferenciar entre dos tipos de ensuciamiento: ensuciamiento reversible o ensuciamiento irreversible. El ensuciamiento

reversible corresponde a materiales débilmente adheridos a la superficie de la membrana o entre sí que puede eliminarse fácilmente mediante procesos físicos de limpieza como relajación, contralavado, inyección de gas o, en el caso de las membranas tubulares externas, circulación tangencial sobre la superficie de la membrana. El ensuciamiento irreversible se debe al bloqueo de los poros de la membrana o la consolidación de materiales sobre su superficie que a largo plazo dan lugar a la formación de la torta incluso operando en condiciones en las que el ensuciamiento reversible resulta inapreciable. El ensuciamiento irreversible se encuentra firmemente adherido y solo puede ser eliminado tras una limpieza química [69].

Por último, hay que tener en cuenta el ensuciamiento irrecuperable asociado a operación a largo plazo donde ningún tipo de limpieza es capaz de recuperar el valor original de resistencia de la membrana nueva. Se trata de un ensuciamiento permanente que da lugar a un valor de resistencia remanente que se va acumulando a largo plazo y que determina la vida útil de la membrana [54,75]

Sin embargo, esta clasificación es insuficiente cuando se pretende explicar otros mecanismos de ensuciamiento cuyo comportamiento puede presentar rasgos propios de dos o más tipos de ensuciamiento. Por ejemplo, el bloqueo de poro se considera irreversible, sin embargo, es posible que estas partículas sean retiradas por un contralavado muy intenso, de modo que en tal caso se trata de ensuciamiento reversible [76]. La diferenciación entre las distintas componentes de la resistencia es muy heterogénea y depende del criterio de cada autor[77] directamente relacionado con el procedimiento empleado para su caracterización.

La resistencia total, R_T, viene determinada por la ley de Darcy, Eq. 3, y permite calcular la resistencia total a la filtración incluyendo la resistencia de la membrana y la resistencia debida a los distintos tipos de ensuciamiento. El modelo de resistencias en serie Eq. 4, [78] permite discriminar la resistencia debida a la membrana y la resistencia debida a los distintos mecanismos de ensuciamiento.

$$R_T = \frac{TMP}{J \cdot \mu} \quad (3)$$

$$R_T = R_m + \sum R_i \quad (4)$$

donde *TMP* es la presión transmembranal, μ es la viscosidad del permeado y *J* es el flujo de permeado. La resistencia total, R_T, se debe a la resistencia de la membrana, R_m, y a la suma de las resistencias parciales, R_i, son las componentes de la resistencia relacionado con el tipo de mecanismo de ensuciamiento.

Numerosos autores emplean el modelo de resistencias en serie, como la suma de la contribución relativa de cada mecanismo de ensuciamiento, para explicar el ensuciamiento de la membrana. Una de las distinción más extendida es aquella que diferencia entre la resistencia debida a la deposición superficial responsable de la formación de una torta superficial, R_C, y la resistencia debida al bloqueo de poro, R_{pb} [79,80]:

$$R_T = R_m + R_C + R_{pb} \quad (5)$$

Otros autores describen una contribución específica para cada tipo de ensuciamiento como por ejemplo Li y Wang [81] quienes dividieron la resistencia total en la suma de la resistencia de la membrana, R_m, resistencia por bloqueo interno de poro, R_{pb}, la resistencia debida a la deposición dinámica del lodo, R_{sf} y la resistencia estable unida a la membrana, R_{sc}:

$$R_{tot} = R_m + R_{pb} + R_{sf} + R_{sc} \quad (6)$$

Algunos autores [82–84] tienen en cuenta los fenómenos de adsorción, R_{ad}, la concentración por polarización, R_{cp}, o el ensuciamiento de la membrana, R_f, a la hora de diseñar sus modelos de resistencias en serie:

$$R_{tot} = R_m + R_{ad} + R_{cp} + R_f \quad (7)$$

Busch y col. [83] consideraron R_{cp} despreciable, incluyeron $R_{ad,}$ como parte de R_f, también consideraron R_{pb} y R_c y la resistencia debida a la capa de material biológico $R_{b.}$ Choi y col. [82,84] diferenciaron R_f entre resistencia reversible e irreversible que no corresponde exactamente con la formación de la torta o el bloqueo de poro ya que como se explicó anteriormente, los mecanismos de la formación de torta y bloqueo de poro pueden presentar características propias de ensuciamiento reversible o irreversible.

Diez y col. [85] consideraron la resistencia de la membrana, R_m, la resistencia irreversible, R_{if} y la resistencia reversible, $R_{rf,}$ como las componentes de la resistencia total, R_T (Eq. 8). Dependiendo de dónde tenga lugar el ensuciamiento irreversible esta resistencia se divide en irreversible externa, R_{ef}, y resistencia irreversible interna, por bloqueo de poro, R_{pb} (Eq. 9):

$$R_T = R_m + R_{if} + R_{rf} \quad (8)$$

$$R_{if} = R_{ef} + R_{pb} \quad (9)$$

En la Tabla 2 se recogen algunas de las nomenclaturas utilizadas por diversos autores a la hora de desglosar los mecanismos implicados en la resistencia de la membrana (adaptado de Di Bella y Di Trapani [77])

Tabla 2. Componentes de la resistencia total (adaptado de Di Bella y Di Trapani [77]).

Mecanismo de ensuciamiento	Abreviatura
Ensuciamiento reversible	R_{rev}
Ensuciamiento irreversible	R_{irr}
Resistencia al contralavado	R_{bw}
Ensuciamiento irreversible interno	$R_{irr,in}$
Ensuciamiento irreversible externo	$R_{irr,ex}$
Ensuciamiento por adsorción	R_{ad}
Ensuciamiento por bloqueo de poro	R_{pb}
Ensuciamiento por bloqueo irreversible del poro	R_{p}
Resistencia por deposición superficial reversible o bloqueo interno	R_{reb}
Resistencia debida a formación de la torta	R_{C}
Formación irreversible de la torta superficial	$R_{C,irr}$
Formación reversible de la torta superficial	$R_{C,rev}$
Ensuciamiento por deposición interna de coloides	R_{co}
Ensuciamiento por polarización por concentración	R_{cp}
Deposición dinámica de material biológico de forma reversible	R_{sc}
Deposición irreversible de material biológico	R_{sf}

2.4 Estrategias para el control del ensuciamiento de las membranas

El ensuciamiento puede ser controlado indirectamente actuando sobre las condiciones de operación del proceso biológico (SRT, HRT, OLR, F/M, etc) o directamente actuando sobre las condiciones de operación de la membrana.

En este apartado se describen los métodos directos de control de ensuciamiento que se aplican sobre el proceso de filtración como son el tipo y diseño de la membrana, las condiciones de filtración y el tipo de limpieza de la membrana.

2.4.1 Selección de la membrana

Una membrana puede caracterizarse por su rugosidad, porosidad, carga superficial o hidrofobicidad que dependen del material con que estén fabricadas y que le otorga unas condiciones de filtración propias. Se ha comprobado que los materiales **e**mpleados en la fabricación de las membranas presentan distinta propensión al ensuciamiento. La principal ventaja de emplear membranas orgánicas son su bajo coste, pese a su menor permeabilidad y menor estabilidad frente a temperaturas elevadas del medio o los productos químicos empleados en la limpieza, comparado con las membranas cerámicas [86]. Yamamoto y col. [87] compararon el ensuciamiento de dos membranas de PE y PVDF y observaron que la membrana de PE tiene una mayor tendencia a ensuciarse de forma irreversible que la membrana de PVDF. Zhang y col. [88] estudiaron la afinidad entre EPS extraídos de fango aerobio en 3 membranas de PAN, PVDF y PES mediante contacto directo en una celda de filtración y observaron que la membrana de PAN tiende a ensuciarse menos y que la membrana de PES fue la que más se ensució debido a su rugosidad e hidrofobicidad. La rugosidad y la carga neta de la superficie de la membrana afectan más a la interacción entre biomasa y membrana que su hidrofobicidad. Cierta aspereza y un mayor potencial zeta disminuyen el ensuciamiento [89]. De acuerdo con Kang y col. [73] las membranas inorgánicas pueden favorecer el ensuciamiento por aumentar la concentración de materiales inorgánicos, de modo que, pese a su gran capacidad de filtración, únicamente se

emplean cuando son estrictamente necesarias como, por ejemplo, ante vertidos cuya temperatura sea demasiado alta como para emplear membranas orgánicas.

La configuración del módulo de filtración también puede favorecer en mayor o menor medida el ensuciamiento de las membranas. En el caso de la configuración externa, la recirculación requerida para la alimentación de la membrana contribuye a la reducción del ensuciamiento por arrastre de materiales superficiales, sin embargo el estrés mecánico provocado por la recirculación da lugar a alteraciones en el fango y rotura de flóculos que hacen que aparezcan más partículas de menor tamaño y se liberan al medio una mayor cantidad de EPS y SMP provocando un mayor ensuciamiento [90]. Uno de los desafíos a los que se enfrenta este tipo de membranas para su mayor implementación es lograr establecer un equilibrio entre la recirculación que permita arrastrar materiales con la mínima alteración del fango [4].

Algunos autores han realizado estudios comparativos donde han observado cómo filtrar en configuración externa o sumergida puede afectar a la capacidad de filtración de las membranas. Sin embargo, las diferencias propias de las condiciones de estudio pueden dar lugar a resultados confusos. Le-Clech y col. [91] compararon los efectos del ensuciamiento en una membrana tubular en dos configuraciones, externa y sumergida, y observaron una menor tendencia al ensuciamiento cuando la membrana se operó en configuración sumergida debido al régimen de flujo obtenido como resultados de los caudales de gas-líquido empleados. Por otro lado, Cheng y col. [92] compararon el ensuciamiento en una misma membrana de fibras huecas en dos configuraciones distintas, sumergida en un tanque externo y sumergida directamente en el reactor biológico, en un AnMBR que trataba agua residual municipal, y observaron una mayor tendencia al ensuciamiento en la membrana sumergida directamente en el reactor que en la membrana sumergida en un tanque externo debido el grado de disrupción de flóculos dentro del reactor. Hay que tener en cuenta que el efluente del tanque externo estaba libre de biomasa de modo que las condiciones de filtración de las membranas no eran exactamente iguales.

2.4.2 Limpieza física

Es posible reducir el ensuciamiento de la membrana durante la operación en continuo mediante determinadas estrategias de control como son la agitación por burbujeo con biogás, la recirculación de suspensiones de carbono activo o la vibración/rotación de membranas.

El burbujeo con biogás es una técnica muy extendida, observándose una relación directa entre flujo de biogás y el incremento de la permeabilidad de la membrana [93,94]. Judd and Chang [95] compararon dos formas de suministrar el gas en dos módulos de filtración de membranas tubulares, una en configuración sumergida y otra en configuración externa. En la membrana externa se suministraba el gas directamente a través de los canales tubulares de la membrana facilitando la recirculación en modo air-lift y, por otro lado, en la configuración sumergida de la membrana tubular el gas se suministraba inyectadolo directamente en los canales en modo intermitente, air-jet. Observaron una recuperación de flujo del 43% cuando el gas se inyecta en modo air-lift, sin embargo, no observaron una mejora notable cuando el flujo de gas aumentó de a 1 a 10 L/min en la membrana que operaba en modo air-jet debido a la obstrucción de los canales.

Otros autores han hecho recircular una suspensión de partículas o gránulos de carbono activo sobre la superficie de la membrana. Las partículas de carbono activo adsorben materia orgánica presente en el fango. Además, como consecuencia de la propia recirculación, la eliminación de materiales se ve favorecida[96]. Johir y col. [97] observaron una reducción de la resistencia de $5.1 \cdot 10^{12} m^{-1}$ a $2.1 \cdot 10^{12} m^{-1}$ al añadir gránulos de carbono activo con una concentración entre 0.2 y 2 g/L en un reactor de membrana plana sumergida que opera con un flujo de aire de 1.0 $m^3/m^2 \cdot h$, y un flujo de filtración de 25 $L/m^2 \cdot h$.

Por otro lado, la vibración de membranas mediante distintas fuerzas mecánicas y movimientos que pueden ser longitudinales, transversales o la combinación de ambas facilita el desprendimiento de materiales de la superficie de la membrana. Kola y col. [98] fueron capaces de mantener un flujo crítico elevado y constante, de 26 L/m^2h, cuando sometían a una vibración de 6.7 Hz un módulo de ultrafiltración de membrana sumergida de fibra hueca formado por 5

fibras con un área de filtrado de 0.003 m^2, pese al progresivo aumento de la concentración de sólidos entre 0.005 g/L y 5 g/L. Sin embargo, en las mismas condiciones, pero sin vibración, la velocidad de flujo crítico se redujo de 16 L/m^2h a 1 L/m^2h.

En el caso de las membranas tubulares externas la recirculación requerida para alimentar la membrana tiene una doble función, por un lado, alimenta la membrana y, por otro, arrastra materiales acumulados durante la filtración. Sin embargo, Le-Clech y col. [91] observaron que al tratar dos tipos de fango distintos, uno de agua residual real y otro de agua residual sintética, en dos MBR con configuraciones de membrana diferentes, sumergida y externa, operando con un flujo de gas entre 0.07 – 0.11 m/s y una velocidad de recirculación de 0.25 – 0.55 m/s respectivamente, la efectividad de la recirculación era menor que el flujo de gas. Mientras que el flujo de gas era capaz de reducir la velocidad de ensuciamiento de 0.12 a 0.01 mbar/min cuando se operaba entre 0.05 y 0.25 m/s, el efecto de la recirculación en la membrana en configuración externa apenas fue apreciable. Operando condiciones sub-críticas la velocidad de ensuciamiento reversible se mantuvo constante en torno a 0.17±0.06 mbar/min independientemente de la velocidad de recirculación.

2.4.3 Modo de filtración

Las estrategias de filtración habitualmente empleadas para minimizar el ensuciamiento es la filtración cíclica con periodos de filtración, relajación y contralavado, como se explicó en la Fig. 8 del apartado 2.3.1. Seleccionar una adecuada combinación entre la duración y los flujos de filtración y contralavado, es muy importante a la hora diseñar el proceso. No existe un criterio unificado que determine cuáles han de ser las condiciones de filtración ya que cada proceso es distinto. El éxito de un proceso de filtración está en ajustar los tiempos y los flujos para que el ensuciamiento de la membrana sea el menor posible y la cantidad de permeado la mayor posible.

La recomendación más extendida en relación con la selección del flujo de filtración es el empleo de flujos sub-críticos [99]. Operar en condiciones sub-críticas permite minimizar el ensuciamiento irreversible de la membrana y prolongar el funcionamiento del MBR en continuo

durante más tiempo, reduciendo el número de paradas para la limpieza intensiva. La determinación del flujo crítico no se encuentra normalizada, mientras que unos autores emplean ensayos de corta duración, inferiores a 1 hora, aumentando el flujo en cada ciclo mientras se controla la presión transmembranal, otros autores, como van der Marel y col. [100], determinan el flujo crítico a partir de la medida de TMP intercalando un periodo de filtración con un flujo mínimo entre flujos superiores ascendentes y descendentes. Otros autores emplean ensayos de larga duración de varios días o semanas a un flujo constante [101].

La relajación y la intensidad de contralavado son factores clave en la eliminación del ensuciamiento acumulado durante la etapa de filtración. La intensidad del contralavado viene determinada por el tiempo y el flujo empleado en esta etapa. La relajación consiste en la detención de la filtración durante un corto periodo de tiempo de modo que favorece la descompresión de la torta y facilita el desprendimiento de materiales durante el contralavado.

Zsirai y col. [102] estudiaron el efecto de la intensidad del contralavado, la relajación y el contralavado químico, sobre la mejora de la permeabilidad en un módulo de membrana sumergida de fibra hueca y observaron que para un mismo volumen de contralavado el flujo de contralavado fue ligeramente más efectivo que la duración del contralavado. Respecto al contralavado químico observaron que no era efectivo en operaciones a largo plazo bajo condiciones desfavorables como eran filtrar a flujos superiores a 35 $L/m^2 \cdot h$ y un burbujeo de tan solo 0.25 $Nm^3/m^2 \cdot h$.

2.4.4 Limpieza química

Tras largos periodos de operación, aún en las mejores condiciones posibles, llega un punto en el que el ensuciamiento de la membrana es tal que las operaciones físicas de limpieza son insuficientes para mantener la permeabilidad de la membrana. En este punto es necesaria una intervención más efectiva sobre la membrana mediante una limpieza química intensiva que permita recuperar un valor de resistencia lo más cercano posible al valor de resistencia inicial de la membrana.

Es un proceso no deseado, es costoso y para llevarlo a cabo es necesario detener la planta. Incluso en el caso de las membranas sumergidas puede ser necesario abrir el reactor biológico lo que complica las labores de limpieza y pone en peligro la estabilidad del reactor anaerobio.

La limpieza química se lleva a cabo con ácidos, bases, reactivos oxidantes, surfactantes o quelantes. Los ácidos y las bases favorecen la hidrólisis de los componentes depositados sobre y dentro de los poros de la membrana facilitando la solubilización de los compuestos. Los productos ácidos pueden ser empleados en la eliminación de precipitados inorgánicos o minerales [54]. Las bases como el hidróxido sódico son efectivas en la eliminación de materiales orgánicos [103]. Las limpiezas con productos ácidos como ácido oxálico o ácido cítrico también son efectivas en la eliminación y desinfección de materia orgánica y biológica [2]. Sin embargo, la forma más habitual de limpiar la membrana es mediante oxidantes como en NaClO. El mantenimiento habitual semanal de las membranas en MBR aerobios consiste en la limpieza con concentraciones entre 200-300 mg/L de NaClO y limpiezas intensivas al cabo de varios meses con entre 1000 y 5000 mg/L de NaClO [104].

Raffin y col [105] llevaron a cabo una serie de ensayos sobre distintos protocolos de limpieza química probando 3 productos químicos distintos a diferentes concentraciones, temperatura y tiempos de contacto y observaron que no se puede definir un único protocolo de limpieza general para todos los sistemas de filtracion si no que cada protocolo de limpieza debe ser optimizado individualmente.

Capítulo 3: Material y Métodos

3.1 Montajes experimentales

Dos montajes experimentales a escala pre-piloto de 20 L fueron operados en paralelo en los ensayos de ultrafiltración de fangos anaerobios. Además, un montaje a escala laboratorio de 1 L de volumen se empleó para el estudio del comportamiento de los EPS sobre una fibra hueca de membrana de PVDF de ultrafiltración.

3.1.1 Membrana tubular externa

En la Fig. 11 se muestra un esquema del montaje empleado en el estudio de filtración de fango anaerobio con membrana tubular externa.

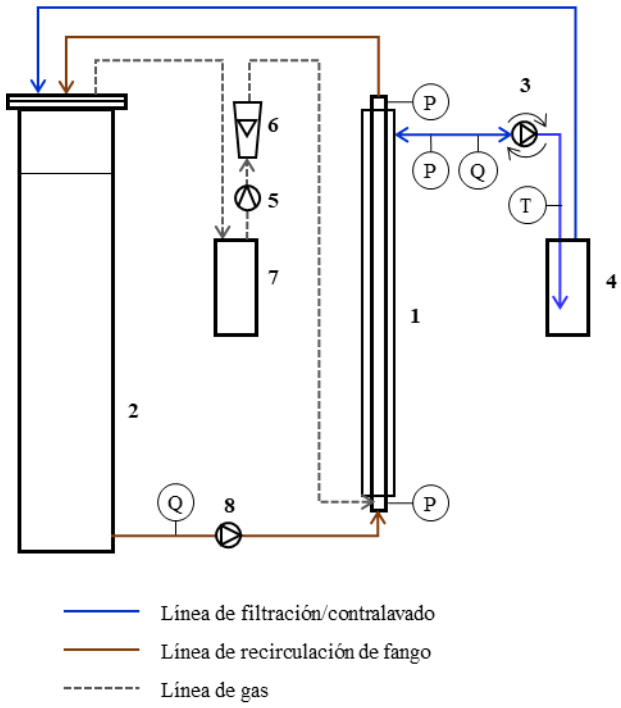

Fig. 11. Sistema de filtración de fangos anaerobios en configuración externa. 1. membrana tubular externa, 2. tanque, 3. bomba de filtración y contralavado, 4. bote de permeado, 5. compresor de biogás, 6. rotámetro, 7. bote de condensados, 8. bomba de recirculación.

Este montaje consta de una membrana tubular (1) (Berghof 63.03I8) de PVDF de ultrafiltración en configuración externa y régimen de filtración in-out acoplada a un tanque de alimentación de 20L. La membrana mide 1 m de longitud y tiene 8 tubos internos de 13 mm de diámetro con un diámetro nominal de poro de 0.04 µm y 0.31 m^2 de superficie de filtración. La

bomba de recirculación (8) alimenta y ejerce la presión necesaria para filtrar el licor de mezcla a través de la membrana. Una bomba de filtración reversible (3) (Micropump Eagle Drivef GJ-N21) ejerce una presión de vacío y controla el flujo de filtración. El filtrado queda recogido en un bote de permeado de 1 L disponible para su reutilización en el contralavado. Un compresor (5) (Secoh SV50, Kantauri) toma el biogás libre de espumas de un bote de condensados (7) que está conectado a la parte superior del tanque. Un rotámetro (6) mide el flujo de gas que se inyecta en la parte inferior de la membrana facilitando el flujo ascendente de la mezcla del licor de mezcla y el biogás. Este fluido tiene una menor densidad que el licor de mezcla lo que facilita el ascenso de la mezcla de la parte inferior de la membrana hasta la parte superior y su retorno al tanque. Este sistema genera una gran cantidad de espumas que son retenidas en el bote de condensados evitando que entren en el compresor de biogás.

El proceso de filtración está controlado remotamente por un PLC (M-Duino 42, Industrial Shields). Los datos registrados por los sensores de presión (PN2069, IFM Electronics), caudal (MIK 5NA, Kobold Mesura) y temperatura (TR2432, IFM Electronics) son enviados por el PLC a un ordenador. Un programa escrito en Visual Basic calcula y representa en tiempo real las velocidades de ensuciamiento.

3.1.2 Membrana sumergida de fibras huecas

En la Fig. 12 se muestra un esquema del montaje experimental empleado para los ensayos de filtración de fango anaerobio con membrana sumergida de fibras huecas.

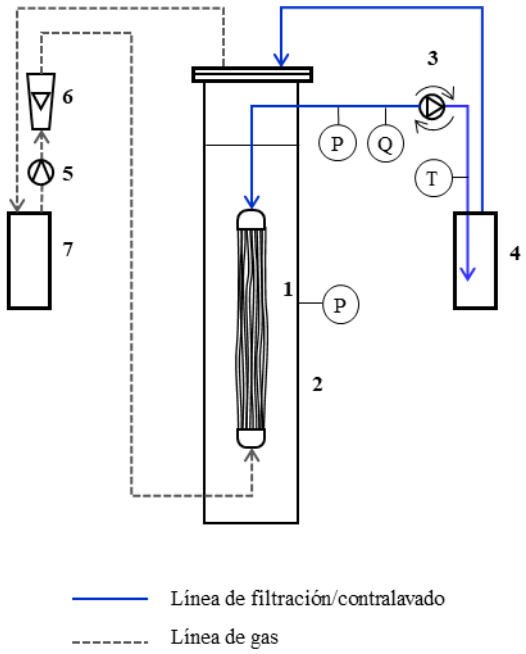

Fig. 12. Sistema de filtración de fangos anaerobio en configuración sumergida. 1. membrana sumergida de fibras huecas, 2. tanque, 3. bomba de filtración y contralavado, 4. bote de permeado, 5. compresor de biogás, 6. rotámetro, 7. bote de condensados.

Este sistema consta de una membrana sumergida de fibras huecas (1) de PVDF de ultrafiltración en régimen de filtración out-in. La membrana mide 69 cm, cada fibra tiene un diámetro de 2 mm con un diámetro de poro de 0.04 µm y una superficie de filtración de 0.93 m^2. La membrana se encuentra sumergida en contacto directo con el licor de mezcla a presión atmosférica. Una bomba de vacío reversible de velocidad regulable (3) (Micropump Eagle Drivef GJ-N21) provoca una presión negativa haciendo que el efluente atraviese la membrana y quede recogido en un bote de permeado donde queda disponible para el contralavado. El biogás se toma del bote de condensados (7) libre de espumas y un compresor (modelo marca) lo inyecta en la parte inferior de la membrana provocando la vibración de las fibras y el arrastre ascendente de materiales depositados sobre la superficie de la membrana. El sistema de registro y control de datos es el mismo que el descrito en el apartado 3.1.1

3.1.3 Fibra hueca sumergida

En la Fig. 13 se muestra un esquema del montaje a escala laboratorio empleado en ensayos de filtración de soluciones de EPS

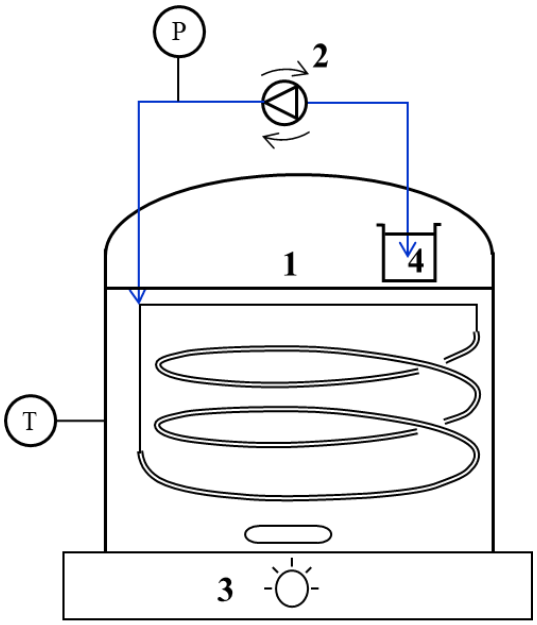

Fig. 13. Sistema de filtración de membrana de fibra hueca a escala laboratorio, de 1 L. 1. bote hermétido, 2. bomba reversible de filtración y contralavado, 3. placa calefactora con agitación, 4. recipiente de permeado. P y T corresponde a los sensores de presión y temperatura

Se trata de un depósito cerrado herméticamente (1) de 1 L que se llena hasta los 0.8 L con distintas soluciones con concentraciones variables de salinidad y EPS, en su interior se encuentra una fibra hueca de 0.03 μm de tamaño de poro de 0.92 m de longitud y tiene un diámetro de 2.4 mm lo que le confiere un área de filtrado de 0.00694 m^2. El bote se encuentra sobre un agitador (3). El filtrado se recoge en un recipiente (4) situado en el interior del depósito donde queda disponible para su reutilización en el contralavado.

El sistema de control y registro de datos es el mismo que el descrito en el apartado 3.1.1, excepto el caudal de filtración determinado a partir del calibrado de la bomba (3), Watson Marlow 520 U, cuya velocidad era controlada por el PLC.

3.2 Caracterización hidrodinámica del ensuciamiento

La TMP durante la filtración a un flujo J ($m^3\ m^{-2}\ h^{-1}$), se calcula acorde a Eq. 10 para la membrana externa y acorde a Eq. 11 para la membrana sumergida:

$$TMP = \left(\frac{P_I + P_o}{2} - P_f\right)_J - P_{J=0} \quad (10)$$

$$TMP = (P_t - P_f)_J - P_{J=0} \quad (11)$$

P_i y P_o son las presiones en la entrada y la salida de la membrana tubular externa respectivamente, P_f es la presión en la línea de filtración, P_t es la presión en el tanque de filtración de la membrana sumergida y $P_{J=0}$ es la diferencia de presiones cuando J es 0.

La resistencia total se calculó de acuerdo con la Ley de Darcy (Eq. 12):

$$R = \frac{TMP}{J \cdot \mu} \quad (12)$$

donde μ es la viscosidad del permeado (Pa·s) para la que se admitió la viscosidad del agua.

El ensuciamiento reversible corresponde al incremento de TMP a lo largo del tiempo $(dTMP/dt)_{rev}$ durante cada etapa de filtración y el ensuciamiento irreversible corresponde al incremento de la resistencia inicial de cada ciclo de filtración a lo largo del ensayo $(dR/dt)_{irr}$. La velocidad de ensuciamiento irreversible se obtiene a partir del incremento de resistencia irreversible entre el volumen filtrado $(dR/dV)_{irr}$

Se ha utilizado el modelo RIS planteado diferentes resistencias individuales que facilitan la comprensión de las componentes del ensuciamiento:

$$R_T = \frac{TMP}{\mu \cdot J_f} = R_m + R_{irr} + R_{rev} \quad (13)$$

$$R_{bw} = \frac{TMP_{bw}}{\mu \cdot J_{bw}} = R_m + R_{irr,in} \quad (14)$$

$$R_0 = \frac{TMP_0}{\mu \cdot J_f} = R_m + R_{irr} \quad (15)$$

$$R_{irr} = R_0 - R_m = R_{irr,in} + R_{irr,ex} \quad (16)$$

$$R_{irr,ex} = R_{irr} - R_{irr,in} = R_0 - R_{bw} \quad (17)$$

$$R_{irr,in} = R_{bw} - R_m \quad (18)$$

Durante la filtración se considera la resistencia total, R_T, en la Eq. 13, como la suma de la resistencia de la membrana, R_m, la resistencia irreversible, R_{irr}, y la resistencia al ensuciamiento reversible, R_{rev}.

La resistencia al contralavado, R_{bw}, en la Eq. 14, es la suma de la R_m y la resistencia irreversible interna, $R_{irr,in}$, provocada por el bloqueo de los poros y materiales firmemente adheridos a la membrana.

La resistencia inicial, R_0, en la Eq. 15, es la resistencia al inicio del ciclo de filtración y se compone de la R_m y la R_{irr}.

La $R_{irr,}$ en la Eq. 16, está formada por la $R_{irr,in}$ y la resistencia irreversible externa, $R_{irr,ex}$. Esta última se debe a la adhesión irreversible de los materiales que forman la torta y se calcula a partir de la diferencia entre la R_0 y $R_{bw.}$ Por otro lado la $R_{irr,in,}$ en la Eq. 18 se obtiene a partir de la diferencia entre la R_{bw} y R_m.

3.3 Diseño de experimentos de Box-Behnken

El diseño de experimentos de Box-Behnken, BBD, [106] se trata de un diseño de superficie de respuesta que permite determinar cuáles son y en qué medida afectan determinadas variables a una respuesta. Mediante el BBD se puede determinar cuáles son las variables que más afectan a una respuesta determinada, establecer un modelo polinómico de primer o segundo orden capaz de explicar la influencia de las variables y optimizar las condiciones de operación para obtener la respuesta deseada.

El BBD es capaz de estimar eficientemente los coeficientes de primer y segundo orden a partir de un menor número de experimentos, comparado con los diseños factoriales. Los BBD dividen

el espacio experimental de cada variable en 3 niveles (nivel bajo -1, nivel medio 0, nivel alto +1) seleccionando ensayos que combinan dos valores extremos. De este modo el número de experimentos necesarios para estudiar 3 variables son 15 experimentos y en el caso de 4 variables tan solo 27 experimentos, en lugar de los 27 y 81 experimentos, respectivamente, necesarios en el diseño factorial.

Mediante la siguiente ecuación polinómica, Eq. 19, se recoge el efecto de cada variable sobre la respuesta estudiada:

$$Y = b_0 + \sum b_i X_i + \sum b_{ij} X_i X_j \qquad (19)$$

donde Y es la respuesta predicha, b_0 es una constante, b_i es el coeficiente lineal de la variable X_i y b_{ij} es la interacción entre las variables X_i y X_j

Raffin y col. [107] emplearon BBD para la optimización de las condiciones de filtración de un sistema de filtración integrado compuesto por una membrana de MF seguido de una membrana de OI diseñado para estudiar su viabilidad como tratamiento para la potabilización de agua residual. Estudiaron el efecto del flujo de filtración, frecuencia de contralavado, el punto en que se dosificaba el agente de limpieza, sobre el ensuciamiento de la membrana MF y por otro lado el flujo de filtración, la recuperación, la dosis de producto y pH sobre la membrana OI. BBD dio como resultado que, bajo las condiciones de filtración seleccionadas, la frecuencia de contralavado y la filtración de flujo fueron los parámetros que más influyen sobre el ensuciamiento de MF, mientras que el pH y la recuperación son los parámetros de control a tener en cuenta sobre la velocidad de ensuciamiento en OI.

BBD permite optimizar eficientemente los parámetros de estudio dentro del rango seleccionado, no es posible extrapolar los resultados fuera de las condiciones de estudio, por lo que, es importante seleccionar adecuadamente los límites de las variables que se desea optimizar.

3.4 Procedimientos analíticos

3.4.1 Métodos estándar de análisis de aguas residuales

Se analizaron sólidos totales y volátiles, sólidos suspendidos totales y volátiles, la la demanda química de oxígeno, la concentración en aceites y grasas y el nitrógeno total, acorde a los protocolos recogidos en Standard Methods for the Examination of Water and Wastewater [108].

3.4.2 Actividades Metanogénicas

Se estudió la actividad metabólica de los fangos sometidos a distintos procesos de filtración al inicio y al final del experimento.

Para el estudio de la actividad metanogénica del fango se introdujo una muestra de 400 ml en botellas de 2.1 L alimentado con comida de mascotas, con una relación S/X de 1 g COD/g VSS. Se añadió 1 g/L de bicarbonato para regular el pH y macronutrientes y micronutrientes acorde con el procedimiento propuesto por Angelidaki y col. [109] para compensar la posible falta de los mismos en el medio. Se retiró el O_x de cada botella por arrastre con N_2 y se mantuvieron durante un periodo igual o superior a 7 días en una sala a una temperatura constante de 35ºC y con agitación continua en un roller.

La producción de biogás se midió con medidores digitales de presión 1 o 2 veces al día dependiendo de la actividad de los cultivos y al final del ensayo se midió la concentración de metano con un medidor multi-gas móvil (MULTITEC 545 de Sewerin).

3.4.3 Métodos para análisis de EPS

Se analizaron EPS en disolución y ligados al fango obtenido por centrifugación, Fig. 14 (a), en el filtrado del licor de mezcla, Fig. 14 (b). También se analizaron EPS en el sobrenadante de muestras obtenidas por distintas técnicas de extracción que implican agitación mecánica con vortex y disolución por ultrasonidos Fig. 14 (c).

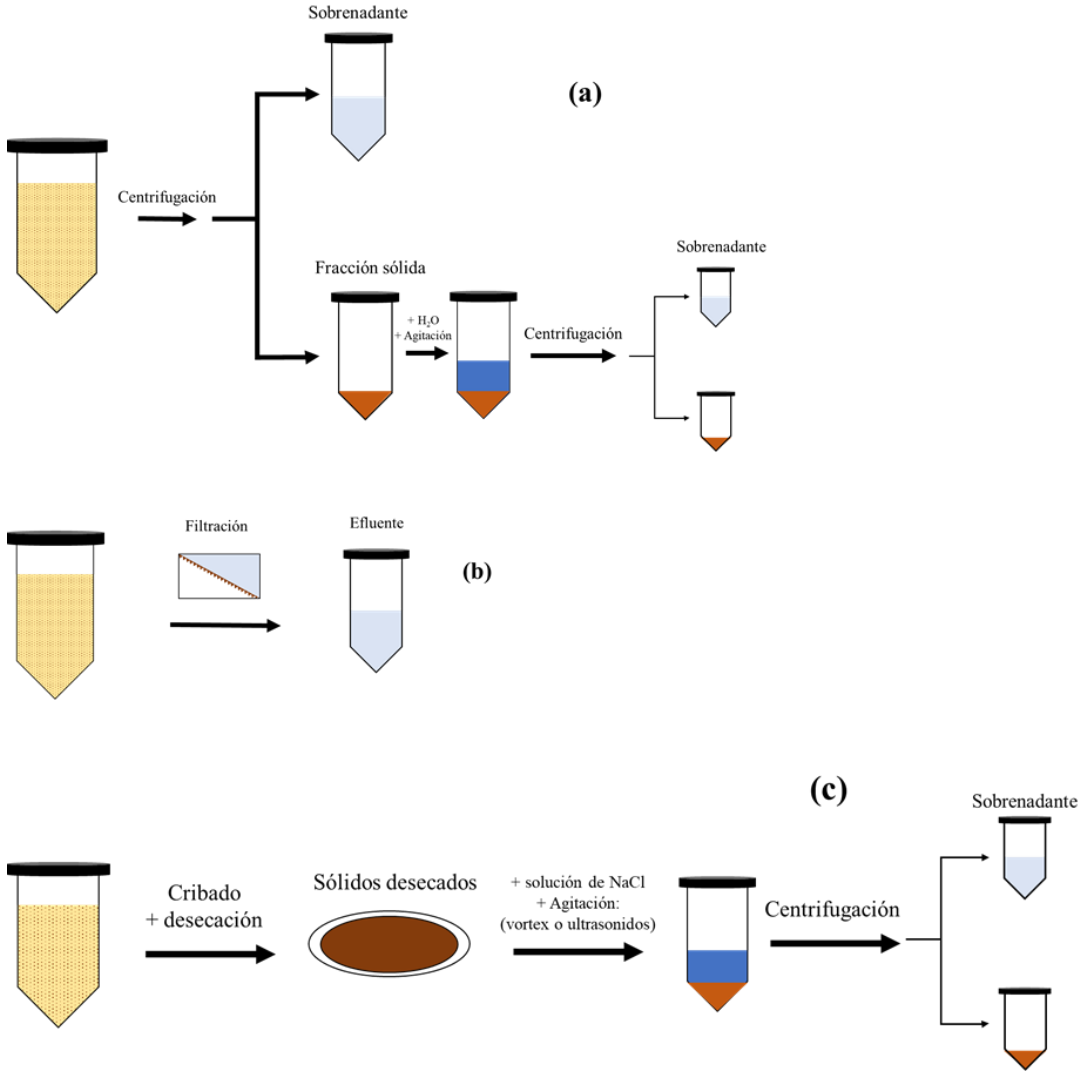

Fig. 14 Sobrenadante y fracción sólida obtenidas por centrifugación (a), filtrado del licor de mezcla (b) y extracción de EPS por agitación o vortex (c) para el análisis de EPS.

La concentración total de hidratos de carbono se determinó utilizando el método de Dubois y D-glucosa como patrón [110–112]. Este método se basa en la medida espectrofotométrica a 490 nm del color amarillo que se forma al reaccionar el fenol con derivados del furfural e hidroximetilfurfural creados en un medio fuertemente ácido.

La determinación de la concentración proteínas en muestras líquidas se ha realizado por el método propuesto por Bradford [113–115]. Este método se basa en la medida espectrofotométrica del color azul que se forma al reaccionar el colorante azul de Coomasie G-250 con los residuos aromáticos de las proteínas y utiliza como patrón seroalbúmina bovina (SAB). Las medidas espectrofotométricas se realizaron a 590 nm y 450 nm.

La determinación de las compuestos húmicos en muestras líquidas se realizó siguiendo el método modificado de Lowry [115–118] que mide espectrofotométricamente de forma simultánea proteínas y ácidos húmicos. Este método se basa en que el $CuSO_4$ reacciona únicamente con las proteínas de la muestra. Las muestras se analizan con y sin $CuSO_4$ para poder eliminar la inferencia de las proteínas en la determinación cuantitativa de las sustancias húmicas. La lectura espectrofotométrica se realizó a 750 nm utilizando como patrón ácido húmico y seroalbúmina bovina (SAB).

SAB de VWR Prolabo Chemicals, compuestos húmicos de SIGMA-ALDRICH y D(+) glucosa anhidra de VWR Prolabo Chemicals fueron empleados como patrones de calibración. Las medidas espectrofotométricas se realizaron con un espectrofotómetro Hitachi U-2000 UV/vis. Todas las muestras se realizaron por triplicado.

3.4.4 Distribución del tamaño de partícula

El tamaño de partícula se determinó a partir de muestras tomadas en el tanque de filtración y a la salida de la bomba de recirculación en el caso del montaje de filtración con membrana externa, mediante medida directa sin tratamiento previo utilizando Mastersizer 2000 de Malvern Instruments acoplado a Hydro 2000SM con un ranto de detección entre 0.02 y 2000 μm.

Dado el impacto que las partículas menores de 100 μm tienen sobre el ensuciamiento de las membranas se determinó el volumen acumulado de partículas de cada diámetro, d_p, en un intervalo entre 0-100 μm calculado a partir de la ecuación 4:

$$Vol.\%\ under\ d_{p[0-100]} = \frac{\sum_0^{d_p}(Vol.\%)_d}{\sum_0^{100}(Vol.\%)_d} \cdot 100 \qquad (20)$$

donde $\sum_0^{d_p}(Vol.\%)_d$ es el volumen acumulado de partículas de cada d_p y $\sum_0^{100}(Vol.\%)_d$ fue el volumen acumulado de partículas menores de 100 μm.

Capítulo 4: Comparison of external and submerged membranes used in Anaerobic Membrane Bioreactors. Fouling related issues and biological activity

Biochemical Engineering Journal
Volume 159, 15 July 2020, 107558
doi.org/10.1016/j.bej.2020.107558

4.1 Introduction

A membrane bioreactor is an innovative and efficient technology used for wastewater treatment combining biological treatment and direct sludge separation by membrane filtration. Membrane fouling, one of the main bottlenecks for the successful operation of a membrane bioreactor, is a complex process that is affected by wastewater characteristics, sludge concentration and properties, membrane configuration, and reactor operating conditions. Fouling appears to be more severe in anaerobic environments, due in part to the lower anaerobic sludge filterability, when compared to aerobic sludge as a consequence of low sludge flocculation and an increase in the supernatant colloidal fraction [6,119]. Higher fouling propensity of the anaerobic sludge has led to low sustainable fluxes in anaerobic membrane bioreactors (AnMBR) even with high biogas sparging intensities [120].

Hydrodynamic conditions are strongly influenced by the mode in which anaerobic reactor and membrane are combined. Two types of membrane arrangements can be distinguished: external or side-stream AnMBR and internal or submerged AnMBR. The external AnMBRs (eAnMBR) commonly apply tubular membranes that operate with a high crossflow velocity for disrupting the formation of a filtration cake on the membrane surface, while submerged AnMBR (sAnMBR) usually apply hollow-fiber membranes or flat-sheet membranes, operating in a vacuum and sparging with biogas for fouling control. A Gas-lift AnMBR (Gl-AnMBR) is a particular type of reactor that combines the two previous technologies. It applies crossflow filtration in tubular membranes, in the same way as the eAnMBR, and low-pressure filtration and gas sparging, in the same way as the sAnMBR configuration, reducing the crossflow velocity that is required in the eAnMBR [94,121]. Each membrane configuration has its own advantages and disadvantages, depending on wastewater characteristics, operational goals, and space availability for the installation. External membrane configurations have well-defined hydrodynamic conditions that permit direct reversible fouling control by adjusting the crossflow velocity, and they are easy to clean and replace [32,46,53]. Chemical cleaning of submerged membranes is more difficult, if

done in place, as the cleaning reagent might affect the biomass, and if done out of place, then the anaerobic system might be exposed to oxygen. That disadvantage can be limited by the combination of a side-stream approach and a submerged configuration in an AnMBR where the membrane is immersed in an external filtration tank [78]. Hollow-fiber membrane modules are often used in sAnMBR, because of their lower capital costs and lower energy consumption [32,53], from 0.038 to 5.68 kWh/m^3, as against the estimated consumption of 3 to 7.3 kWh/m^3 of an external membrane configuration [46,119,122]. On the other hand, optimizing filtration conditions directly affects the positive economic balance of AnMBR technology [123].

Particle Size Distribution (PSD), Extracellular Polymeric Substances (EPS) composition and even microbial activity can be affected by biomass shear stress, which will provoke differences in the fouling behavior between external and submerged membrane processes, due to their different hydrodynamic conditions. The recirculation in the external membrane configuration, required to reach high crossflow velocities that prevent deposition on the membrane surface, causes high shear forces that can lead to a decrease in biomass particle size [124] and the subsequent release of Soluble Microbial Products (SMP) [53,90,125]. Humic substances (HS) are the principal exopolymers in the air-sparged side-stream membrane configuration, and polysaccharides (PS), and proteins (PN) are prevalent in the submerged membrane configuration [126]. The accumulation of SMP on the membrane surface is related to the irreversible membrane fouling rate [35,127] and choosing the appropriate operating conditions could help to minimize major fouling mechanisms by reducing the release of high molecular weight substances [128]. Recent studies have shown that addition of powdered activated carbon in membrane bioreactors would reduce membrane fouling, and so the operating costs [129].

Shear stress can result in decreased microbial activity, due to possible disruption of syntrophic relationships between the different groups of microorganisms, and can even induce cell disruption that lowers biogas production and decreases chemical oxygen demand (COD) removal efficiency in side-stream processes [4,130]. Ghyoot and Verstraete [131] filtered sludge from an anaerobic digestor checking that the shear stress disrupted the interactions between the different species in

the anaerobic consortia, and that the negative effect on the microbial communities depended on the frequency of anaerobic sludge displacement throughout the filtration circuit, due to shear stress in its mechanical parts. However, the effect of side-stream pumping and shear on methanogenic activity is still unclear [86], as it also depends on the type of pump. Brockmann and Seyfried [132] studied the effect of different types of pumps (centrifugal pumps with rough or polished surfaces, mono-pumps, peristaltic pumps, lobular pumps, and centrifugal screw pumps) on the aerobic sludge filtration and found a significant influence of the recirculation pump type on the disintegration of sludge flocs.

The literature includes some comparative studies of the behavior of external and submerged configurations operating under the same conditions, but the results were in some cases contradictory because there were relevant differences in the characteristics of the bioreactors. Le-Clech et al. [91] compared the performance of a tubular membrane bioreactor configured both as a submerged and as a side-stream MBR. They observed a lower fouling propensity in the submerged configuration, due to the prevalent slug flow hydrodynamics regime resulting from the air-liquid flow rates that were employed. Chen et al. [92] compared the performance of external and submerged granular AnMBR configurations operating in parallel to treat municipal wastewater. For the external granular AnMBR, a hollow-fiber membrane was immersed in an external filtration tank fed with the effluent of an upflow anaerobic granular bioreactor, while in the submerged granular AnMBR, an identical hollow-fiber membrane module was directly immersed in the mixed liquor in the settling zone of the bioreactor. The submerged configuration demonstrated higher fouling propensity, higher cake layer resistance and more deposition of EPS in the cake layer, as a consequence of the deteriorated granular sludge properties with granule fragmentation and reduced granule settleability. Martin-García et al. [119] compared submerged hollow fiber and external tubular membrane AnMBR configurations, operating the latter in both pumped and gas-lift mode. The filtration performance of flocculated and granulated AnMBR treating domestic wastewater was compared. Higher critical fluxes and lower fouling rates were achieved for the granular anaerobic sludge using either submerged hollow fibers or external

tubular membranes operated in pumped side-stream mode; however, the specific energy demand was significantly lower for the submerged hollow fibers membranes than for the pumped side-stream configuration.

It is difficult to compare the behavior of external and submerged membrane bioreactors when there are differences in reactor configuration, sludge characteristics, wastewater composition, and operating conditions. Likewise, few studies have compared fouling in tubular membranes and hollow-fiber membranes filtering anaerobic sludge under the same conditions, in order to assess the impact of hydrodynamic conditions imposed by each configuration. The aim of this work is therefore to provide a direct comparison of the anaerobic sludge filtration behavior with external tubular membranes and submerged hollow-fiber membranes under the same conditions: biomass concentration filtration and backwash flux and duration, and biogas sparging flow per unit of membrane area. Thus, an integrated study is performed, of the factors relating to shear stress, such as PSD, EPS and SMP concentrations, and biomass methanogenic activity, in addition to reversible and irreversible fouling rates, and the efficiency of physical and chemical cleaning processes.

4.2 Material and Methods

4.2.1 Filtration set-ups and operating conditions

Two filtration set-ups, equipped with an external tubular membrane (eM) and a submerged hollow-fiber membrane (sM), were simultaneously operated under the same conditions (Table 3). A simplified diagram of the eM and sM set-ups is shown in Fig. 15 Each of the two set-ups had a 20 L tank, 160 mm in diameter, that was loaded with sludge from an anaerobic digestor of food industries biowastes diluted with effluent from a pilot scale AnMBR, to obtain an initial total suspended solids concentration of 4 g/L.

Table 3. Membrane characteristics and operating conditions of each one.

Membrane	External	Submerged
Type	multitube	hollow fiber
Material	PVDF	PVDF
Filtration mode	in-out	out-in
Nominal pore diameter (μm)	0.04	0.04
Filtration area (m^2)	0.31	0.93
Effective membrane length (mm)	1000	692
Membrane diameter (mm)	8	2
Number of tubes	13	n/a
Cross flow velocity (m/s)	0.51	n/a
Gas flow (m^3/h)	0.3 – 0.4	1.0 – 1.2
Specific gas demand ($m^3/m^2 \cdot h$)	1.2±0.1	1.2±0.1
Superficial gas velocity (m/s)	0.15±0.02	0.015±0.001
Filtration flow (L/h)	4.65	14.0 – 18.5 – 23.0
Filtration flux ($L/m^2 \cdot h$)	15	15 – 20 – 25

n/a not applicable

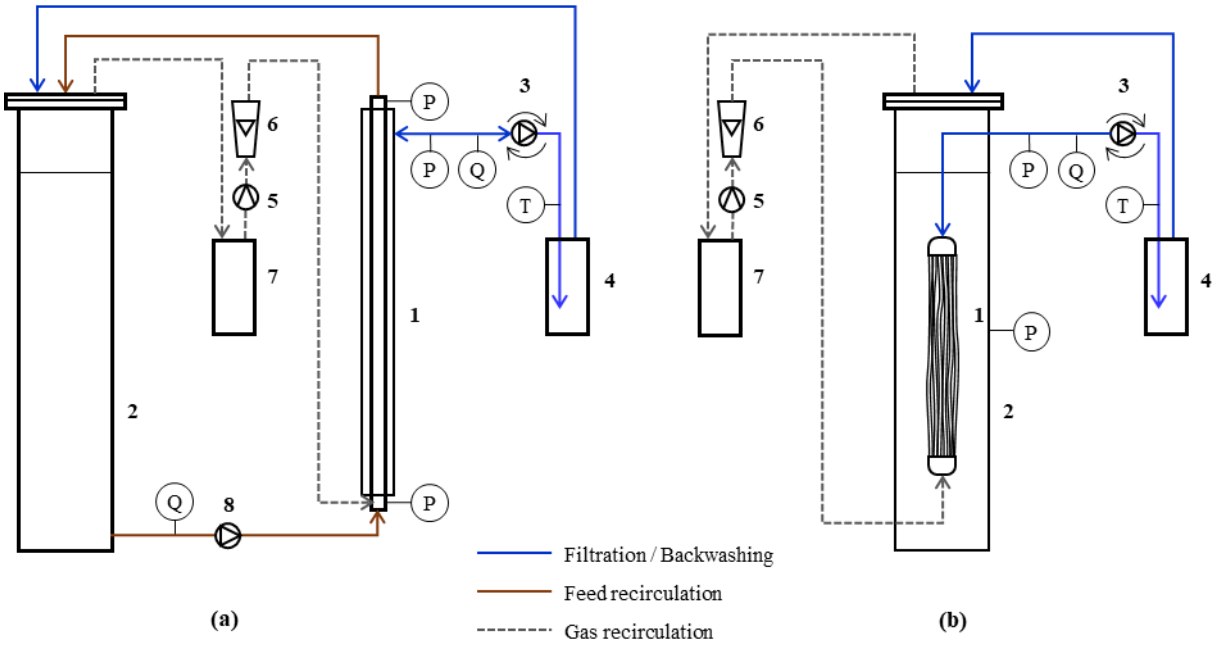

Fig. 15. Experimental set-ups: (a) external membrane set-up, and (b) submerged membrane set-up. (1.a) tubular membrane, (1.b) hollow-fiber membrane, (2) feed tank, (3) reversible filtration/backwashing pump, (4) permeate vessel, (5) biogas compressor, (6) rotameter, (7) condensate trap, (8) recirculation pump, P, Q, T pressure, flow, and temperature gauges.

In eM, Fig. 1(a), a backwashable ultrafiltration multi-tubular membrane is detailed (Berghof 63.03I8) with a surface area of 0.31 m^2, a bore size of 8 mm and a nominal pore size of 0.04 µm. It runs a recirculation pump with a low maximum rotational velocity (950 rpm) and a two-blade open impeller for wastewater with high levels of suspended particles. A frequency converter is used for crossflow control, avoiding flow control valves. The eM set-up, had a biogas recirculation circuit to operate as a gas-lift side-stream filtration system for increasing shear over the membrane surface and reducing pumping requirements for recirculation. In sM, Fig. 1(b), an ultrafiltration hollow-fiber membrane module is detailed (ZeeWeed ZW-10) with a surface area of 0.93 m^2 and a nominal pore size of 0.04 µm that is directly submerged in the filtration tank.

Reversible wear pumps (Micropump Eagle Drivef GJ-N21) were used for filtration and backwashing and membrane scouring by biogas recirculation was performed with Secoh SV50 (Kantauri) compressors in each set-up. Electronic pressure gauges (PN2069, IFM Electronics), electronic-inductive flowmeter (MIK 5NA, Kobold Mesura), and digital temperature sensors (TR2432, IFM Electronics) were applied for filtration monitoring. Ardunino-based PLCs

(M-Duino 42, Industrial Shields) were programmed for flux, filtration/backwash cycle, biogas sparging, and crossflow control. A desktop application running on a PC connected to the PLCs collected the data relayed from the sensors and calculated the filtration and backwashing resistances and the fouling rates on-line.

The filtration cycle duration was 15 minutes with 30 seconds for backwash and 30 seconds for relaxation before and after the backwash, the same for both membranes. The specific gas demand per square meter of membrane area (SGD_m) was 1.2±0.1 $Nm^3/m^2 \cdot h$, also identical, apparently high for full-scale membrane modules, but not so high for lab-scale modules [2,133]. Crossflow velocity was maintained at 0.51 m/s during filtration and backwash in eM, in the order of Gl-AnMBR, between 0.3 and 1.0 m/s [121]. Backwashing flux was 20 $L/m^2 \cdot h$ for both membranes. Filtration flux was set at 15 $L/m^2 \cdot h$ over the first 7 days and was then increased up to 25 $L/m^2 \cdot h$ in the sM.

4.2.2 Filtration and fouling characterization

Filtration performance is characterized by total resistance at the beginning of the filtration, R_0, the resistance during the backwash, R_{bw}, the reversible fouling rate, $(dTMP/dt)_{rev}$, from the increase in transmembrane pressure, during each filtration cycle and irreversible fouling rate, $(dR/dt)_{irr}$, from the increase in the initial filtration resistance throughout the assay.

Transmembrane pressure, TMP (Pa), for a flux J ($m^3 \cdot m^{-2} \cdot s^{-1}$), was calculated for the external membrane as:

$$TMP = \left(\frac{P_i + P_o}{2} - P_f\right)_J - P_{J=0} \quad (21)$$

where, P_i and P_o are the pressure at the membrane inlet and outlet, respectively, P_f is the pressure in the filtration line, and $P_{J=0}$ is the previous difference for J = 0, which value depends of the relative height of the pressure gauges, neglecting the head loss in the filtration line. TMP for the submerged membrane was calculated as:

$$TMP = \left(P_t - P_f\right)_J - P_{J=0} \quad (22)$$

where, P_t is the pressure in the filtration tank.

Total resistances, R (m^{-1}), were determined according to Darcy's law

$$R = \frac{TMP}{J \cdot \mu} \quad (23)$$

where, μ is the viscosity of permeate (Pa·s) approximately represented by the viscosity of tap water, dependent on its temperature , T (°C), in accordance with the correlation [134]:

$$\mu = \frac{479 \cdot 10^{-3}}{(T + 42.5)^{1.5}} \quad (24)$$

From the irreversible fouling rate $(dR/dt)_{irr}$, the irreversible increase in resistance over the filtered volume per unit of area, $(dR/dV)_{irr}$ (m^{-2}), was determined as:

$$\left(\frac{dR}{dV}\right)_{irr} = \frac{(dR/dt)_{irr}}{J} \quad (25)$$

where, V is the filtrated volume per unit of membrane surface area ($m^3\ m^{-2}$).

4.2.3 Analytical methods

Proteins (PN), Polysaccharides (PS), and Humic Substances (HS) were analyzed in the mixed liquor and in the permeate. Soluble Microbial Products (SMP) in the sludge were determined from the supernatant obtained by centrifugation at 4500 rpm. From the solid fraction, loosely bound extracellular polymeric substances (LB-EPS) were determined after water extraction at room temperature.

PN were determined using the modified Bradford method [114], PS were measured using the method suggested by Dubois [111], and HS were determined using Lowry's modified method [117] and a Hitachi U-2000 UV/vis spectrophotometer. Bovine serum albumin (VWR Prolabo

Chemicals), humic acid (SIGMA-ALDRICH), and D(+)-anhydrous glucose (VWR Prolabo Chemicals) were used as the calibration standards. Each sample was analyzed in triplicate.

Anaerobic activity tests were performed in glass bottles of 2.1L. 400 ml of initial anaerobic sludge were fed with pet food at an S/X ratio of 1 g COD/g VSS Bicarbonate, macro and micronutrients were also added according to Angelidaki et al. [109]. After removing O_2 with N_2, the samples were incubated at 35°C in a temperature controlled room, and softly agitated in a Wheaton roller culture apparatus. Biogas production was monitored by a digital pressure sensor throughout the assay. A blank sample with the initial anaerobic sludge was prepared. The assays were performed in duplicate and the biogas production of blank assays without substrate was subtracted from the fed assay. The methane concentration was determined with a multi-gas measuring device, mobile MULTITEC 545 (Sewerin).

Analyses of Total Suspended Solids (TSS) and Volatile Suspended Solids (VSS) were completed in accordance with the protocols described in the Standard Methods for the Examination of Water and Wastewater [108]. PSD was obtained using a Mastersizer 2000 (Malvern Instruments) coupled to a Hydro 2000SM with a detection range of 0.02–2000 µm.

4.2.4 Membrane cleaning

The cleaning of both membranes was performed sequentially under increasingly strong conditions. The cleaning protocol was divided into 4 steps: physical rinsing with tap water, chemical rinsing with diluted sodium hypochlorite, 100 mg/L of NaClO, oxidizing cleaning with 500 mg/L of NaClO, and acid cleaning with 100 mg/L of oxalic acid. The length of each step was 2 hours during which filtration and backwash resistances were measured. After each cleaning stage the membranes were rinsed with tap water to remove detached materials. The efficiency of each cleaning step was evaluated on the basis of the total and backwashing resistances at the end of the stage, before the removal of the detached solids with tap water [135].

4.3 Results and Discussion

4.3.1 Particle size distribution

Fig. 16 shows the PSD of the initial anaerobic sludge, and the PSD of the samples taken on days 1 and 7 from the eM tank (a), and from the sM tank (b). In the case of eM, the PSD of a sample taken from the outlet of the pump after 1hour of operation is also represented.

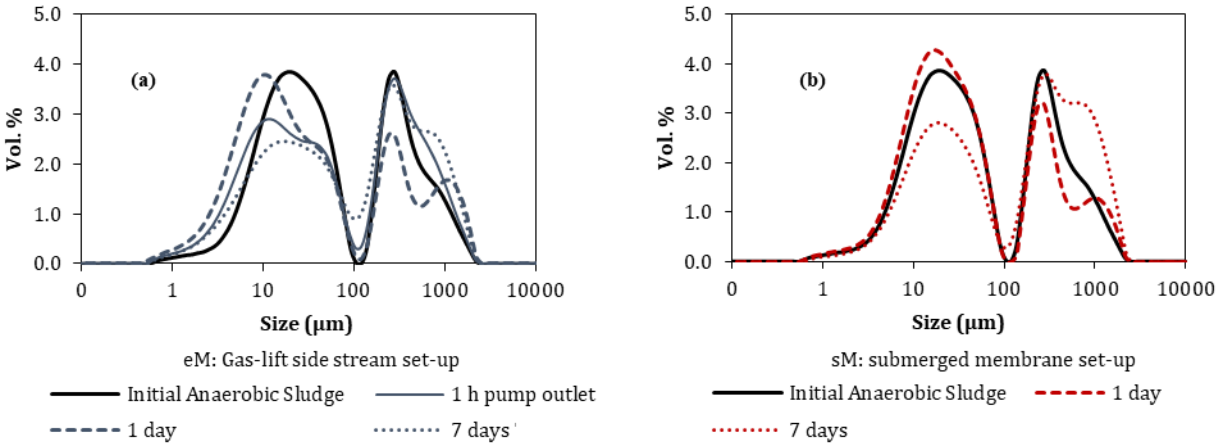

Fig. 16. Particle size distribution of the initial anaerobic sludge and (a) samples taken from the gas-lift side-stream membrane set-up and (b) from the submerged membrane tank.

The PSD of the initial anaerobic sludge shows a bimodal curve with central peaks at 20 µm and 120 µm. This type of distribution is maintained throughout the whole experience in both membrane set-ups with decreasing percentages of the larger size particles in favor of the smaller ones.

The difference in the concentration of particles of around 100 µm between eM and sM is noticeable. 100 µm particles were neither found in the initial anaerobic sludge nor in the samples taken from the sM tank, and the presence of those particles in the eM tank was clear evidence of the breakup of the larger particles when using the side-stream configuration. However, with regard to membrane fouling, the smallest particles had a higher contribution in the fouling process [124,136–139], because their back-transport from the membrane is less effective and they form a less porous cake [140], and it is therefore of greater importance to highlight the different size distributions of the particles smaller than 100 µm.

With the aim of specifically determining the behavior of the particles with the highest impact on the fouling process, particles larger than 100 μm were excluded in the PSD analysis. To that end, the cumulative volume of particles under d_p in the 0-100 μm interval, were recalculated as:

$$Vol.\%\ under\ d_{p[0-100]} = \frac{\sum_0^{d_p}(Vol.\%)_d}{\sum_0^{100}(Vol.\%)_d} \cdot 100 \quad (26)$$

where, $\sum_0^{d_p}(Vol.\%)_d$ is the cumulative volume of particles under d_p and $\sum_0^{100}(Vol.\%)_d$ is the cumulative volume of particles under 100 μm.

Fig. 17 presents the cumulative volume curves of the initial anaerobic sludge, and samples taken on the days 1 and 7 in both the eM and the sM tanks. It is worth noting that the cumulative curve of particles under 100 μm in the sM tank after 7 days practically matched the initial value. However, the cumulative curve of the sludge was notably altered in the eM tank. A significant increase in the fine particles in the eM tank was observed; for instance, the percentage of particles smaller than 10 μm increased from 25.1% to 34.6% within only 24 hours and to 44.8% after 7 days, while the increase in the sM tank (negligible on the first day, not represented) reached only 31.5% on day 7. These results indicated that the hydrodynamic conditions in the eM set-up had promoted a sharp increase in the breakup rate of the anaerobic biomass over time that was barely observable in the sM set-up. The breakage of particles has already been reported as a consequence of shear stress [53,125,130,141,142], which is higher in the external AnMBRs, because the sludge recirculation required to maintain an adequate crossflow velocity. Jeison et al. [4] highlighted the need to establish the recirculation rate under which surface shear would be enhanced, but avoiding exposure of the sludge to shear stress levels that could reduce the size of the flocs and even induce cell disruption.

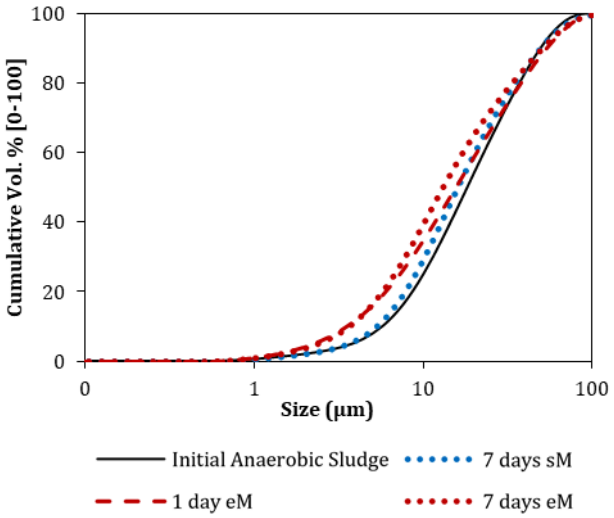

Fig. 17. Cumulative volume of particles under 100 µm of initial anaerobic sludge, after 1 day in the external membrane set-up and after 7 days in both set-ups.

4.3.2 EPS development

LB-EPS and SMP were analyzed from initial anaerobic sludge and samples from the filtration set-ups on day 7. PN, PS, and HS were also analyzed in the permeate samples after 1 hour and on day 7. The membrane rejection of SMP was calculated from the concentration of SMP in the initial sludge and in the permeate samples and is summarized in Table 4.

Table 4. PN, PS, and HS content in LB-EPS, SMP, SMP in permeate and percentage of retention of SMP in eM and sM at day 0, after 1 hour and after 7 days.

Set-up	Parameter	Time (days)	LB-EPS (mg/g VSS)	SMP (mg/L)	$SMP_{PERMEATE}$ (mg/L)	Retention (%)
eM		Initial sludge	5.62 ± 0.03	25.0 ± 1.0		
	PN	1 hour			10.6 ± 0.8	57 ± 4
		7 days	6.62 ± 0.09	42.4 ± 1.0	4.9 ± 1.3	88 ± 3
		Initial sludge	5.00 ± 2.51	31.1 ± 0.9		
	PS	1 hour			23.7 ± 0.4	24 ± 3
		7 days	5.53 ± 0.12	59.5 ± 3.1	30.3 ± 0.4	49 ± 2
		Initial sludge	18.88 ± 0.53	183.0 ± 2.0		
	HS	1 hour			63.1 ± 2.4	66 ± 1
		7 days	2.00 ± 0.21	151.1 ± 13.6	88.6 ± 8.9	41 ± 10
sM		Initial sludge	5.62 ± 0.03	25.0 ± 1.0		
	PN	1 hour			12.5 ± 0.1	50 ± 2
		7 days	6.64 ± 0.03	35.4 ± 1.1	10.6 ± 0.5	70 ± 2
		Initial sludge	5.00 ± 2.51	31.1 ± 0.9		
	PS	1 hour			23.1 ± 0.2	26 ± 2
		7 days	6.26 ± 0.26	43.3 ± 1.4	23.8 ± 4.8	45 ± 9
		Initial sludge	18.88 ± 0.53	183.0 ± 2.0		
	HS	1 hour			77.3 ± 3.6	58 ± 2
		7 days	1.79 ± 0.21	145.3 ± 9.3	105.9 ± 11.3	27 ± 11

The LB-EPS behavior was similar in both the eM and the sM set-ups, meaning that no significant difference in LB-EPS behavior were induced by differences in the hydrodynamic conditions. Loosely bound PN and PS remained constant or slightly increased, however loosely bound HS significantly decreased by 89% in the eM set-up and by 91% in the sM, due to its release in the liquid phase, which also increased the levels of HS in the permeate.

With regard to SMP in the sludge, soluble PN and PS increased significantly in both set-ups on day 7. However, the prevalent SMP, HS, decreased from 183.0 mg/L in the initial anaerobic sludge to 151.1 mg/L and 145.3 mg/L in the eM and sM, respectively. The concentration of the three compounds was higher in the eM than in the sM set-up, with a more significant difference for PN than for PS, which brings new evidence of the difference between HS versus PN and PS

behavior. The higher increase in soluble PN and PS in the eM sludge indicated that the shear stress imposed on the biomass could have caused the release of microbial polymeric substances. Yu et al. [143] observed an increase of soluble COD in the sludge of an AnMBR as a consequence of SMP release, due to shear forces caused by a crossflow velocity of 1.0 m/s. Xiong et al. [144] detected a significant increase in PN and PS concentrations in the soluble EPS of an AnMBR fed with synthetic wastewater, however they attributed it to accumulation in the retentate of higher molecular weight SMP produced in the microbial process.

It was found that PN was always higher than PS rejection, which is probably explained by the higher propensity of PN than PS to attach to the membrane surface, due to electrostatic interactions with the polymeric membrane [145]. PN and PS rejection rates were higher over time. The increased retention of PN and PS was also observed by Chen et al. [92] who assumed that the TMP increase, due to the fouling, enhanced SMP retention by the cake layer, which might explain why SMP rejection was higher in the eM.

The HS in the permeate showed an unexpected behavior over time. The HS rejection decreased on day 7, from 66% to 41% in the eM set-up and from 58% to 27% in the sM set-up. Two phenomena could explain these results, on the one hand the above-mentioned loosely-bound HS release, and on the other hand the likely breakdown of the HS complex molecules that made possible its permeation.

Chen et al. [92] on the contrary, when comparing submerged and external granular AnMBR, reported fewer microbial products, better biomass granule quality, and less fouling propensity in the external AnMBR. However, it should be considered that these authors compared a membrane submerged in the mixed liquor with an external membrane fed with the biomass-free effluent of an upflow anaerobic granular bioreactor.

4.3.3 Membrane fouling

Fouling development was very different in the eM and the sM filtration set-ups. Under the same filtration conditions, fouling of the gas-lift side-stream set-up was faster and higher than that of the submerged membrane set-up. Fig. 18 shows the behavior of filtration and backwashing resistance of (a) the eM and (b) the sM. The eM filtration resistance quickly increased reaching a value of $9.3\pm0.6\times10^{12}m^{-1}$ in just 7 days. The most pronounced fouling appeared on days 3 and 4, in which the TMP exceeded 300 mbar. At that point, the filtration pump flow control system was unable to maintain the desired flux rate, which decreased throughout each cycle from 15 $L/m^2\cdot h$ to values around 12 $L/m^2\cdot h$, reducing the fouling rate and increasing the resistance data dispersion. The fouling rate of sM under the same conditions was notably lower than the eM, reaching, over the same period, a resistance of 1.1×10^{12} m^{-1}, so that between day 7 and 10 the flow rose to 20 $L/m^2\cdot h$, thereafter increasing to 25 $L/m^2\cdot h$. Under those conditions, the fouling rate was significantly higher and the filtration resistance reached $3.6\pm0.2\times10^{12}$ m^{-1} on day 12, clearly lower than the eM resistance.

The irreversible increase in resistance over the filtered volume per unit of area, $(dR/dV)_{irr}$, rose rapidly from 1.4×10^{12} m^{-2} to 11.5×10^{12} m^{-2} during the first four days of eM operation. During the same period, the irreversible fouling rate in the sM was held between 0.3 and 0.8 $\times10^{12}$ m^{-2}. The $(dR/dV)_{irr}$ in the sM increased with the flux, however it remained below 1.2 $\times10^{12}$ m^{-2} at 25 $L/m^2\cdot h$.

The development of the backwash resistance, R_{bw}, related to irreversible fouling by pore-blocking [85], followed the same pattern as for filtration resistance. Starting with similar backwashing resistances, 0.5×10^{12} m^{-1} and 0.3×10^{12} m^{-1} for the eM and the sM, respectively, the increase in R_{bw} for eM was notably higher than for sM, up to $3.3\pm0.4\times10^{12}$ m^{-1} for the first one and only $1.4\pm0.1\times10^{12}$ m^{-1} for the second one, despite higher operating fluxes.

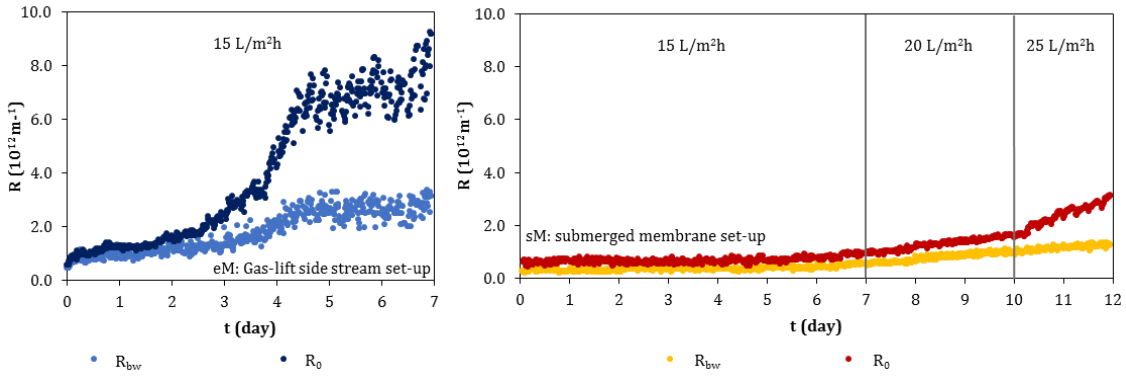

(a) (b)

Fig. 18. Filtration and backwash resistance behavior: (a) external; and, (b) submerged membrane.

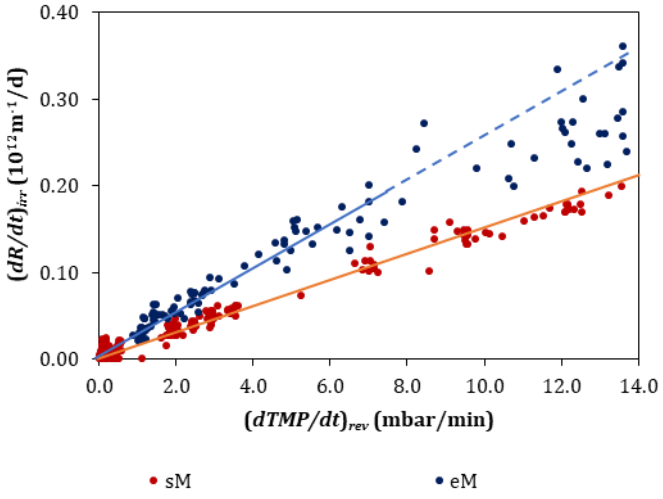

Fig. 19. Development of irreversible fouling, dR/dt, with regard to reversible fouling, dTMP/dt, in the external and in the submerged membranes.

Fig. 19 shows the irreversible fouling rate $(dR/dt)_{irr}$ versus the reversible fouling rate $(dTMP/dt)_{rev}$. A quasilinear relationship between both fouling rates can be observed, with proportionality constants of 0.027 and 0.014×10^{12} $m^{-1}\cdot min/(mbar\cdot d)$, for both the eM and the sM, respectively. The eM worked in a stable manner with a reversible fouling rate of up to 7 mbar/min. The flow control problems that took place from day 4 explain the data dispersion for the highest reversible fouling rate. The sM operated without any difficulty with a reversible fouling rate of up to 14 mbar/min, reaching an irreversible fouling rate of 0.2×10^{12} m^{-1} d^{-1}.

Ersahin et al. [130] using dynamic membrane AnMBRs equipped with flat sheet membrane modules operating in gas-lift mode, observed that filtration resistance in the eAnMBR was lower than in the sAnMBR. Nevertheless, as the authors indicated, the observed differences could be due to the gas diffusers in the sAnMBR that were placed inside the mixed liquor, which implied a lower efficiency of the gas bubbles in the control of the dynamic membrane thickness.

Stricot et. al. [146] studied the impact of hydrodynamic stress on sludge in two different side-stream MBRs, demonstrating that high shear stresses associated with a crossflow velocity induced significant modifications of the sludge, floc breakage, and release of polymeric substances, which increased its fouling potential drastically from 5×10^{14} m^{-2} to 50×10^{14} m^{-2}.

Choo and Lee [138], during a continuous long-term experiment with an anaerobic bioreactor coupled to a plate and frame membrane by a gear-type pump, also observed that the permeation flux dropped sharply from 100 $L/m^2\cdot h$ to 10 $L/m^2\cdot h$ within less than 20 days.

4.3.4 Physical and chemical cleaning

The cleaning efficiency as the membrane fouling behavior could be influenced by operating conditions [147]. A comparative study of physical and chemical cleaning processes on both membrane set-ups, was performed, determining the efficiency of a series of cleaning steps: rinsing with tap water, and chemical cleaning with sodium hypochlorite solutions of 100 and 500 mg/L, and an oxalic acid of 100 mg $H_2C_2O_4$/L. Table 5**¡Error! No se encuentra el origen de la referencia.** summarizes the filtration and backwash resistances values at the end of each cleaning step for both membranes.

Table 5. Initial resistance, R_0, and backwash resistance, R_{bw}, at the end of each cleaning step for both membranes.

Cleaning step	eM		sM	
	$\mathbf{R_0}$ (10^{12} m^{-1})	$\mathbf{R_{bw}}$ (10^{12} m^{-1})	$\mathbf{R_0}$ (10^{12} m^{-1})	$\mathbf{R_{bw}}$ (10^{12} m^{-1})
Initial conditions	7.4	3.3	3.6	1.3
Tap water	6.9	3.3	1.4	0.9
NaClO (100 mg/L)	2.7	1.9	1.1	0.6
NaClO (500 mg/L)	1.6	1.6	0.6	0.6
$H_2C_2O_4$ (100 mg/L)	0.8	0.5	0.6	0.3

Given that, as stated in the preceding section, the fouling of the eM was worse than the fouling of the sM, the resistances of both membranes were not initially equal. It is worth highlighting the different resistances to backwash, which were 3.3 and 1.3×10^{12} m^{-1}, for the eM and the sM, respectively, suggesting that the effectiveness of the cleaning stages might also foreseeably be different, because of their relation with the internal fouling of the membrane [85].

Rinsing the eM with tap water showed a very low efficiency, under 7% of the filtration resistance and without any effect on backwash resistance. On the contrary, rinsing the sM with tap water reduced its resistance to around 60% in the filtering stage and to 36% in the backwash stage.

This difference might be related to the degree of consolidation of the fouling layer [142]. The TMP of almost 300 mbar that was reached in the eM consolidated the fouling layer by compression, which reduced the effectiveness of the rinsing. On the contrary, operating at under 50 mbar, a relaxed fouling layer was maintained in the sM, which facilitated its elimination in the rinsing stage.

Cleaning with low concentrations of NaClO, 100 mg/L can be considered as a form of "chemical rinsing", which permits the foulants to be removed from the system. The low concentration of NaClO enable the withdrawal of the detached foulants avoiding the higher membrane fouling potential of the sludge exposed to NaClO [148]. In this way, the effectiveness of the subsequent stages was increased, in which the cleaning agent detached the materials that adhered most firmly to the membrane.

Chemical rinsing permitted the removal of over 60% of the eM resistance, both in filtration and in backwash, although its effectiveness was lower in the sM, due to the weakly attached materials that could be removed by rinsing with tap water.

The oxidizing cleaning with 500 mg/L NaClO was capable of eliminating over 40% of the resistance to filtration from both membranes. Finally, an acid-based cleaner with 100 mg/L of oxalic acid was used. The sM practically recovered its initial permeability with the acid cleaning, however, the eM never recovered its original resistance to filtration, 0.5×10^{12} m^{-1}, staying at 0.8×10^{12} m^{-1}. The cause of the different behaviors of both membranes through the chemical cleaning stages has to be looked for in the different chemical compositions both of the caked layer and of the materials that caused the pore blocking, which in the final analysis was a consequence of the shear stress to which the biomass of the eM was subjected.

4.3.5 Biomass concentration and methanogenic activity

Samples from the initial anaerobic sludge were taken after 1 day and 7 days from both experimental set-ups for methanogenic activity control.

Specific methanogenic activity was barely affected by shear stress, remaining at values of 11.5±0.5 ml CH_4/g VSS·d in the eAnMBR and at values of 12.3±0.6 ml CH_4/g VSS·d in the sAnMBR. However, a decrease was observed in mixed liquor VSS in the eM tank over time, from 3.3 g VSS/L in the initial anaerobic sludge, to 2.8 g VSS/L within 1 day and to 1.2 g VSS/L within 7 days, a period in which VSS concentration only decreased to 2.7 g VSS/L in the sM tank.

Beaubien et al. [149] demonstrated that the high shear rates generated by the circulation pump in a side-stream anaerobic reactor were not detrimental to methanogens that maintained their specific methanogenic activity. Jeison et al. [4] operating a side-stream thermophilic AnMBR also observed a biomass concentration decrease, although lower, from 17 g VSS/L to 15.3 g VSS/L that was attributed to the low apparent yield of thermophilic anaerobic sludge and the washout of active thermophilic microorganisms. Ersahin et al. [130] comparing side stream and submerged anaerobic dynamic membrane configurations, detected less biogas production and less methane concentration in biogas for eAnMBR, however, those same authors also observed a decrease in methanogenic activity of 25% from 0.20 g CH_4-COD/g VS·d in sAnMBR to 0.15 g CH_4-COD/g VS·d in eAnMBR. It may be noted that both authors determined the activity from the concentration of Volatile Solids (VS), so no solid breakdown can eventually be corrected, while methanogenic activity in this work was determined on the basis of the suspended fraction.

Choo and Lee [138] observed an increase in supernatant turbidity and a decrease in biomass from 3000 mg VSS/L to 300 mgVSS/L in an anaerobic bioreactor coupled to a UF membrane when a gear-type recycling pump was used for a CFV between 0.67-0.95 m/s, and from 2410 mgVSS/L to 920 mgVSS/L for a lower mechanical shear pump (mono-pump) and 0.5 m/s in sludge velocity. The authors attributed their findings to cell lysis caused by mechanical shear stress and biomass displacement from the bioreactor onto the membrane surface.

4.4 Conclusions

Two filtration set-ups respectively equipped with an external tubular membrane and a submerged hollow-fiber membrane, fed with anaerobic sludge, were simultaneously operated to discern the effects of the hydrodynamic conditions on the characteristics of the sludge and on the fouling of the membranes.

Operating the external membrane set-up with gas sparging and low crossflow, the shear stress observed in a series of batch assays has been shown to cause a reduction in the particle size, increasing the concentration of the particles under 10 µm, from 25.1% to 34.6%, within only one day.

After 7 days, the concentrations of soluble proteins and polysaccharides in the sludge were 20% and 37%, respectively, greater in the external than in the submerged membrane set-up. The degree of polysaccharide retention was similar in both membranes, however, the retention of proteins and humic substsances was notably greater in the external membrane.

The concentration of anaerobic sludge in the eM tank was reduced from 3.3 g VSS/L to 1.2 g VSS/L, over 7 days, but the specific methanogenic activity remained nearly constant.

By operating both set-ups under the same filtration cycle (15 minutes), flux (15 $L/m^2 \cdot h$), SGD_m (1.2±0.1 $Nm^3/m^2 \cdot h$), and at a CFV of 0.51 m/s for the external membrane, filtration resistance after 7 days reached 9.3×10^{12} m^{-1} in the eM and 1.1×10^{12} m^{-1} in the sM. The irreversible fouling rate on the filtered volume basis reached 11.5×10^{12} m^{-2} in the eM, in so far as the irreversible fouling rate of the sM was maintained at 0.3×10^{12} m^{-2}, which increased to 1.2×10^{12} m^{-2} when the flux was raised to 25 $L/m^2 \cdot h$.

The effectiveness of the membrane cleaning processes was also different. Rinsing with tap water followed by chemical rinsing of the sM with 100 mg/L of NaClO decreased the resistance to filtration to 1.1×10^{12} m^{-1}. Under the same conditions, the resistance of the eM remained at 2.7×10^{12} m^{-1} and a chemical cleaning with 500 mg/L of NaClO was insufficient to recover its original permeability.

Capítulo 5: Influence of flux, backwash intensity, gas sparging and cross flow velocity on ultrafiltration performance of anaerobic sludge in submerged and external membranes

5.1 Introduction

Membrane bioreactors combine either biological aerobic (MBR) or anaerobic (AnMBR) degradation processes of organic matter with complete physical sludge retention of biomass by either microfiltration or ultrafiltration, preventing biomass losses and improving organic matter removal and effluent quality. As the filtration progresses, membrane fouling by accumulation of materials on the membrane surface and concentration polarization reduces membrane permeability, increasing operating, maintenance, and replacement costs.[69,150–152] Depending on the attachment strength of the foulant materials, fouling may be considered as reversible or irreversible. Reversible fouling can be easily removed by simple physical processes such as gas sparging, relaxation, or backwashing, while irreversible fouling requires more intensive cleaning processes, including the use of chemical agents.[85]

The main factors affecting membrane fouling are membrane configuration, operating conditions and biomass properties.[69,137,153] The type and configuration of the membranes have an important impact on their fouling. Andrade et al.[90] studied two membrane bioreactors equipped with submerged hollow fiber modules for the treatment of dairy wastewater. In one of them, the membrane module was submerged in the main biological tank. In the other, the module was submerged in a side-stream tank in series, with recirculation pumps ensuring recirculation to the main biological tank. The authors observed that shear stress provoked by recirculation led to the breakdown of the biomass that significantly reduced the concentration of mixed liquor suspended solids, improving the performance, in terms of fouling, of the side-stream arrangement of the hollow fiber membrane. Martínez et al.[154] compared fouling related issues in a tubular membrane and a hollow fiber membrane commonly employed in side-stream and submerged membrane bioreactors. They also found a decrease in suspended solids concentration, due to shear stress. However, the EPS release and the increase in concentration of fine particles contributed to severe fouling of the external membrane.

Proper control of the operating conditions will lessen fouling and will improve the economic balance of MBRs.[123] Due to the complexity of fouling processes, it is frequent to use sub-optimal operational conditions based either on conservative recommendations from the membrane manufacturer or according to operator experience and risk avoidance criteria.[104] Conservative criteria negatively impacts on capital costs but should not be undervalued, specially at the lowest flow plant, where labour costs contribute up to 63% of the total operating expenditure in submerged MBR and 79% in side-stream MBR, and therefore, process robustness is likely to be as cost effective as process productivity.[155] Zsirai et al.[102] studied the effect of backflushing, relaxation, and chemically enhanced backwashing on permeability decline and recovery in a submerged hollow fiber membrane module. They observed that, for the same backwash volume, the backwash flux was slightly more efficient than the backwash duration. Regarding chemically enhanced backwashing, the authors observed that it was not effective for long-term operation under unfavorable filtration conditions: flux higher than 35 $L/m^2 \cdot h$ and air sparging of only 0.25 $Nm^3/m^2 \cdot h$.

Filtration, backwash flux, relaxation, and air sparging flow are used for both fouling control and to minimize energy consumption. Monclús et al.[156] applied a control system for daily regulation of air sparging flow from short-term and long-term permeability slopes, determined at 4 and 14 days, respectively. The system was validated at full-scale reaching a maximum energy saving of 22% without modifying its fouling rate trend. Villaroel et al.[157] likewise improved the performance and permeate productivity of a pilot scale MBR equipped with a hollow fiber membrane, by automatically adjusting the relaxation and backwash frequency, based on a pre-selected TMP set-point between 280 and 360 mbar, to minimize the residual fouling resistance. The initiation of backwashing regulated by a TMP set-point has been used to manage peak flux conditions in MBR treating municipal wastewater.[158] The adjust of the filtration duration according to the degree of membrane fouling permitted increasing the process productivity maintaining sustainable operation at high peak flux for peak periods up to 6 h. The combination of a TMP set-point for backwash initiation and intermittent gas sparging further improved the

process productivity by increasing filtration cycle duration as well as reduced gas consumption more than 75% with respect to the continuous gas-sparging mode.[159]

Mathematical fouling-process models were applied to the optimization of operating conditions of membrane bioreactors. Amini *et al.*[160] used computational fluid dynamics to model the three phase turbulence, considering gas, mixed liquor, and biomass as the solid phase, to predict the membrane fouling resistance. Kim *et al.*[161] proposed a mechanistic fouling model by combining four well known fouling mechanisms: complete blocking, intermediate blocking, cake filtration, and standard blocking mechanisms. They demonstrated that the combined model predicted the fouling evolution of a pilot-scale MBR more accurately than single mechanistic fouling models. Li and Wang[81] developed a mathematical model to determine the pressure increase on the basis of filtrated volume per unit of area, using a potential equation of the main operating variables: filtration flux, aeration intensity, sludge concentration, and sludge stickiness. The model parameters were selected based on laboratory test but also on previous reported data and some other assumptions. The simulated results showed that membrane fouling was mainly affected by filtration flux, followed by aeration intensity and sludge concentration. Wu et al.[162] modified the aforementioned model, to include the effect of colloidal and soluble components and solids of different floc size distribution, which revealed a detailed cake structure, including the spatial distribution of cake porosity, the specific cake resistance, and the synergistic interactions among major fouling factors. The main limitation of these models for their widespread application is the calibration of model parameters, including the density of deposited soluble, colloidal components and suspended solids within the layer, as well as online analysis of particle size distribution for real-time prediction of membrane fouling.

The main parameters governing fouling behavior have also been analyzed using statistical methods. Factorial experimental designs require a high number of experiments, particularly p^k for determining the effect of k variables at p levels. Yi et al.[163] studied flux decline during the filtration of synthetic wastewater with an ultrafiltration membrane in a dead end stirred filtration cell. They applied factorial design for 4 variables with 2 levels: pH, total dissolved solids,

concentrations of anionic polyacrylamide and transmembrane pressure, to study membrane fouling, showing how factorial analysis is a powerful tool for gaining an understanding of the influence of the main variables and their interactions, identifying the most influential ones and determining their optimum values. Schoeberl et al.[164] used a 2^3 factorial design to study the influence of filtration and backwashing duration and specific air demand on the irreversible fouling rate in an MBR equipped with a submerged membrane. Akhondi et al.[165] applied a Taguchi experimental design method for the optimization of filtration performance and energy consumption of a hollow fiber membrane filtering a baker's yeast suspension as the model foulant. Five parameters with four levels were investigated: filtration flux, feed concentration, backwash duration, backwash strength, and aeration rate during backwash. They highlighted that the application of the Taguchi experimental design was an effective approach for such exhaustive investigation by reducing the number of factorial combinations, to only 16 experiments. Taguchi experimental design greatly reduces cost and time constraints, however it requires guess work, before any experimental results, to find the variable combinations with a greater likelihood of significativeness.

Box-Behnken experimental design (BBD) notably reduces the required number of experiments of the factorial design, by dividing the experimental range of each variable into three levels: low-level (−1), middle-level (0) and high-level (+1), and selecting only those experiments that combine two extreme levels.[106] In this way, the number of runs to study the effect of a process involving 3 variables is reduced to 15, and for 4 variables to only 27 runs, instead of 27 and 81, respectively. Zhang *et al.*[166] used a Box-Behnken experimental design to study the effect feed flow rate, transmembrane pressure and rotating speed of three types of ultrafiltration membranes to select the optimal hydraulic conditions in a shear-enhanced membrane system for dairy wastewater treatment. They obtained regression coefficients R^2 between 0.904 and 0.988 for the polynomial regression of the studied responses: average flux, flux decline, permeability index, chemical oxygen demand, total protein, turbidity, conductivity, and pH.

Raffin et al.[107] used the BBD for optimization of the operating conditions of an integrated filtration demonstration plant, composed of a microfiltration membrane followed by a reverse osmosis membrane, constructed to study its applicability for indirect potable reuse. On the one hand, they studied the effects of flux, backwash frequency, chloramine dose, and the point where the cleaning reagent was added on fouling propensity in the microfiltration membrane unit and, on the other hand, flux, recovery, pH and anti-scalant dosages in the osmosis reverse membrane unit. They observed that, in the studied experimental range, backwash frequency and flux were the parameters with most influence on microfiltration membrane fouling propensity, whereas pH and recovery were the controlling factors of fouling rate in the reverse osmosis membrane. BBD was also used to optimize membrane cleaning processes. Raffin et al.[105] conducted a bench scale study of different chemical cleaning protocols and their effects on the permeability recovery of a hollow fiber membrane, including three cleaning reagents at different concentrations, cleaning temperatures, and soaking times. They observed that the variables under study showed synergic effects and that the cleaning method has to be optimized for each installation and application. They also highlighted the benefit offered by BBD as a robust and time-efficient method for the required optimization with the fewest number of experiments.

Obtaining representative results for long-term irreversible fouling rate from mid-term experimental assays is a challenge in membrane bioreactors field. The aim of this work is therefore to study reversible and irreversible fouling rates in submerged and side-stream membranes, in gas-lift configuration, by evaluating the effect of filtration and backwash flux, filtration and backwash duration, specific gas demand and, in the case of external membrane, the crossflow velocity. A BBD implemented in the control system of the experimental set-ups will be used, to reduce the number of assays and the duration of the experiment and to avoid sludge alteration throughout the study.

5.2 Materials and methods

5.2.1 Experimental set-ups

Two filtration set-ups with two different types of ultrafiltration membranes were used. One was equipped with an external tubular membrane operated in gas lift mode and the other with a submerged hollow fiber membrane, referred to as “external membrane” (E) and “submerged membrane” (S), respectively. Further details about the set-ups may be found elsewhere.[154]

Anaerobic sludge from an industrial anaerobic digester treating food waste (Ecoalia Group, Burgos, Spain) was used. Once in the laboratory, the sludge samples were not fed until the daily biogas production was negligible. The sludge, free of biodegradable organic matter, was diluted to a concentration of 4.0 g TSS/L with effluent from an AnMBR pilot plant treating slaughterhouse wastewater (Campofrio Food Group, Burgos, Spain).

The membranes were cleaned following a three-step protocol, using consecutively 100 mg/L and 500 mg/L of sodium hypochlorite solutions and 100 mg/L of oxalic acid. Then the membranes were conditioned with the sludge during 24 h under gentle filtration conditions, with filtration and backwash fluxes of 8 and 14 $L/m^2 \cdot h$ for the external membrane, and 12 and 18 $L/m^2 \cdot h$, for the submerged one, with filtration cycles of 10 minutes with 30 seconds for backwashing. Then the BBD started with the same sludge. The aim of the conditioning period was to exclude the transitory stage of biofouling during the initial deposition of anaerobes and prevent any rapid increase in fouling over the course of the first hours of filtration, after the membrane cleaning,[56,102,167] which might corrupt the fouling rate determination of the first runs of the experimental design. Schoeberl et al.[164] needed to eliminate the abrupt rise in total resistance, observed at the very beginning of filtration, in order to obtain comparable and reliable results of irreversible fouling rates, during the first day after the chemical cleaning of the membrane when the increase in resistance was clearly faster than the linear behavior that followed.

The operating conditions of the BBD were programmed in an Arduino-based PLC (M-Duino 42, Industrial Shields) connected to a PC for real-time monitoring, online determination of reversible fouling rates, and remote control. The BBD is a complement of the basic control program of an AnMBR pilot plant, with the possibility of selecting the operating conditions and their levels to perform the BBD with a minimal change to bioreactor performance, depending only on the level that is selected.

5.2.2 Reversible and irreversible fouling

Since the filtration assays were performed at room temperature, before determining fouling rates, transmembrane pressure fluctuations due to temperature differences were corrected, by means of Eq.27, normalizing them at a reference temperature of 30ºC:

$$TMP = TMP_T \frac{\mu}{\mu_T} \quad (27)$$

where, TMP is the normalized transmembrane pressure at the reference temperature (Pa), μ is the permeate viscosity at that temperature (Pa·s), TMP_T is the observed transmembrane pressure at the operating temperature, T (ºC), measured in the permeate line, and, μ_T is the permeate viscosity at the same temperature, approximately represented by the viscosity of water, determined by Eq. 28:[134]

$$\mu_T = \frac{0.497}{(42.5 + T)^{1.5}} \quad (28)$$

Fig. 20 shows graphically the determination of the reversible fouling rate $(dTMP/dt)_{rev}$, the transmembrane pressure at the beginning of the filtration period, TMP_0, and the irreversible fouling rate in transmembrane pressure terms, $(dTMP_0/dt)_{irr}$, determined from the increase of TMP_0 throughout the experimental run. Schoeberl et al. [164] suggested a minimum filtration time of 7 days, in order to obtain good linear fits ($R^2 = 0.92$) when determining the irreversible fouling rate from the increase of resistance over time, although such long periods of time can

hardly be used to perform 15-28 runs using unaltered biomass. Zsirai et al.[168] calculated the irreversible fouling rate through a linear-regression of TMP_0 data monitored during the 15-hour filtration cycles, assuming that it offered useful qualitative and comparative trends of the extrapolated fouling behavior, even though mid-term determination might overestimate the irreversible fouling rate. Calculation of the fouling rate determinations, TMP_0, $(dTMP/dt)_{rev}$, and $(dTMP_0/dt)_{irr}$, was improved through the use of robust linear regressions using Huber's method, so that the TMP outliers associated with bubbling and, in general, system heterogeneity, contaminated the slope and intercept estimations of the least squares regression. Huber's tuning constant was fixed at 1.345 according to the 95% asymptotic efficiency rule.[169]

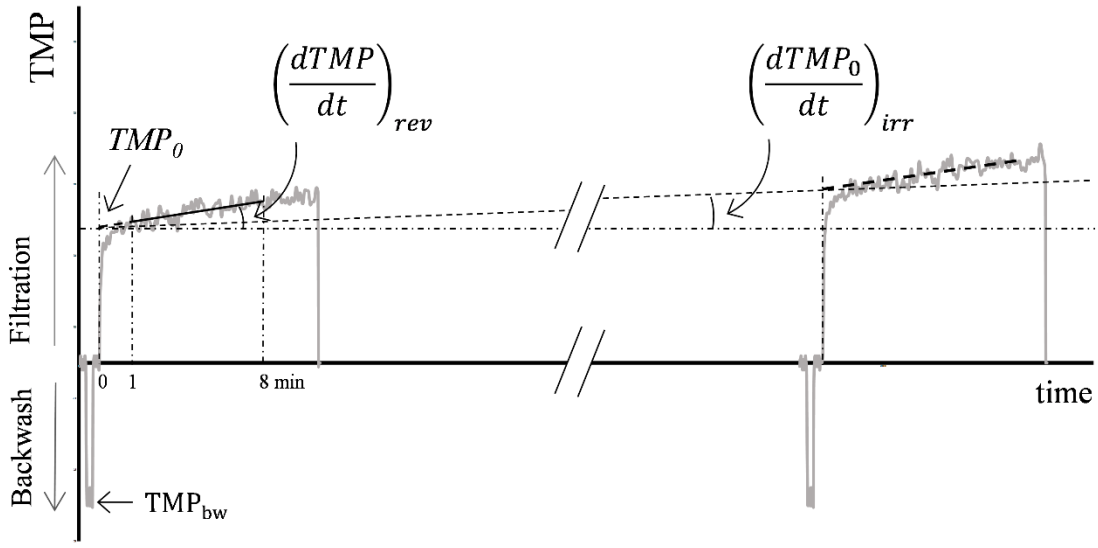

Fig. 20. Normalized TMP profile at the reference temperature, where TMP_0 is TMP at the beginning of filtration; TMP_{bw} is TMP during backwashing; reversible fouling is the TMP slope during a filtration step, $(dTMP/dt)_{rev}$; and, irreversible fouling is the TMP_0 slope throughout the experimental run $(dTMP_0/dt)_{irr}$.

The resistance at the beginning of the filtration stage, R_0 (m^{-1}) was determined by Darcy's law, Eq. 29:

$$R_0 = \frac{TMP_0}{J_f \cdot \mu} \tag{29}$$

where, J_f is the filtration flux ($m^3 \cdot m^{-2} \cdot s^{-1}$). The irreversible fouling rate was calculated in terms of resistance and on the basis of the net production of permeate per unit of membrane surface

area, to take into account the different membrane production levels, depending on the flux and on the duration of filtration and backwashing. The irreversible fouling rate on transmembrane pressure terms $(dTMP_0/dt)_{irr}$ (Pa·s^{-1}), was recalculated in resistance terms $(dR_0/dt)_{irr}$ (m^{-1}·s^{-1}) with Eq. 30. The irreversible increase in resistance over the net production of permeate per unit of membrane surface area, $(dR_0/dv)_{irr}$ (m^{-2}) was determined (Eq.31) from the net flux, J_{net}, (m^3 m^{-2}·s^{-1}) calculated with Eq. 32:

$$\left(\frac{dR_0}{dt}\right)_{irr} = \left(\frac{dTMP_0}{dt}\right)\frac{1}{\mu \cdot J_f} \tag{30}$$

$$\left(\frac{dR_0}{dv}\right)_{irr} = \frac{(dR_0/dt)_{irr}}{J_{net}} \tag{31}$$

$$J_{net} = \frac{J_f \cdot t_f - J_{bw} \cdot t_{bw}}{t_c} \tag{32}$$

where, v is the net filtrated volume per unit of membrane surface area (m^3 m^{-2}); t_f is the duration of filtration (s); J_{bw} is the backwash flux (m^3 m^{-2}·s^{-1}); t_{bw} is the duration of backwash (s); and, t_c is the duration of the entire filtration cycle (s) composed of both the filtration and the backwash stages, and two relaxation steps with a 30 s interval between each one.

5.2.3 Box-Behnken experimental design

Four BBDs were used to evaluate the effect of filtration and backwash flux, the duration of the filtration and the backwash steps, specific gas demand (SGD), and, in the case of the external membrane, the crossflow velocity (CFV), on both the reversible and the irreversible fouling rates. In the experimental designs labelled 'A', the variables t_c, J_f, and SGD were studied in both membranes, and CFV was also studied in the external membrane. In the experimental designs labelled 'B', the operating conditions directly related to backwash, t_c, t_{bw} and J_{bw}, were studied in both membrane set-ups. The operating conditions used in each BBD in the external and

submerged membranes are presented in Table 6, where −1, 0, and +1, represent the low, middle, and high levels of the variables.

Table 6. Operating conditions of the Box-Behnken experimental designs.

	External Membrane						**Submerged Membrane**					
BBD	AE			BE			AS			BS		
Level	−1	0	+1	−1	0	+1	−1	0	+1	−1	0	+1
t_c (min)	10	15	20	10	15	20	10	15	20	10	15	20
J_f (L/m^{2}h)	11	12	13		12		18	20	22		20	
J_{bw} (L/m^{2}h)		20		20	25	30		30		27	30	33
SGD (m^3/m^{2}h)	1.2	1.3	1.4		1.3		1.2	1.3	1.4		1.3	
t_{bw} (s)		30		20	30	40		30		20	30	40
CFV (m/s)	0.43	0.51	0.59		0.51			n/a			n/a	

t_c: cycle duration, J_f: filtration flux, J_{bw}: backwash flux, SGD: specific gas demand, t_{bw}: backwash duration, CFV: crossflow velocity.

In the BBD labelled AE, 27 runs were performed to study 4 variables, while in the BBD labelled BE, AS, and BS 15 runs were conducted to study 3 operating conditions. Therefore, the entire duration of the experimental designs was 6.75 days for AE and 3.75 days for BE, AS and BS, which can be considered relatively short mid-term assays in relation to the number of variables and levels that are studied. The combination of the levels of each operating condition in the runs and the statistical analysis of the results were performed using Statgraphics® Centurion XVIII. A two-factor interaction response surface model was defined for both fouling rates with the following polynomial equation:

$$Y = b_0 + \sum b_i X_i + \sum b_{ij} X_i X_j \qquad (33)$$

where, Y is the predicted reversible fouling rate, $(dTMP/dt)_{rev}$, or the predicted irreversible fouling rate, $(dR_0/dv)_{irr}$; b_0 is the corresponding intercept coefficient; b_i is the linear effect

coefficient of the operating condition X_i; and, b_{ij} is the interaction effect coefficient of the operating conditions, X_i and X_j.

5.3 Results and Discussion

5.3.1 Observed reversible and irreversible fouling rates

The experimental results of the reversible and irreversible fouling rates from the BBDs both with the external membrane (Table 7) and with the submerged membrane (Table 8) are presented in this section. The $(dTMP/dt)_{rev}$ for each operating condition was calculated as the robust average of the $(dTMP/dt)_{rev}$ of the filtration cycles monitored throughout each run. The coefficients of variation (CV) were calculated from the weighted data, according to the robustness criteria.

The external membrane operated under very low reversible fouling rates, between 0.07 and 0.55 mbar/min (Table 7), in the range of those reported by Drews[170] for long-term operation of typical full-scale MBR at subcritical conditions.[171] The coefficients of variation of $(dTMP/dt)_{rev}$, up to 17.9%, were relatively high. However, the difficulty of determining such small slopes of the TMP profiles should be considered. Even so, these $(dTMP/dt)_{rev}$ deviations were lower than those reported by Le-Clech et al.[91]: 0.17±0.06 mbar/min, using a side-stream tubular membrane operating at a similar CFV.

Table 7. Reversible and irreversible fouling rates of external membrane runs.

AE					BE				
Level t_c, J_f, SGD, CFV	$(dTMP/dt)_{rev}$ (mbar/min)	CV	$(dR_0/dv)_{irr}$ (10^{12} m^{-2})	CV	Level t_c, t_{bw}, J_{bw}	$(dTMP/dt)_{rev}$ (mbar/min)	CV	$(dR_0/dv)_{irr}$ (10^{12} m^{-2})	CV
0 0 0 0	0.19	14.4%	4.0	6.9%	0 0 0	0.19	9.2%	1.03	5.3%
−1 −1 0 0	0.25	12.0%	1.5	6.5%	−1 −1 0	0.08	7.9%	0.43	6.3%
+1 −1 0 0	0.17	7.9%	1.2	3.9%	+1 −1 0	0.12	11.2%	1.13	5.3%
−1 +1 0 0	0.33	6.3%	4.5	3.3%	−1 +1 0	0.36	5.4%	0.44	5.9%
+1 +1 0 0	0.32	10.3%	4.5	3.6%	+1 +1 0	0.36	12.3%	0.44	9.2%
0 0 −1 −1	0.39	6.1%	4.1	4.9%	−1 0 −1	0.19	8.1%	0.46	5.7%
0 0 +1 −1	0.22	15.9%	5.2	3.9%	+1 0 −1	0.14	5.5%	0.54	5.0%
0 0 −1 +1	0.42	5.5%	1.4	3.8%	0 0 0	0.22	4.7%	1.66	6.7%
0 0 +1 +1	0.11	16.2%	0.5	5.0%	−1 0 +1	0.44	10.3%	1.29	6.4%
−1 0 0 −1	0.27	16.9%	7.2	4.1%	+1 0 +1	0.32	7.5%	1.08	6.5%
+1 0 0 −1	0.32	11.6%	2.5	5.9%	0 −1 −1	0.07	6.5%	0.45	6.7%
−1 0 0 +1	0.33	10.3%	1.0	5.9%	0 +1 −1	0.17	7.9%	1.94	7.8%
+1 0 0 +1	0.26	9.5%	1.1	6.3%	0 −1 +1	0.26	14.5%	3.38	5.4%
0 0 0 0	0.26	7.3%	1.2	3.0%	0 +1 +1	0.55	12.2%	1.02	6.4%
0 −1 −1 0	0.23	7.1%	1.4	4.4%	0 0 0	0.17	7.2%	2.51	5.3%
0 +1 −1 0	0.42	4.4%	4.5	3.6%					
0 −1 +1 0	0.21	17.9%	0.5	4.8%					
0 +1 +1 0	0.32	10.3%	4.1	4.6%					
−1 0 −1 0	0.38	4.9%	1.5	4.3%					
+1 0 −1 0	0.28	5.6%	1.5	3.1%					
−1 0 +1 0	0.34	7.7%	1.1	4.2%					
+1 0 +1 0	0.15	14.8%	2.9	3.7%					
0 −1 0 −1	0.22	10.8%	4.1	4.7%					
0 +1 0 −1	0.34	12.5%	6.3	4.0%					
0 −1 0 +1	0.28	9.2%	1.2	9.9%					
0 +1 0 +1	0.32	6.2%	0.9	4.6%					
0 0 0 0	0.23	9.7%	1.2	4.5%					

Despite operating under subcritical conditions, the irreversible fouling rate of the external membrane reached values between 0.43 and 7.2×10^{12} m^{-2}, that expressed as $(dTMP_0/dt)_{irr}$ corresponded to 3.0 – 49.8 mbar/d. Those values could be considered normal residual fouling rates in lab-scale time frames,[170] but were above those recommended for long-term operation for full-scale MBR, 1.4 – 14 mbar/d. Using a tubular membrane module immersed in an aerated activated sludge tank, with an air sparging intensity of 0.3–0.9 m^3/m^2 h, a filtration flux of

5 $L/m^2 \cdot h$, and a netflux-ratio of around 0.85, Schoeberl et al.[164] obtained higher irreversible fouling rates, $(dR_0/dt)_{irr}$ between 0.11 and $1.82 \cdot 10^{12}$ $m^{-1} \cdot d^{-1}$, which in terms of permeate production, $(dR_0/dv)_{irr}$, were in the range $1.1 – 18.2 \cdot 10^{12}$ m^{-2}, higher than those presented here, probably because of the lack of pumped recirculation.

It is remarkable that the CV of the observed $(dR_0/dv)_{irr}$ in the external membranes were always below 10%, usually between 5% and 7%. Results that corroborate how robust statistics can obtain an appropriate quality estimation of irreversible fouling rates in 6-hour runs. The $(dR_0/dv)_{irr}$ values in BE BBD were slightly lower than in AE, which could be due to the use of a higher J_{bw}, although it could also be due to the fact that the highest J_f and lowest SGD and CFV used in the AE BBD were not attempted in BE. Therefore a direct comparison of the observed fouling rates was insufficient to elucidate the causes of the observed effects, justifying the need for the following statistical analysis.

Table 8: Reversible and irreversible fouling rates in submerged membrane runs.

AS					BS				
Level t_c, J_f, SGD	$(dTMP/dt)_{rev}$ (mbar/min)	CV	$(dR_0/dv)_{irr}$ ($\times 10^{12}$ m^{-2})	CV	Level t_c, J_{bw}, t_{bw}	$(dTMP/dt)_{rev}$ (mbar/min)	CV	$(dR_0/dv)_{irr}$ ($\times 10^{12}$ m^{-2})	CV
0 0 0	0.87	12.6%	0.11	0.6%	0 0 0	1.57	6.0%	0.88	6.0%
−1 −1 0	0.67	21.5%	0.12	4.7%	−1 −1 0	1.24	7.6%	0.99	9.0%
+1 −1 0	0.48	22.0%	1.15	16.5%	+1 −1 0	1.31	10.5%	0.66	7.5%
−1 +1 0	1.28	37.8%	0.50	3.7%	−1 +1 0	1.87	13.4%	0.23	4.6%
+1 +1 0	1.89	20.5%	1.13	45.3%	+1 +1 0	1.71	13.1%	1.70	8.3%
−1 0 −1	1.17	15.4%	0.47	3.2%	−1 0 −1	1.22	8.2%	0.81	4.9%
+1 0 −1	1.27	16.2%	1.16	13.1%	+1 0 −1	1.19	7.3%	1.29	7.3%
0 0 0	0.83	16.2%	1.24	44.0%	0 0 0	1.25	12.2%	0.88	7.3%
−1 0 +1	1.19	31.1%	0.50	0.5%	−1 0 +1	1.71	6.7%	0.50	8.2%
+1 0 +1	0.60	18.6%	0.69	58.9%	+1 0 +1	1.43	13.8%	1.16	12.5%
0 −1 −1	0.72	16.6%	0.58	37.6%	0 −1 −1	1.02	7.6%	1.51	6.0%
0 +1 −1	2.04	27.1%	0.86	1.9%	0 +1 −1	1.45	11.9%	0.41	6.1%
0 −1 +1	0.81	20.5%	0.77	4.9%	0 −1 +1	1.32	14.0%	0.90	9.6%
0 +1 +1	0.87	20.0%	0.46	7.6%	0 +1 +1	2.08	14.5%	0.52	6.1%
0 0 0	1.38	10.4%	0.36	51.5%	0 0 0	1.25	11.2%	0.80	4.4%

The filtration fluxes in the submerged membraned were around or over the critical flux. The observed $(dTMP/dt)_{rev}$ in both the AS and BS BBD (Table 8) were between 0.48 and 2.08 mbar/min, approximately four times higher than the one reached in the external membrane. This difference cannot only be due to the difference in flux, just 1.5 times higher, and shows how tangential flow and gas sparging used in the gas-lift configuration of the external membrane setup was more effective at avoiding solid depositions than the scouring used in the submerged hollow fiber membrane setup. It is remarkable that $(dR_0/dv)_{irr}$ was substantially lower in the submerged

membrane than in the external one, between 0.10 and $1.70 \cdot 10^{12}$ m^{-2}, which in terms of $(dTMP/dt)_{irr}$ was 3.6 – 31.8 mbar/d, notably lower than the figure reported by Zsirai et al.[168], between 53 and 96 mbar/d for a flux of 20 $L/m^2 \cdot h$, but still above the recommended values for long-term MBR operation.

5.3.2 Standardized effect of the operating conditions and their interactions on fouling

The analysis of the standardized effects was done to asses which of the operating conditions studied, or interactions between them, were most significant in the experimental range. The Pareto diagrams were modified to display the standardized effects of each operating condition on both fouling rates (Fig. 21 and Fig. 22) in the same graph, and to compare the significance level of each variable and interaction on reversible and irreversible fouling. Reference vertical lines on these diagrams can be used to judge which effects are statistically significant, with a 95% confidence level. The bars that exceed the reference line correspond to variables or interactions with potentially important effects on the fouling rate. The signs (+) and (−) represent "positive" and "negative" effects, respectively. A "positive" effect indicates that the fouling rate increases with the respective variable within the range studied; whereas a "negative" effect indicates that the fouling rate decreases when the variable increases.

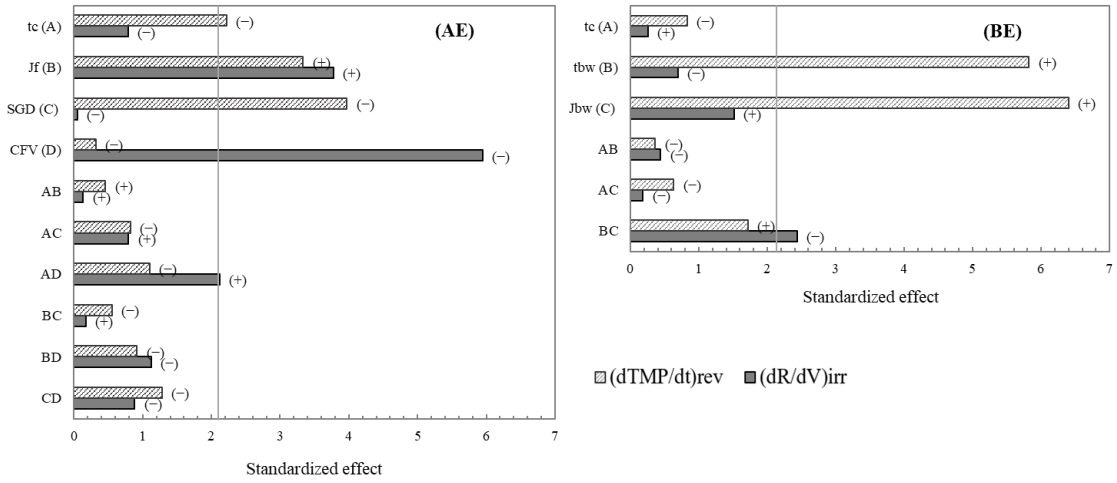

Fig. 21 Standardized effect of each operating condition and its interactions in external membrane in AE and BE BBDs. t_c, cycle duration (min); J_f, filtration flux (L/m^2·h); SGD, specific gas demand (m^3/m^2·h); CFV, crossflow velocity (m/s); t_{bw}, backwash duration (s); J_{bw}, backwash flux (L/m^2·h).

The duration of filtration cycle, filtration flux, and specific gas demand all had significant effects on the observed reversible fouling rate in the external membrane (Fig. 21 – AE). $(dTMP/dt)_{rev}$ increased with J_f, whereas it decreased with t_c and SGD. It is noteworthy that the effect of CFV on $(dTMP/dt)_{rev}$ was not statistically significant, at least in the experimental conditions analyzed, i.e. using low filtration flux with regard to the common side-stream MBR, and particularly applying gas-sparging, distinctive of gas-lift configuration. Le-Clech et al.[91] compared the effects of aeration and CFV on reversible fouling in an MBR equipped with a side-stream tubular membrane using the flux-step method, confirming that the increase in superficial gas velocity from 0.07 to 0.11 m/s (SGD 0.9 to 1.4 m^3/m^2·h) had a greater effect than the increase of CFV from 0.25 to 0.55 m/s. On the other hand, the effect of t_c on $(dTMP/dt)_{rev}$ was also noteworthy. It was checked that the increase in backwashing frequency caused the increase of the reversible fouling rate. The BE experimental design corroborated that backwash intensity, especially the increase in backwash flux and duration, caused a statistically significant increase of $(dTMP/dt)_{rev}$, which cannot be due to an increase in the convective transport of suspended materials from the bulk mixed liquor. This effect of backwashing conditions on reversible fouling rate suggested that backwashing could not detach all the weakly attached materials in the cake, but a part is only loosed without resuspension. Thus when filtration resumes a faster increase in

TMP was observed due to cake rearrangement and colloidal entrapment, rather than to the transport of new materials.

The operating conditions with the highest statistical significance on the irreversible fouling rate of the external membrane were J_f, that increased $(dR_0/dv)_{irr}$, and CFV, that reduced it with the highest standardized effect. On the contrary, SGD had the lowest standardized effect on $(dR_0/dv)_{irr}$, even though it was the parameter with the highest significance level for $(dTMP/dt)_{rev}$. The backwash frequency, flux and duration, separately, had no statistically significant effects on $(dR_0/dv)_{irr}$ within the range of the BE BBD. However, with a confidence level of 95%, the product $J_{bw}{\cdot}t_{bw}$, i.e. the volume of permeate used for backwashing, slowed down the irreversible fouling rate.

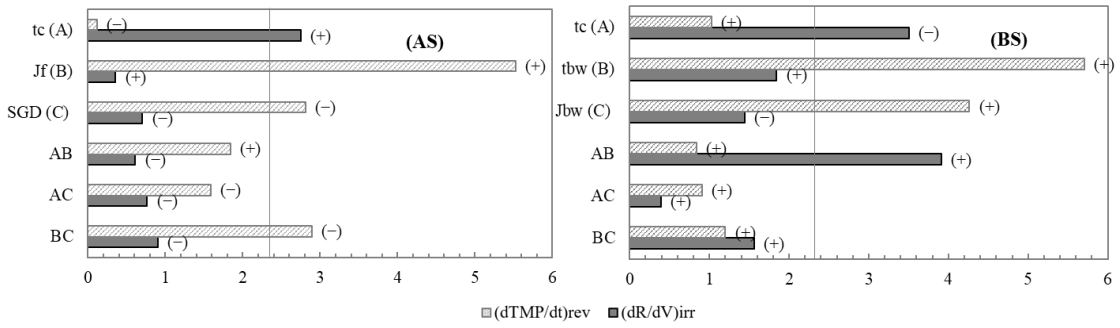

Fig. 22. Standardized effects of the variables studied in submerged membrane in AS and BS BBDs. t_c, cycle duration (min), J_f, filtration flux ($L/m^2{\cdot}h$), SGD, specific gas demand ($m^3/m^2{\cdot}h$), t_{bw} backwash duration (s), J_{bw}, backwash flux ($L/m^2{\cdot}h$)

According to the standardized effects shown in Fig. 22 – AS, the operating conditions with higher effects on $(dTMP/dt)_{rev}$ in the submerged membrane were J_f, SGD and its interaction, $J_f{\cdot}SGD$. The reversible fouling rate increased with J_f and decreased with SGD, with a higher effect of SGD as J_f increased, according to the sign of the standardized effect of $J_f{\cdot}SGD$. This interaction was in disagreement with the findings of Nywening and Zhou[93] who, by comparing the relative effects of filtration flux and gas sparging intensity on reversible membrane fouling in three submerged membrane MBR pilot plants. They concluded that the effects of both parameters on the reversible fouling were independent of each other. The backwash intensity effect on $(dTMP/dt)_{rev}$ in the submerged membrane (Fig. 22 – BS), agreed with the results previously

presented for the external membrane. The reversible fouling rate increased with the flux and duration of backwash. According to this finding, after removing pore blocking via backwashing, a relaxation period longer than 30 s should be considered to favor the detachment of the loosened materials. Christensen et al.[172] using a flat-sheet MBR concluded that the relaxation time should be determined for each sludge, with the optimal value between 0.2 and even 4 min.

In the submerged membrane, within the experimental range of AS BBD, the significance level of the effect of t_c on $(dR_0/dv)_{irr}$ was higher than the effect of either J_f or SGD, the effects of which were not statistically significant. The irreversible fouling rate reached $0.66 – 1.16 \cdot 10^{12}$ m^{-2} for the longest filtration time, 20 minutes, significantly higher than $(dR_0/dv)_{irr}$ for the filtration time of 10 min, between 0.12 and $0.50 \cdot 10^{12}$ m^{-2} (Table 8). This could be due to cake consolidation over the filtration time by deformation and rearrangement of foulant particles exposed to compressive forces, lowering the cake porosity that becomes more prone to consolidation by the colloidal material entrapment[142,162,173,174]. González et al.[171] performed an experimental study on a submerged membrane MBR using filtration times in the range 5 -18 min, verifying that cake consolidation caused severe fouling effects for the higher filtration duration, > 12 min, that were slowed down when filtration duration was fixed at the lower values. Finally, the analysis of the standardized effects of flux and backwash duration on the submerged membrane (Fig. 22 - BS) showed no statistically significant effect on $(dR_0/dv)_{irr}$.

5.3.3 Response surface diagrams of reversible and irreversible fouling rates.

Table 9 and Table 10 show the intercepts and coefficients of the polynomial model (Eq. 33) of the reversible and irreversible fouling rates, respectively, in each experimental design. A regression of the responses calculated from the polynomial models, and the experimental fouling rates are presented and compared to the 1:1 dashed line in Fig. 23, to assess the quality of the adjustments. The correlation coefficients were in the range 0.530 - 0.908 that, according to the difficulty of experimentally determining fouling rates in mid-term assay, can be considered in line with the coefficients of variation presented in Table 9 and Table 10, and with the intrinsic

complexity of the fouling processes. It is important to take into account the challenge of obtaining long-term projection of mid-term as a prerequisite to evaluate the combined effects of three or more variables, even using optimized experimental designs, a difficulty that has previously been highlighted by other authors.[168]

Table 9. Model parameters (Eq.33) for the reversible fouling-rate estimation $(dTMP/dt)_{rev}$.

BBD	b_0	t_c	t_{bw}	J_f	J_{bw}	SGD	CFV	$t_c \cdot J_f$	$t_c \cdot$ SGD	$t_c \cdot$ CFV	$t_c \cdot t_{bw}$	$t_c \cdot J_{bw}$	$t_{bw} \cdot J_{bw}$	$J_f \cdot$ SGD	$J_f \cdot$ CFV	SGD· CFV
AE	-7.56	0.06		0.37		4.08	10.50	0.003	-0.005	-0.008				-0.15	-0.31	-4.38
BE	-0.42	0.03	-0.003		0.004						-0.001	-0.001	0.001			
AS	-42.02	0.05		1.96		34.51		0.02	-0.35					-1.57		
BS	-1.64	0.2	0.007		0.07						-0.002	-0.01	0.002			

Table 10. Model parameters (Eq. 33) for the irreversible fouling rate estimation $(dR_0/dv)_{irr}$.

BBD	b_0	t_c	t_{bw}	J_f	J_{bw}	SGD	CFV	$t_c \cdot J_f$	$t_c \cdot$ SGD	$t_c \cdot$ CFV	$t_c \cdot t_{bw}$	$t_c \cdot J_{bw}$	$t_{bw} \cdot J_{bw}$	$J_f \cdot$ SGD	$J_f \cdot$ CFV	SGD· CFV
AE	-30.03	-2.93		3.76		6.21	107.2	0.02	0.90	3.00				1.00	-7.94	-62.5
BE	-19.37	0.47	0.56		0.71						-0.003	-0.01	-0.002			
AS	-26.69	0.59		1.13		17.69		-0.01	-0.25					-0.74		
BS	11.95	-0.53	-0.35		-0.22						0.02	0.005	0.005			

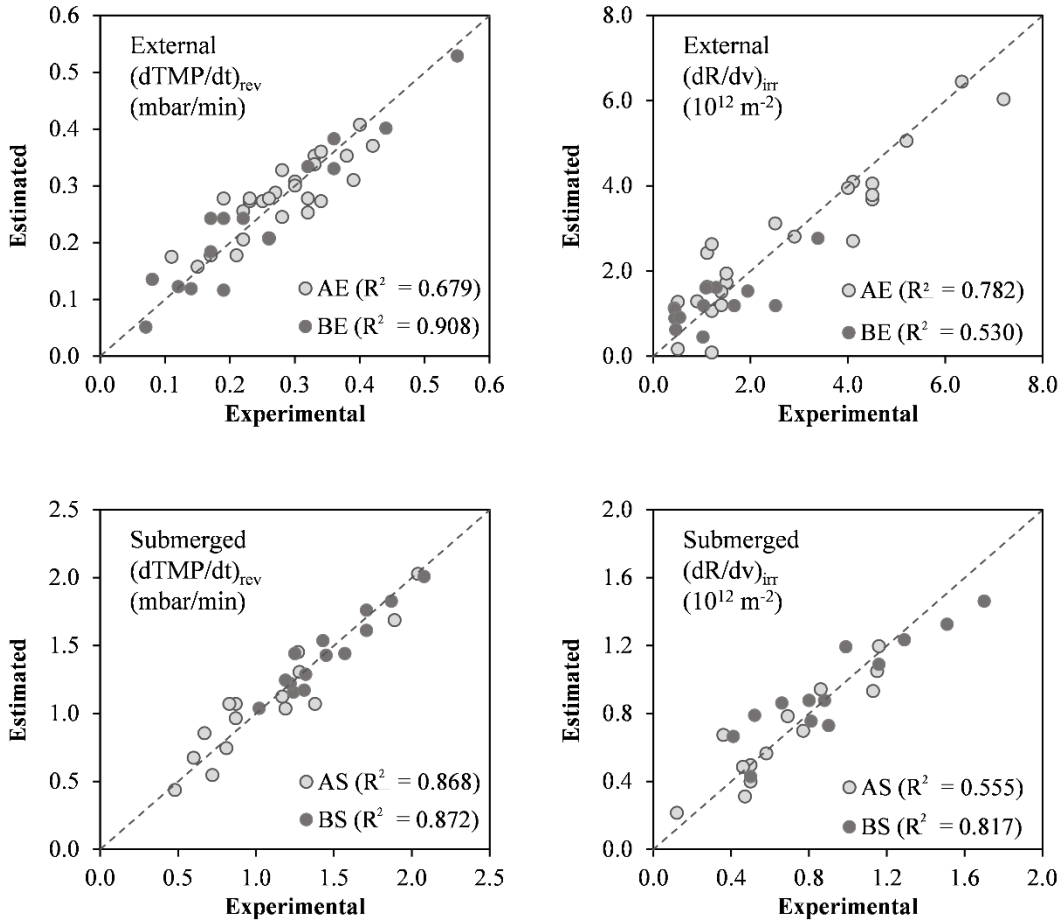

Fig. 23. Estimated results fitted by modeling the experimental results both for reversible, $(dTMP/dt)_{rev}$, and for irreversible, $(dR/dv)_{irr}$, fouling rates in external and submerged membrane

Fig. 24 presents the three-dimensional response surfaces of the effect of operating conditions on external membrane fouling (a-d), and submerged membrane fouling (e-h). The reversible and the irreversible fouling rates obtained in the same experimental design can be compared by rows, and those obtained in different experimental designs can be compared by columns for the reversible fouling rates (a, c, e, g) , and for the irreversible fouling rates(b, d, f, h).

The $(dTMP/dt)_{rev}$ of the external membrane, Fig. 24 (a) and (c), were clearly lower than that of the submerged membrane, Fig. 24 (e) and (g), as a consequence of the difference in filtration flux, 12±1 L/m^2·h and 20±2 L/m^2·h, respectively. In a previous work, using the same flux in both membranes, 15 L/m^2·h, it was verified that the reversible fouling rates of the external membrane were up to twice the $(dTMP/dt)_{rev}$ of the submerged membrane.[154] However, TMP considerably increased, due to the higher irreversible fouling rate and the external membrane setup had

difficulty maintaining a flux of 15 L/m^2·h over a 7-day period. By comparing response surfaces (a) and (c), it may be noted that J_f and CFV had a lower effect, on $(dTMP/dt)_{rev}$ than J_{bw} and t_{bw}, within the experimental range. Reversible fouling rate increased with backwashing intensity, which can be explained because strong backwash contributes to the loosening of a part of reversible fouling that remains weakly bound, without resuspension, so when filtration resumes, the TMP increase is faster than expected, due to the transport of suspended materials. The effects of both J_f and CFV on the irreversible fouling rate were very pronounced (Fig. 24 (b)). For the highest flux and the lowest CFV, $(dR_0/dv)_{irr}$ reached a level of 6.0×10^{12} m^{-2} that could be reduced to 1.3×10^{12} m^{-2} by increasing CFV from 0.43 to 0.59 m/s. The control of $(dR_0/dv)_{irr}$ by CFV was also significant at the lowest flux, 11 L/m^2·h, at which the increase in CFV allowed decreasing the irreversible fouling rate from 2.7 to 0.5×10^{12} m^{-2}. The effect of t_{bw} and J_{bw} on the irreversible fouling rate does not follow the trend of the reversible one. An increase in t_{bw} was not effective and was counterproductive at worst, when the J_{bw} was insufficient, 20 L/m^2·h, and an increase in t_{bw} at only the highest J_{bw} slightly decreased the $(dR_0/dv)_{irr}$ of the external membrane. The increase in pore blocking with backwash, was reported by Wu et al. [175], who considered that the cake layer might protect the membrane from internal fouling by macromolecules. Frequent backwashing with permeate may therefore provide additional opportunities for pore blocking, responsible for irreversible fouling.

The effect of SGD on $(dTMP/dt)_{rev}$ in the submerged membrane, Fig. 24 (e), is noteworthy in that it shows that SGD had no effect on $(dTMP/dt)_{rev}$ at a low flux, 18 L/m^2·h, remaining constant at around 0.5 mbar/min. However, as the filtration flux increased and with it, the reversible fouling rate, the alleviating effect of scouring on $(dTMP/dt)_{rev}$ became increasingly important. So for the highest flux, 22 L/m^2·h, it was possible to reduce the reversible fouling rate from 2.0 to 1.0 mbar/min by increasing SGD from 1.2 to 1.4 m^3/m^2·h. The effect of backwashing intensity on the reversible fouling rate in the submerged membrane was the same, even more pronounced than in the external membrane. The effects of J_f and SGD on $(dR_0/dv)_{irr}$ presented the same trend as on $(dTMP/dt)_{rev}$. Some decrease in $(dR_0/dv)_{irr}$ with SGD can be appreciated for the highest J_f,

although, as discussed in the previous section, it was not statistically significant in the experimental range under study. However, from an energetic point of view, increasing SGD is of no interest for the lower J_f. Schoeberl et al.[164] reported SGD efficiency on irreversible fouling control with the netflux-ratio (ratio between permeate production and volume filtrated) concluding that high gas sparging did not contribute to fouling amelioration for netflux-ratios under 0.85. Finally, it is important to highlight that the results obtained for the control of the reversible fouling rate may not be directly transferable to the control of the irreversible fouling rate.

Zsirai et al.[102] reported that an increase in backwash volume generally reduced the irreversible fouling rate in submerged membranes, but operating at TMP in the order of 100-300 mbar, and very high irreversible fouling level, in the order of 100 mbar/day. However Fig. 24 (h) shows that backwash intensity had slight impact on $(dR_0/dv)_{irr}$, making it necessary to consider that the cake layer in the external membrane never became overly cohesive, with TMP remaining below 120 mbar.

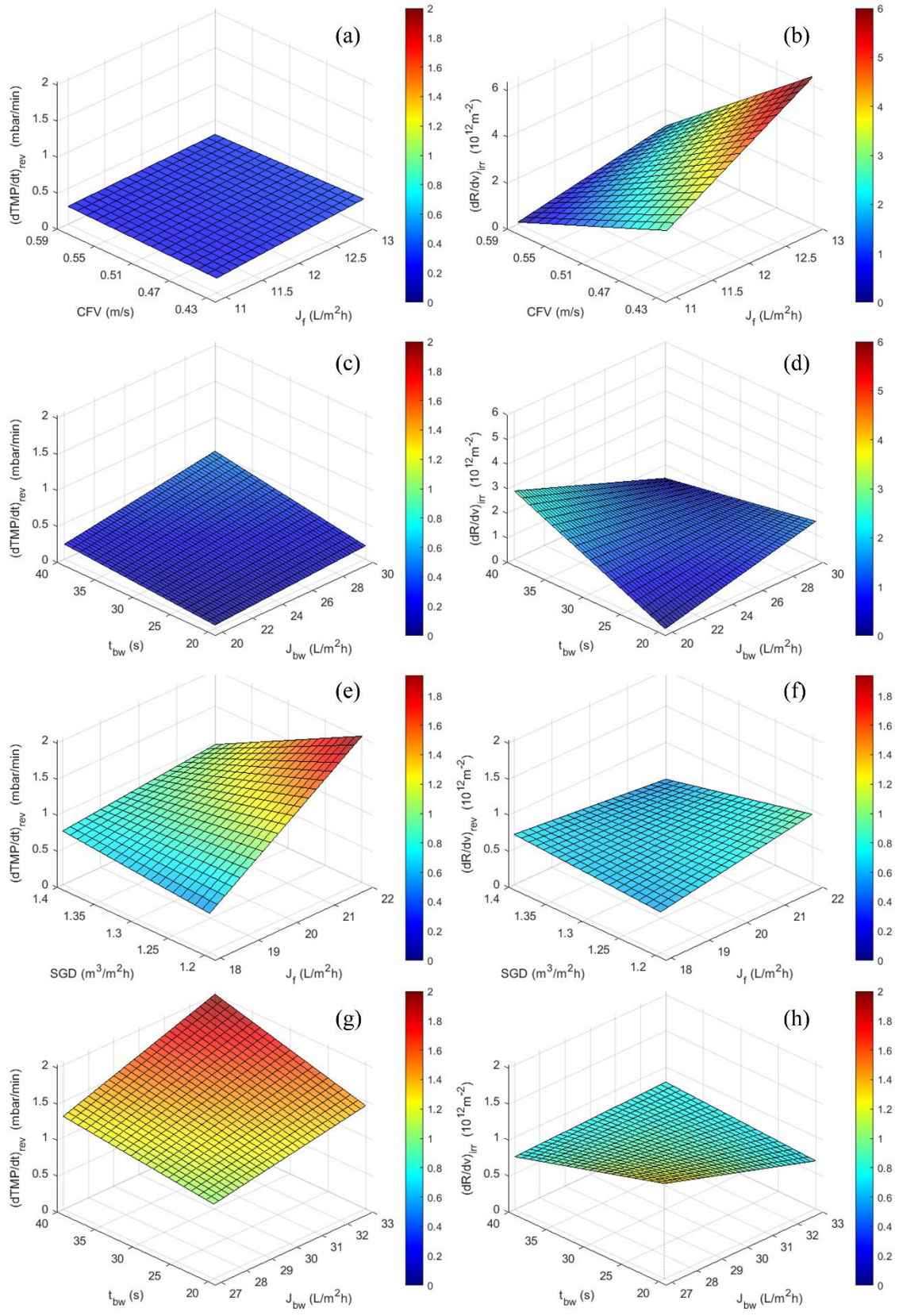

Fig. 24. Three-dimensional response surface of both the reversible and the irreversible fouling rates for AE, BE, AS and BS assays. All the response surfaces corresponded to the 15 min test. Furthermore, test (a) and (b) show the results corresponding to a specific gas demand of 1.3 Nm^3/m^2h.

5.4 Conclusions

The influence of flux and filtration duration, flux and backwash duration, specific gas demand, and crossflow velocity on reversible and irreversible fouling rates has been evaluated both in a hollow-fiber submerged membrane and in an external tubular membrane with gas sparging. Despite the clearly lower reversible fouling rate of the external membrane, $(dTMP/dt)_{rev}$, 0.08 – 0.55 mbar/min, than of the submerged membrane, 0.48 – 2.08 mbar/min, the irreversible fouling rate of the external membrane, $(dR_0/dv)_{irr}$, was notably higher, by up to $7.2 \cdot 10^{12}$ m^{-2}, whereas the submerged one never exceeded $1.7 \cdot 10^{12}$ m^{-2}.

The variables that controlled the reversible fouling were not always capable of controlling the irreversible fouling. In the external membrane, within this experimental study, SGD had a statistically significant effect on $(dTMP/dt)_{rev}$, although not on $(dR_0/dv)_{irr}$, unlike with CFV allows controlling the irreversible fouling rate, despite its effect on the reversible fouling was not statistically relevant.

An unexpected effect of the frequency, the flux, and the duration of backwash on reversible fouling rates was observed in both membranes. The standardized effects of backwash showed that the more intense the backwash, the higher the $(dTMP/dt)_{rev}$, which may be due to a loosening of part of the weakly attached foulants that are not resuspended during the backwash. Even so, backwash intensity decreased $(dR_0/dv)_{irr}$ to a moderate extent.

Box–Behnken experimental design has proven to be suitable for both qualitative and comparative analysis of the combined effects of the main filtration operating conditions in mid-term experiments, in this study between 15-27 assays, each of 6 hours.

New efforts focused on longer mid-term experiments in pilot and real-scale plants will help in the future to improve the accuracy of irreversible fouling rate measures, and experimental designs will facilitate to establish the optimal operating range of the main factors affecting filtration performance of AnMBR.

Capítulo 6: Batch filtration of anaerobic sludges from the treatment of food-processing wastewater with ultrafiltration membranes

6.1 Introduction

The Anaerobic Membrane Bioreactor (AnMBR) is a well-known and widespread technology, successfully employed in wastewater treatment, that combines biological treatment with a membrane filtration process that retains both total solids and biomass [16] and can recover biogas [176]. The industrial application of AnMBR technology has been very significant [17,177], due to its high wastewater treatment efficiency, higher than 90% in terms of COD removal [178,179], the absence of aeration and the associated lower energy demand, as well as for simultaneous recovery of clean water, and nutrient in soluble forms from wastewater [180]. Recently, AnMBR technology is attracting interest in emerging environmental applications that require long solid retention times and/or short hydraulic retention times, such as antibiotics removal and biohydrogen production [181–184].

The critical obstacle limiting the widespread application of this technology is membrane fouling. Few control strategies have been validated to improve the filtration process in AnMBRs, while a wide range of control strategies to optimize membrane performance have been reported in literature in aerobic MBRs [78]. The main factors affecting membrane fouling are membrane characteristics, biomass properties, operating conditions, and wastewater composition [43,103]. In Table 11, the factors causing membrane fouling and the parameters that influence them are listed. Appropriate selection of the operating parameters is important for the minimization of membrane fouling and energy consumption and the maximization of membrane filtration capacity. In an attempt to reduce membrane fouling, some authors have studied the effects of different operating conditions on the filtration process [93,175]. Even so, fouling is inevitable in the long term and filtration process periodically have to be stopped for intensive membrane cleaning.

Table 11. Main parameters affecting membrane fouling (adapted from Bagheri and Mirbagheri (2018))

Membrane set-up	Operating conditions	Biomass properties	Wastewater
Material	Flux	Floc morphology	Dissolved matter
Pore size	Filtration time	Particle size	Chemical
Type	Backwash frequency	distribution	composition
Configuration	Gas bubbling	Suspended solids	Nutrients
State of cleanliness	Crossflow velocity	Extracellular	Chemical oxygen
	Relaxation	polymeric substances	demand (COD)
	Temperature	Soluble microbial	Organic loading rate
		products	(OLR)

AnMBR technology has been applied in numerous studies for the treatment of different industries or municipal wastewater [16,179] even high-strength food waste slurry [185,186]. Filtration process is affected by wastewater characteristics and the operating condition of the biological process. Organic loading rate and food to microorganism ratio, determine the influence of suspended solid concentration on microbial metabolism and EPS and SMP production, thus changing biomass characteristics as floc structure and viscosity [57,187].

Some authors studied the effect of sludge hydrophobicity on membrane filtration. Low hydrophobicity of biomass results in floc deterioration and therefore low hydrophobicity of the sludge is expected to be related to high levels of membrane fouling [170,188]. Dereli et al. [189] studied the influence of high lipid concentrations on the fouling in AnMBRs treating corn-to-ethanol thin stillage. They determined that the adsorption of non-degraded long chain fatty acids on sludge has a negative impact on filtration performance by modification of flocs hydrophobicity and their fouling capacity.

In other studies, severe membrane fouling has been found in high protein/polysaccharide ratio mixtures when filtering synthetic solutions [190,191]. Although membrane fouling is potentially more severe when treating slaughterhouse wastewater than in other applications, due to the high protein content, Jensen et al [34] observed that the treatment of slaughterhouse wastewater in an

AnMBR equipped with microfiltration membranes presented a similar behavior to the treatment of other types of wastewater.

In addition to the effect of wastewater properties, it is also important to understand the influence of the membrane configuration and the operating conditions. Le-Clech et al. [91] studied two different membrane configurations, submerged and side-stream, with the same tubular membrane to treat synthetic and domestic sewage. They observed similar fouling behavior when operated at an aeration rate of 0.07 - 0.11 m/s in the submerged configuration and a crossflow velocity, CFV of 0.25 - 0.55 m/s in the side-stream configuration.

Inappropriate operating conditions result in higher membrane fouling. A filtration flow that is too high will provoke high fouling rates that will reach very high transmembrane pressures, TMP, notably reducing filtration capacity [85]. On the contrary, intense backwash or excessive chemical cleaning can be counterproductive, because, despite reducing membrane fouling, it will also reduce the volume of filtrate, increasing the consumption of both energy and chemical reagents [165]. Liu et al. [192] assessing mitigation strategies for membrane fouling in an AnMBR treating brewery wastewater, observed that regular aeration was more effective than backflushing and the combination of both could inhibit fouling more effectively.

Inadequate operating conditions could also provoke high shear stress affecting biomass properties. High crossflow velocity or gas sparging rate can cause floc disruption releasing substances and particles onto the membrane surface [82,193]. Soluble microbial products, affecting biomass properties, are the main causes of membrane fouling [170]. Other authors have highlighted the influence of food to microorganism ratio, F/M, on membrane resistance. Liu et al. [145] investigated the effect of two F/M ratio, 0.1 g COD/g MLSS and 3.8 g COD/g MLSS and they found that membrane fouling was higher when the bioreactor was operated at the highest F/M ratio and that the cake layer was responsible for over 98% of total resistance.

Although the membrane fouling behavior has been studied on different types of membranes and wastewater, at different scales, no parallel comparative studies have been conducted on the fouling capacity of different sludges over different membrane configurations.

In this paper, a direct comparison of membrane fouling behavior will be presented for two membrane configurations glT and sHF filtering three different anaerobic sludges from a snack food factory, a slaughterhouse, and a brewery. Resistance caused by external and internal membrane fouling, reversible and irreversible fouling rates, critical flux, soluble microbial products and the effectiveness of different cleaning protocols are shown in this study.

6.2 Materials and methods

6.2.1 Anaerobic sludges

With the aim of simulating the characteristics of anaerobic sludge from different food and beverage industries, sludge from an anaerobic digestor at a biowaste treatment plant, (Grupo Ecoalia, Burgos, Spain) was fed over 90 days with concentrated discharges form a snack factory (Pepsico Iberia, Burgos, Spain), a slaughterhouse (Campofrio Frescos, Campofrío Food Group, Burgos, Spain), and a local brewery (Table 12) in completely mixed reactors in fill-and-draw mode and with an OLR of 1.8 kg COD/m^3·d, at a VSS concentration of 4 g/L. Each of the sludges fed with wastewaters from either the snack factory, or the slaughterhouse, or the brewery will now be referred to as SF, SL, and BR, respectively.

Table 12. Characteristics of the wastewater employed for the preparation of the three sludges.

	Snack Factory (SF) (g/L)	Slaughterhouse (SL) (g/L)	Brewery (BR) (g/L)
COD	14.6	6.8	4.0
TKN	0.2	0.8	0.1
FOG	5.0	0.3	0.0
TSS	3.8	3.6	0.5
VSS	3.7	3.5	0.4

6.2.2 Filtration set-ups and operating conditions

Two filtration set-ups, equipped with glT and sHF, were operated in parallel with each sludge. The external set-up employed ultrafiltration multi-tubular membrane (Berghof 63.03I8) with a surface area of 0.31 m^2. The membrane was connected to a 20 L tank and fed with a recirculation pump at a crossflow velocity of 0.51 m/s during filtration and backwash, and was operated in gas-lift side-stream filtration mode with biogas recirculation at a specific gas demand of 1.3 $Nm^3/m^2 \cdot h$.

The submerged set-up was equipped with an ultrafiltration hollow-fiber membrane module (ZeeWeed ZW-10) with a surface area of 0.93 m^2, immersed in a 20 L tank, and with a biogas recirculation rate of 1.3 $Nm^3/m^2 \cdot h$.

Filtration flux was set at 15 $L/m^2 \cdot h$ for the tubular membrane, and 20 $L/m^2 \cdot h$ for the submerged membrane over 7 days. The filtration cycle duration was 12.5 minutes with 30 seconds for backwash and 30 seconds for relaxation before and after the backwash. According to previous studies, backwashing flux was set at 22.5 $L/m^2 \cdot h$ for the tubular membrane and 30 $L/m^2 \cdot h$ for the submerged membrane.

6.2.3 Filtration and fouling characterization

6.2.3.1 Hydraulic resistances

Filtration performance is characterized by the resistance in-series model (RIS). The following individual resistances were selected to describe the filtration process [85]:

$$R_T = \frac{TMP}{\mu \cdot J_f} = R_m + R_{irr} + R_{rev} \quad (34)$$

$$R_{bw} = \frac{TMP_{bw}}{\mu \cdot J_{bw}} = R_m + R_{irr,in} \quad (35)$$

$$R_0 = \frac{TMP_0}{\mu \cdot J_f} = R_m + R_{irr} \quad (36)$$

$$R_{irr} = R_0 - R_m = R_{irr,in} + R_{irr,ex} \quad (37)$$

$$R_{irr,ex} = R_{irr} - R_{irr,in} = R_0 - R_{bw} \quad (38)$$

$$R_{irr,in} = R_{bw} - R_m \quad (39)$$

where, R_T in Eq. 34 is the total resistance (m^{-1}) determined according to Darcy's law; TMP is the transmembrane pressure (Pa); μ is the viscosity of permeate (Pa·s); and, J_f is the filtration flux ($m^3\,m^{-2}\cdot s^{-1}$). According to RIS model, during filtration R_T was divided in the membrane resistance, R_m, irreversible fouling resistance, $R_{irr,}$ and reversible fouling resistance, R_{rev}. The resistance to backwash, R_{bw}, was calculated in Eq. 35 on the basis of the backwash flow, J_{bw}, and the TMP in the backwash, TMP_{bw}, as represented in Fig. 25 (a), in which a typical operating cycle pressure profile is shown. The initial resistance at the start of filtration, R_0, in Eq. 36, was calculated on the basis of transmembrane pressure at the beginning of filtration, TMP_0, (Fig. 25 (a)), in which the contribution to reversible fouling is negligible.

From the initial resistance, the irreversible resistance, R_{irr}, can be calculated as the difference between R_0 and R_m (Eq. 37). Irreversible resistance was divided into where it occurs, either external irreversible fouling, $R_{irr,ex}$, or internal irreversible fouling, $R_{irr,in}$, according to its backwash behavior. In accordance with. Diez et al.[85], in the backwash, the layer of external fouling loosened in such a way that the internal irreversible resistance contributed solely to resistance to backwash, with which $R_{irr,in}$ may be calculated as the difference between backwash resistance and membrane resistance (Eq. 39). Finally, $R_{irr,ex}$ may be calculated as the difference between R_{irr} and $R_{irr,in}$ or as the difference between R_0 and R_{bw}, (Eq. 38).

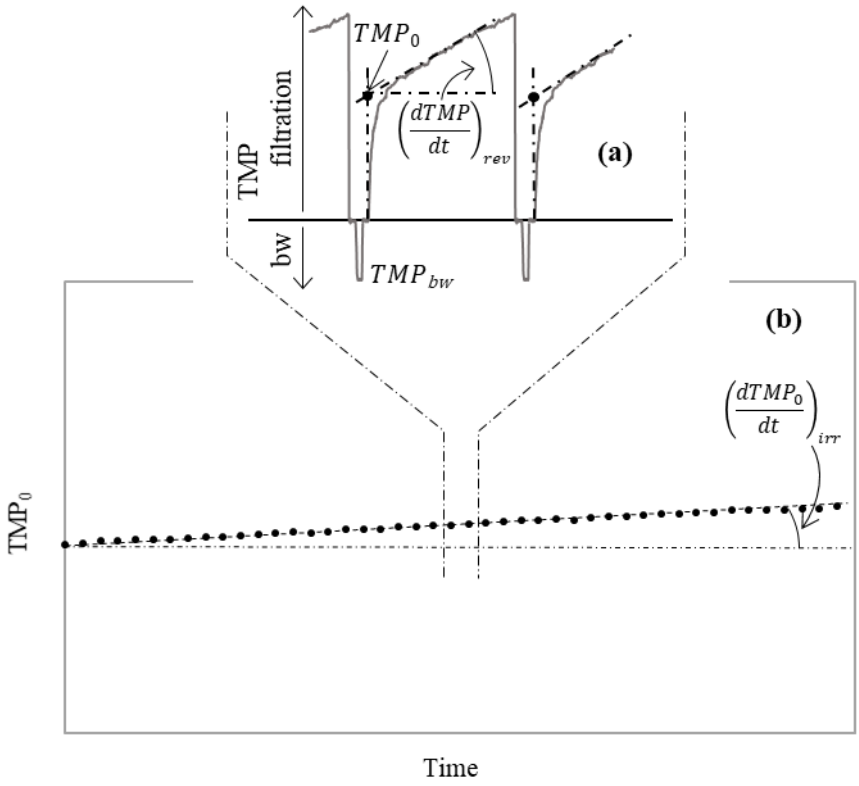

Fig. 25. (a) Transmembrane pressure profile over a 12.5-minute operating cycle. TMP_0 and the slope of the filtration cycle for the calculation of reversible fouling (dTMP/dt) are indicated. (b) Irreversible fouling rate calculation from the slope of TMP_0 in long term assay evolution.

6.2.3.2 Reversible and irreversible fouling rate

The reversible fouling rate, $\left(\frac{dTMP}{dt}\right)_{rev}$, during filtration can be calculated with a linear regression as the slope of TMP versus time (Fig. 25 (a)). The irreversible fouling rate, $\left(\frac{dR}{dt}\right)_{irr}$, (Eq. 40), was calculated, from the long term TMP_0 evolution represented in Fig. 25 (b) as the slope of TMP_0 versus time, $\frac{dTMP_0}{dt}$, divided by the viscosity and flux:

$$\left(\frac{dR}{dt}\right)_{irr} = \left(\frac{dR_{irr}}{dt}\right) = \frac{d(R_0 - R_m)}{dt} = \frac{dR_0}{dt} = \frac{dTMP_0}{dt}\frac{1}{\mu \cdot J_f} \quad (40)$$

Finally, the internal irreversible fouling rate, $\left(\frac{dR}{dt}\right)_{irr,in}$, was determined from long term R_{bw} evolution as:

$$\left(\frac{dR}{dt}\right)_{irr,in} = \frac{d\left(R_m + R_{irr,in}\right)}{dt} = \left(\frac{dR_{bw}}{dt}\right) \quad (41)$$

Huber's robust regression method [169,194] was used for both irreversible fouling rate calculations, by means of a robust filter algorithm to reduce the statistical weight of values deviating from the global linear trend, to increase the confidence interval for the estimated slopes.

6.2.3.3 Critical flux

The critical flux, J_c, was determined twice a day, every 11 hours for 1 hour. The flux-step method was employed for the evaluation of the critical flux using 8 different filtration fluxes between 12-18 L/m^2·h in glT and 17-23 L/m^2·h in sHF. Backwashing flux was 150% of filtration flux. Fig. 26 (a) shows the pressure profile over time used in the assessment of critical flux. The filtration cycle duration was 7.5 minutes with 30 seconds for backwash and previous relaxation and 15 seconds for relaxation between backwash and filtration.

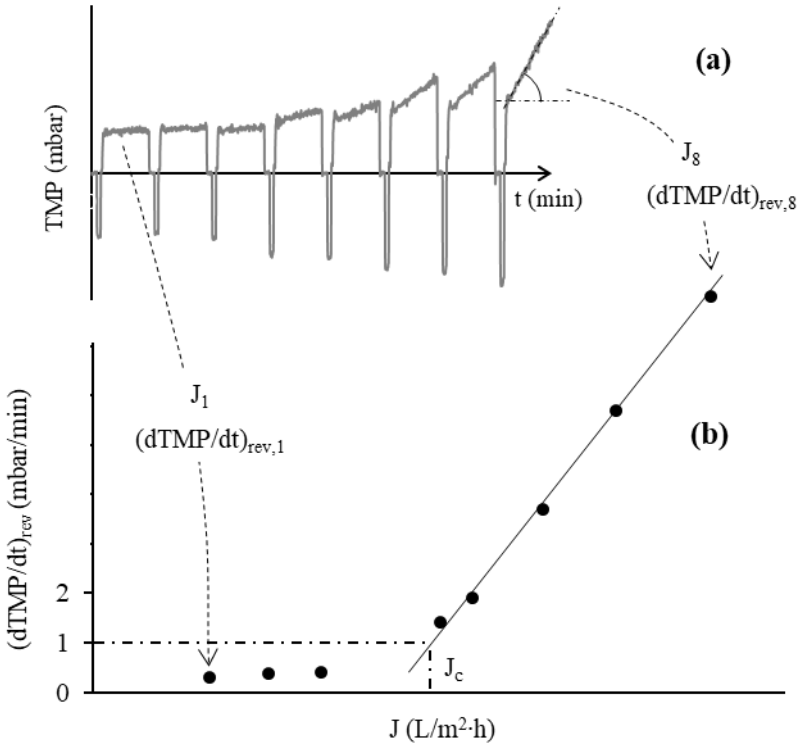

Fig. 26. (a) Pressure profile over 1 hour obtained for the determination of critical flux with different filtration fluxes, and (b) reversible fouling rate versus filtration flux for critical flux determination.

The reversible fouling rate versus the flux, represented in Fig. 26 (b) can be used to determine the critical flux. An arbitrary TMP gradient threshold of 1 mbar/min was chosen to determine the critical flux [195].

6.2.4 Analytical methods

Total Suspended Solids (TSS) and Volatile Suspended Solids (VSS) were analyzed according to the protocols described in the Standard Methods for the Examination of Water and Wastewater [108].

Humic Substances (HS), Proteins (PN) and Polysaccharides (PS) were analyzed in the mixed liquor and in the permeate. SMP in the sludge were determined from the supernatant obtained by simple filtration through a glass fiber filter Millipore AP40 with a 0.7 µm pore size [104,196] and from the permeate. Each sample was analyzed in triplicate.

HS were determined by Lowry's modified method [117], PN were determined using the modified Bradford method [114] and PS were measured using the method suggested by Dubois et al [197]. Humic acid (SIGMA-ALDRICH), bovine serum albumin (VWR Prolabo Chemicals), and D(+)-anhydrous glucose (VWR Prolabo Chemicals) were used as the calibration standards. A Hitachi U-2000 UV/vis spectrophotometer was used for spectrophotometric measurements.

6.2.5 Membrane cleaning

Once each assay was finished, membrane cleaning was sequentially performed under increasingly severe conditions, in order to evaluate the differences in the type of irreversible fouling caused by the three types of sludge. First a physical rinsing with tap water and then with gas sparging, followed by chemical rinsing with a 100 mg/L NaClO low concentrate solution, an oxidizing cleaning with 500 mg/L of NaClO, and finally acid cleaning with 100 mg/L of oxalic acid [154]. Additional acid cleaning with 150 mg/L of oxalic acid was carried out when necessary to reduce membrane resistance.

The length of each step was 2 hours during which time filtration and backwash resistances were measured for the evaluation of the efficiency of each cleaning step [135]. After each cleaning stage, the membranes were rinsed with tap water to remove detached materials.

Cleaning efficiency was calculated in Eq. 42 as:

$$\%\ \text{cleaning efficiency} = \frac{R_i - R_c}{R_i} 100 \qquad (42)$$

where, R_i represents the resistance of the membrane before the cleaning operation and R_c the resistance after the cleaning operation.

6.3 Results and discussion

6.3.1 External and internal membrane fouling

Fig. 27 (a) represents the evolution of TMP_0 in glT operating at a flux of 15 L/m^2·h for the SF, the SL and the BR sludges. In only 7 days, the 3 types of sludge provoked a very significant increase of TMP_0, SF, SL and BR, reaching 250±12, 230±17 and 199±8 mbar, respectively. The increase of TMP_0 stands out especially during the first day of filtration of the sludges, starting from a clean membrane surface and sludges as were prepared in the anaerobic reactors. Such a high increase of TMP_0 highlights that the operating conditions employed in this work could hardly be employed in the long-term continuous operation of this type of biological reactor. Backwash resistance was analyzed, as represented in Fig. 27 (c), employing a J_{bw} of 22.5 L/m^2·h, in order to determine to what extent the fouling was due to irreversible external fouling or to irreversible internal fouling. It may be confirmed that the R_{bw} increased from 0.77±0.02×10^{12} m^{-1} at the start of the experiment up until 2.96±0.07×10^{12} m^{-1}, 2.69±0.12×10^{12} m^{-1} and 2.40±0.16×10^{12} m^{-1}, at 7 days, for SF, SL, and BR, respectively. In accordance with Eq. 39, the hydraulic resistance of irreversible internal fouling, $R_{irr,in}$, was 2.21±0.07 ×10^{12} m^{-1}, 1.92±0.12 ×10^{12} m^{-1}, and 1.62±0.16 ×10^{12} m^{-1} for SF, SL, and BR, respectively.

The fouling capacity of the three sludges in sHF, maintained the order SF>SL>BR, however the level of fouling was notably lower. Fig. 27 (b) and (d) shows that the fouling of the sHF took place in a slower and more progressive manner than in the glT. After 7 days of filtration, the TMP_0 reached values of 124±6, 117±5, and 110±7 mbar in SF, SL, and BR, respectively, approximately half those of the external membrane, despite operating with a higher filtration flow, 20 L/m^2·h. R_{bw} followed the same order as in the external membrane, reaching 1.04±0.05, 1.14±0.04, and 1.23±0.03×10^{12} m^{-1}, at 7 days, with SF, SL, and BR, respectively.

The fact that the fatty sludges generated with snack food factory wastewater caused the highest levels of fouling is not in accordance with what was reported in earlier studies. It has been reported

a significant flux enhancement, due to the increase of sludge hydrophobicity in an aerobic MBR treating frying oil and rhamnolipids as surfactants [198], assuming that hydrophobic flocs caused lower fouling, due to weaker interactions with typically hydrophilic membrane [68,170,188].

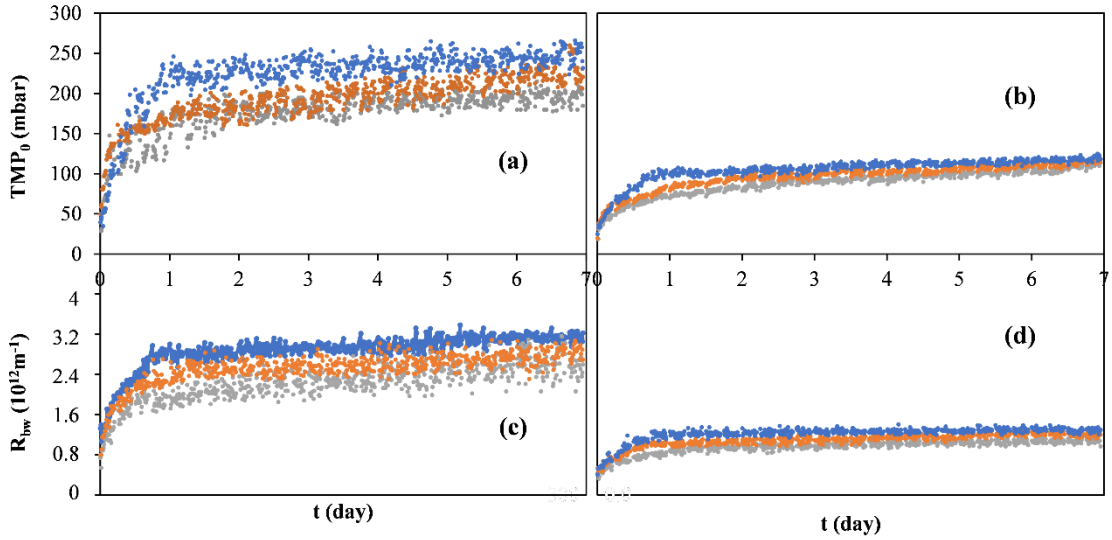

Fig. 27. Initial transmembrane pressure, TMP_0, and backwash resistance, R_{bw}, for 7 days filtering of anaerobic sludge from snack factory, slaughterhouse, and brewery wastewater treatment in glT (a), (c) at 15 L/m^{2}h and a sHF (b) (d) at 20 L/m^{2}h.

6.3.2 Reversible fouling rates

All the tests were performed under supracritical flow conditions. At the start of the experiment, over the period 0 – 6 h, the reversible fouling rates were between 2.0 and 2.8 mbar/min with glT and between 2.0 and 2.4 mbar/min with sHF. The same order of fouling propensity was maintained: SF>SL>BR. The reversible fouling rate also increased over time (Fig. 28). It's worth highlighting that, in spite of the similar fouling rates initially observed in both membranes, the increase in $(dTMP/dt)_{rev}$ over time was particularly high in the external membrane. Its values reaching 5.7, 6.4 nd 9.1 mbar/min for BR, SL and SF respectively from the 2nd day on, corresponding to reversible fouling rates between 220% and 270% for sHF during the same period. In relative terms, the difference between the three different sludges was also significant, with a reversible fouling rate, $(dTMP/dt)_{rev}$, for SF that was 51% and 59% higher than for BR,

in the glT mode and in the sHF membranes, respectively. With regard to the temporal evolution, using SF and SL sludges, the reversible fouling rate, $(dTMP/dt)_{rev}$, progressively increased, above all after 48 h. However, it is worth highlighting that the BR sludge caused a very rapid increase of the reversible fouling rate, $(dTMP/dt)_{rev}$, in the glT over the period 12–24 h, reaching 4.63 mbar/min, with much slighter subsequent increases. In the meantime, the behavior of the BR sludge in the sHF was exactly the contrary, remaining practically stable during the first 24 g, passing from 2.0±0.3 mbar/min over the period 0–12 h, to 1.9±0.2 mbar/min over the period 12–24 h.

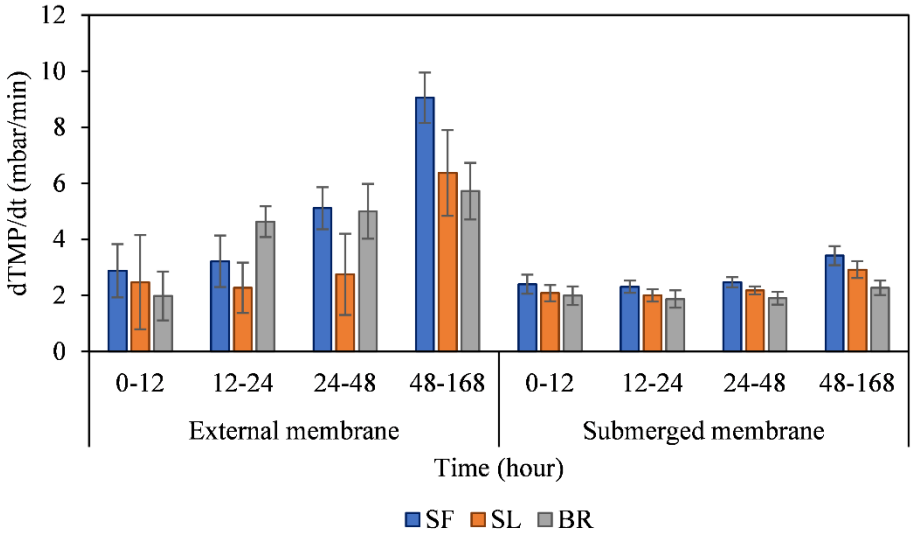

Fig. 28. Reversible fouling rate in glT and sHF when filtering SF, SL and BR anaerobic sludges

6.3.3 Irreversible fouling rates

The irreversible fouling rates confirmed the order by fouling capacity stated in section 3.2, SF>SL>BR.

Table 13 shows both the total irreversible fouling rate, $(dR/dt)_{irr}$, and the total internal irreversible fouling rate, $(dR/dt)_{irr,in}$, in both the glT and the sHF membranes, over 7 days. It is worth highlighting that the highest differences between the glT and the sHF took place during

the first twelve hours. Over the period 0–12 h, the irreversible fouling rate of the glT was between 6.80−7.91×10^{12} m^{-1}/d while that of the sHF was between 2.06−2.49×10^{12} m^{-1}/d, differences that drastically diminished from 12 h, observing that the $(dR/dt)_{irr}$ were maintained at much narrower intervals, with much lower differences between both membranes. This difference concentrated in the first hours of operation was already observed by Ozaki and Yamamoto [199] who studied the effect of shear stress on sludge accumulation on a flat sheet membrane module in bubble and non-bubble driven crossflow filtration. They observed that sludge accumulation rapidly increased during the first 6 hours, after a lag phase at the very beginning of filtration while membrane surface conditions increased the attachability of particles. Subsequently, the surface become more stable and membrane fouling was produced in a linear form over time, being the shear stress the major factor influencing its rate. As the accumulation of sludge increased, it started to detach, that in turn produced a balance in the net accumulation, stabilizing the fouling rate.

The differences between the two membranes might be due to the different hydrodynamic conditions caused by the particular configuration of each membrane that gave rise to greater shear stress on the glT, breaking-up flocs and freeing substances that increased the sludge accumulation on the membrane [154].

The high levels of irreversible internal fouling were very remarkable, representing around 50% of total irreversible fouling. The external irreversible fouling rate, the difference between $(dR/dt)_{irr}$ and $(dR/dt)_{irr,in}$, was especially high in the interval 0–12 h, taking similar values for the three types of sludges, between $4.03 - 4.19\times10^{12}$ m^{-1}/d in the glT and between 0.97−1.14×10^{12} m^{-1}/d in the sHF. The rate then fell drastically after 12 h and stabilized at 0.13 and 0.18×10^{12} m^{-1}/d in the glT and sHF, respectively.

Moreover, it is worth highlighting that reversible and irreversible fouling were not directly related, irreversible fouling, $(dR/dt)_{irr}$, dropping over time while reversible fouling, $(dTMP/dt)_{rev}$, increased sharply. It must be considered that internal fouling, due to pore

blockage, caused a reduction of the useful area of filtration and with it an increase in the local filtration flux [200,201] that was associated with higher reversible fouling rates, $(dTMP/dt)_{rev}$, which was not accompanied by higher irreversible fouling rates towards the end of the experiment.

This can be easily explained in batch filtration experiments with total recirculation of the permeate, in which as time advances, the concentration of materials with greater fouling capacity that are irreversibly retained by the membrane will decrease over time. It should be considered that batch filtration experiments do not keep biological conditions constant what affects sludge accumulation on the membrane, although the aim of this work was limited to evaluate the differences in behavior of the sludges and membranes.

Table 13. Irreversible fouling rate of glT and sHF membranes when filtering SF, SL and BR anaerobic sludge.

	Time (h)	$(dR/dt)_{irr}$ (10^{12} m^{-1}/d)			$(dR/dt)_{irr,in}$ (10^{12} m^{-1}/d)		
		SF	SL	BR	SF	SL	BR
glT	0 – 12	7.91	7.37	6.80	3.81	3.18	2.77
	12 – 24	1.63	2.17	2.32	1.27	1.54	1.60
	24 – 48	1.27	1.06	0.92	0.63	0.69	0.60
	48 – 168	0.51	0.57	0.52	0.28	0.24	0.22
sHF	0 – 12	2.49	2.31	2.06	1.35	1.34	1.06
	12 – 24	1.21	0.92	0.87	0.97	0.71	0.61
	24 – 48	0.57	0.41	0.36	0.37	0.21	0.12
	48 – 168	0.32	0.27	0.24	0.14	0.13	0.11

6.3.4 *Critical flux*

The critical flux, J_c, fell as the filtration process and consequent membrane fouling progressed. The critical flux of the sHF took higher values than glT, initially between 16.5−17.6 L/m^2·h in the first, and between 11.0−12.4 L/m^2·h in the second, which confirmed that the fluxes used throughout this work were supracritical, what is justified by the purpose of obtaining comparable results within a relatively short period of time.

The J_c decay during each filtration assay was linearly regressed versus time. Table 14 shows the equations obtained and the coefficients of determination, that explains over 90% of the J_c variance. Accordingly, it may be confirmed that the SL sludge gave rise to a lower J_c with an initial value of 11.02 L/m^2·h and a slope value of –0.16 (L/m^2·h)/d for glT, and an initial J_c of 16.51 L/m^2·h and an slope of –0.18 (L/m^2·h)/d for sHF. These results corresponded with the fouling data presented in section 3.1, according to with which, higher membrane fouling resulted in a lower J_c.

In the case of SL and BR sludges, with the same slope value, the initial J_c marked the difference of each sludge and of membrane configuration, being SL sludge which kept a lower J_c in both membranes over time.

Table 14. Evolution of critical flux throughout the filtration tests with external and submerged membrane filtering Snack Factory (SF), Slaughterhouse (SL), and brewery (BR) anaerobic sludge.

		J_c (L/m^{2}h); t (d)	R^2
glT	SF	11.02 – 0.16 t	0.92
	SL	11.71 – 0.14·t	0.94
	BR	12.41 – 0.14·t	0.92
sHF	SF	16.51 – 0.18·t	0.98
	SL	17.04 – 0.14·t	0.90
	BR	17.62 – 0.14·t	0.96

Once again, the sludges that caused a greater descent of critical flux, both in the glT and in the sHF were the SF. However, the most significant aspect was that the differences in the decrease in critical flux over 7 days were really small, from only ΔJ_c = 0.85 L/m^2·h in the glT, for BR sludge, to ΔJ_c = 1.17 L/m^2·h in the case of the sHF, and SF sludge. These results thereby demonstrate, that there was no direct relation between the difference of actual flux and critical flux, J−Jc, and fouling rates. For example, in the case of the glT and SF sludge, initially reversible and irreversible fouling rates were 2.8 mbar/min and 7.91×10^{12} m^{-1}/d, respectively, being J − Jc = 3.98 L/m^2·h, and at the end of the experiment the increase in J – JC, up to 5.02 L/m^2·h, was accompanied by an increase in $(dTMP/dt)_{rev}$, up to 9.1 mbar/min, however, $(dR/dt)_{irr}$ was 15 times lower than the initial one, 0.51×10^{12} m^{-1}/d.

6.3.5 Soluble microbial products

The amount of SMP was analyzed in the filtered fraction of sludge and permeate at the beginning and at the end of each experiment. Fig. 29 represents the concentrations of HS, PN, and PS in the sludges of (a) the glT set-up and (b) the sHF set-up. It is notable that the concentration of humic substances in all the samples was higher than the concentrations of proteins and carbohydrates. The differences of HS concentration between glT and sHF, and between sludge were small, only the glT set-up tank showed slightly higher levels than the sHF set-up and the permeate from the BR sludge had slightly higher levels than the permeate from both the SF and the SL sludges. It was observed that the polysaccharide concentrations in the SL sludge were higher than in both the SF and the BR sludges, however, hardly any differences were observed either between the glT set-up and the sHF set-up, and between the concentrations determined within the 1st hour and on the 7th day. The concentration of proteins in the tank of the glT set-up was always higher than the concentration of polysaccharides, however, the permeates had notably lower concentrations than the polysaccharides. It is worth highlighting the falling trends of the proteins, both in the tank and in the permeate, over time in both set-ups.

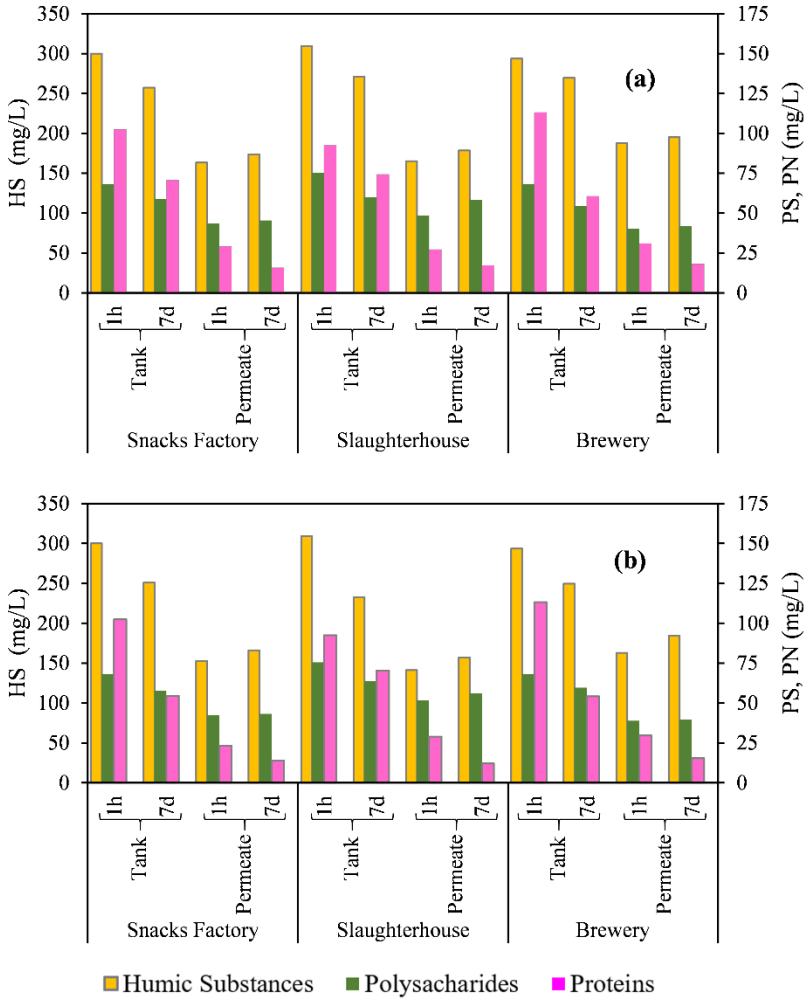

Fig. 29. Concentration of humic substances (HS), carbohydrates (PS) and proteins (PN) in the filtration tank and permeate when starting the filtration test and at the end of the assay, 7 days after filtering SF, SL, and BR wastewaters, in glT (a) and sHF (b).

Table 15 shows the retention percentage of SMP from the 3 sludges by the 2 membranes, in the 1st hour and on the 7th day. The sHF showed a slightly higher SMP retention capacity for the three sludges from the beginning up until the end of the assays. Generally, the retention capacity of the three types of compounds followed the order PN>HS>PS. Choi et al. (2013) and Teychene et al. [203] demonstrated that proteins are the principal compounds retained by the membrane. The retention capacity of HS and PS fell over time, probably as a consequence of the reduction in the concentration of HS and PS in the sludge, due to the prior retention, in accordance with the

batch nature of the experiments. Kimura et al. [204] associated initial fouling with humic substances and later on, fouling with polysaccharides.

On the contrary, protein retention remained almost constant in the BR sludge, clearly increasing for the SL sludge, especially in sHF, and slightly increasing in the SF sludge, in the glT. This increased PN retention capacity over time demonstrated that proteins are retained in an effective way by the fouling layer [202,203]. Finally, it was not observed a direct relation between the concentration of SMPs and the degree of membrane fouling with each sludge.

Table 15. Retention of SMP from the 3 sludges by the 2 membranes, in the 1st hour and on the 7th day.

Sludge	glT			sHF		
	HS	PS	PN	HS	PS	PN
SF	46%−32%*	36%−23%	71%−78%	49%−34%	38%−25%	77%−75%
SL	47%−34%	36%−3%	71%−77%	54%−32%	31%−12%	69%−83%
BR	36%−28%	41%−23%	73%−70%	45%−26%	43%−34%	74%−72%

(*) 1 hour−7 days

Humic Substances (HS); Polysaccharides (PS); Protein (PN); anaerobic sludge from Snack Factory (SF), Slaughterhouse (SL), and brewery (BR).

6.3.6 Membrane cleaning

The membrane cleaning process efficiency was different in the two set-ups and, likewise, differences were observed between the three sludges. The cleaning protocol presented in section 2.5 was sufficient to recover the resistance of the sHF but was insufficient for the cleaning of the glT, which as has been seen in section 3.1 reached higher levels of fouling. The cleaning of the glT was, for that reason, completed with a second addition of a slightly higher concentrate of oxalic acid, 150 mg/L, with which the initial resistance of the glT was recovered.

Fig. 30 (a) shows the filtration and backwash resistance values during the cleaning stages of the glT. The efficacy of the NaClO at cleaning the glT after filtration of the BR sludge may be highlighted. Rinsing with 100 mg NaClO/L was sufficient to reduce the resistance from 8.35 to 3.17×10^{12} m^{-1}, which was reduced to up to 1.68×10^{12} m^{-1} with subsequent cleaning with 500 mg NaClO/L, with similar levels of efficacy in the backwash, which fell by 41%. Rinsing with NaClO had a notably lower effectiveness on the cleaning of glT after the filtration of SF and still less so after the filtration of SL, with an efficiency on the R_{bw} of only 21 and 3% for SF and SL, respectively. The cleaning acids were especially effective on the cleaning of the glT after filtration of the SL sludge.

Even though numerous authors have employed sodium hypochlorite as a cleaning reagent, citric acids can offer a better cleaning efficiency than other chemical reagents under some circumstances [103]. Calderón et al. [205] observed that backflushing and chemical cleaning with NaClO was insufficient for complete membrane cleaning. Liikanene et al. [206] tested several cleaning agents and procedures on nanofiltration membrane cleaning process and achieved high cleaning efficiency when combining cleaning agents and a multi-stage procedure.

Finally, the second acid cleaning was sufficient to recover the original resistance of the glT membrane with the three types of sludge, $0.77\pm0.02\times10^{12}$ m^{-1}.

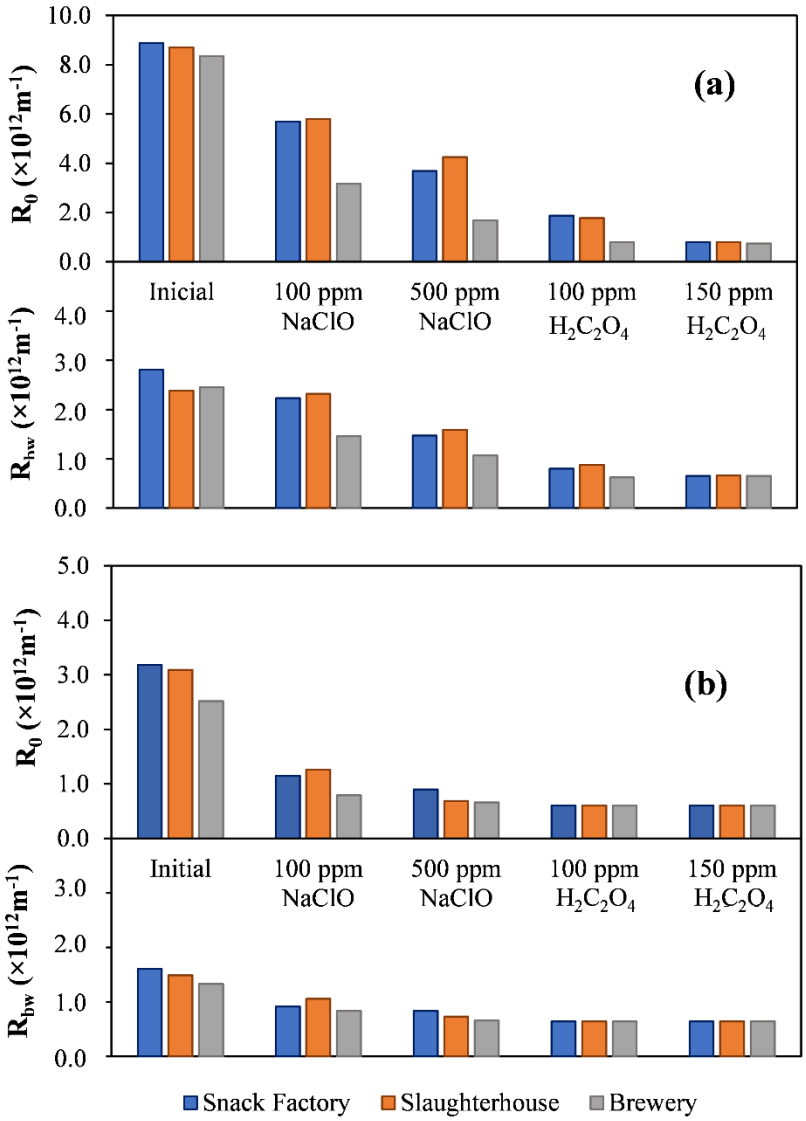

Fig. 30. Filtration resistance (R0) and backwash resistance (Rbw) of glT (a) and sHF (b) at the end of each stage of cleaning, having filtered anaerobic SF, SL, and BR wastewater.

The initial state of the sHF membrane, Fig. 30 (b), $R_0 \leq 3.2\ 10^{12}\ m^{-1}$ and $R_{bw} \leq 1.3\ 10^{12}\ m^{-1}$, meant that the cleaning was notably more effective, with lower differences between the three types of sludge. Similarly to glT, it was observed that the cleaning process of the sHF membrane was more efficient after the filtration of the BR sludge. In the same way, after filtering the SL sludge, the efficiency of the rinsing with 100 mg/L NaClO was notably lower than chemical rinsing after filtering the SF and the BR sludges. Cleaning with 500 mg/L of NaClO was practically sufficient to recover the resistance of the membranes used in the filtration of the SL and the BR sludges. However, the membrane employed with the SF sludge maintained its

resistance of 1.48±0.59 and 0.87±0.13×$10^{12}$$m^{-1}$, both to filtration and to backwash, respectively, so it was necessary to use 100 mg/L oxalic acid to recover the initial resistance of the membrane.

6.4 Conclusions

Three different anaerobic sludges from a snack factory, a slaughterhouse, and a brewery have been filtered with a tubular external membrane in gas-lift mode and a submerged hollow fiber membrane module. glT was operated at 15 L/m^2h for filtration and sHF was operated al 20 L/m^2h and backwash flux was stablished at 150% of filtration flux in both set-ups.

It has been proven that all indicators of fouling such as external and internal membrane fouling, reversible and irreversible fouling rate, and critical flux showed higher fouling capacity for the SF than for the SL and the BR sludges in both membranes and they also showed that fouling propensity of the glT set-up was always higher than of the sHF set-up for the three sludges.

Fouling of the sHF took place in a slower and more progressive way than in the glT. After 7 days of filtration the values of TMP_0 reached by glT were approximately twice those of the sHF, despite operating with a lower filtration flux.

There was no direct correspondence between the reversible and irreversible fouling rates, while $(dR/dt)_{irr}$ fell over time, $(dTMP/dt)_{rev}$ rapidly increased.

The highest differences with regard to the irreversible fouling rates took place over the initial period when glT reached values between 6.80−7.91×10^{12} m^{-1}/d, while the irreversible fouling rates of sHF were 3 times lower, between 2.06−2.49×10^{12} m^{-1}/d, drastically falling in subsequent periods with lower differences between both membranes. The reversible fouling rates in glT mode were between 220% and 270% higher than in sHF as from 2nd day.

The difference observed in the fouling rates between the two membranes in the initial periods may be due to the rupture of floc caused by the shear stress on the sludges.

The critical flux was measured for 1 hour every 11 hours. J_c, in glT were initially between 11.02−12.41 L/m^2·h, depending on the sludge, and those of the sHF were between

16.51−17.62 L/m^{2}h. It was observed that as the filtration test advanced and fouling built up on the membranes, J_c decreased especially with SF sludge, both in glT and in sHF.

SMP were analyzed in the filtered fraction of sludge and permeate at the beginning and at the end of each experiment. sHF has shown a slightly higher retention capacity, for the three sludges since the start until the end of the experience. Despite the HS concentration that was higher than PN and PS, the retention capacity was higher in PN than in HS and PS.

Capítulo 7: Effect of salinity and temperature on the anaerobic sludge-released organic matter and fouling in submerged membranes

7.1 Introduction

Extracellular polymeric substances (EPS) and soluble microbial products (SMP) have high fouling potential in membrane bioreactors [170,207]. Loosely and tightly bound EPS are mainly involved in cake deposition on the membrane surface, while SMP often cause pore blocking [208]. It is widely known that EPS and SMP are mainly composed of proteins (P), polysaccharides (PS), humic substances (HS), nucleic acids, and lipids, which can be originated from cell lysis, microbial metabolism, or similar unmetabolised wastewater components [57]. EPS concentration is closely connected to sludge characteristics, such as sludge volume index, flocculation ability, hydrophobicity, surface charge, and sludge viscosity. EPS production depends on different factors, such as solid retention time (SRT), organic loading rate (OLR), food-to-microorganism ratio (F/M), carbon-to-nitrogen ratio (C/N), shear stress, and, in the case of aerobic processes, dissolved-oxygen concentration. It has already been reported that P and PS cause severe fouling due to bei collected upon the pores and spread over the surface of the membrane [69,170].

Different solvents such as water [208], sodium chloride solution [209–211], EDTA [212], formaldehyde [212], formaldehyde plus sodium hydroxide [212], acetone, and ethanol [213], have already been used in the EPS extraction. Conventional stirring [115,212], vortex agitation [208,210,211,213,214], and ultrasonication [209,212,214,215] are commonly used to increase the EPS diffusion rate during extraction. Although short contact times of between 1 and 2.5 minutes are generally used, contact times of up to 45 min [216] and 8 h [217] have also been reported. The literature gives variable values for temperature of extraction. Frølund et al. [115] and Liu et al. [212] carried out the extraction with refrigeration at 4 ºC, Morgan et al. [213] at room temperature, Ding et al. [211] used the solvent at 50 ºC, Han et al. [209] held the extraction mixture for 30 min at 60 ºC, and Li et al. [210] carried out EPS extraction at 70 ºC. Finally, Cosenza et al. [208] after 1 min of vortex agitation, held the mixture in a water bath at 80 ºC for 10 min, although such a high temperature can produce partial EPS denaturation [218]. After the

extraction stage, filtration [212,214] or centrifugation [115,208,210,211] are commonly used to separate the solid and liquid phases.

D'Abzac et al. [218] compared four physical and four chemical EPS extraction methods; their results showed that different extraction techniques led to a slightly preferential extraction of different EPS compounds. Liu et al. [212] have already analysed the effectiveness of different solvents under different extraction conditions, and higher extraction of P and PS were observed by using a binary mixture of formaldehyde with NaOH as solvent. However, the extraction of HS was increased by using EDTA. The research reported by Wingender et al. [219] shows that EPS amount and composition depend on the extraction method used.

High salt concentrations hindered the formation of biofilms and granules required in conventional anaerobic reactors, however, the complete biomass retention provided by membrane in anaerobic membrane bioreactors (AnMBR) enables anaerobic treatment of saline wastewaters [220]. It has been proven that an increase in the concentration of sodium chloride causes a decrease in membrane permeability in MBR systems, being recovered when the salt is removed [221]. Several researchers determined the importance of osmotic pressure in cake-layer filtration originating from the interception of ions in the matrix of biopolymers in the cake layer [222–224]. Ionic strength directly affects osmotic pressure and filtration resistance by reducing cake-layer porosity when the ionic concentration increases in the solution flowing through the cake layer [223]. The effect of osmotic pressure depends not only on salt concentration in the mixed liquor, but also on the compression of the cake layer. When transmembrane pressure increases, water migrates from the cake and osmotic pressure increases, acting as a resistance to external forces applied to the cake [224]. Although the gel layer is very porous and has a large pore size, gel pores contain large amounts of SMP and colloids that provide negatively charged sites holding counter-ions, increasing gel layer filtration resistance even above that of the cake layer [225].

The aim of this study was to evaluate the EPS extraction from sludge of a pilot scale side-stream anaerobic membrane bioreactor in order to determine the real effect of polymeric

substances on the membrane fouling. The response surface methodology with a Box-Behnken design (BBD) was employed to examine the combined effect of contact time, temperature, and salinity on the extraction efficiency. The ratios of P, PS and HS in the total extracted organic matter in each BBD run were calculated based on the experimental and theoretical values of the total organic carbon. A kinetic study was also performed under the BBD optimal to obtain kinetic parameters such as the extraction velocity and the minimum contact. Hollow-fibre ultrafiltration assays were carried out and the effect of polymeric substances and salinity on the membrane fouling has been examined. A novel fouling model has also been proposed to determine the SRF and degree of retention of EPS under the same filtration/backwashing cycles of an AnMBR system.

7.2 Materials y methods

7.2.1 Materials

The sludge used came from a pilot side-stream AnMBR plant installed in a snack factory. Total and volatile solid concentration were 26.3 g TS/L and 15.3 g VS/L, respectively. Bovine serum albumin, D(+)-anhydrous glucose and sulphuric acid were supplied by VWR Chemicals (Germany) and humic acid was supplied by Sigma-Aldrich (USA). Sodium chloride and phenol were purchased from Labkem (Spain) and Riedel-de Haën (Germany), respectively. Folin-Ciocâlteu reagent, copper (II) sulphate pentahydrate, potassium antimony (III) tartrate trihydrate and sodium hydroxide were provided by Panreac AppliChem (Spain).

7.2.2 Extraction tests

Extraction was carried out on sludge that had previously been dried at room temperature, using distilled water or NaCl solutions as solvent and 0.5 wt% of total solids in the solvent. Contact between the sludge/solvent phases was performed using vortex agitation (VORTEX MVOR-03-SBS) or by ultrasonication (Ultrasons-H Selecta). EPS analysis was

carried out on the supernatant obtained by centrifugation (Eppendorf centrifuge, Centrifuge 5804) at 4500 rpm for 3 min. Total organic carbon (TOC) was measured using a TOC-VCSN (Shimadzu) analyser. Total concentration of proteins (P), polysaccharides (PS) and humic substances (HS) were determined according to the Bradford method [114], Dubois method [111] and Lowry's modified method [226], respectively. Standards for calibration were dissolved in distilled water with 0, 0.9 and 1.8 wt% of NaCl. Spectrophotometric readings were taken using a Hitachi U-2000 UV/vis spectrophotometer. The experimental extraction results were expressed in units of mass of P, PS, HS, and TOC extracted per unit of mass of sludge as total solid (w_P , w_{PS}, w_{HS} and w_{TOC} , mg/g TS). A Statgraphics Centurion 18 software package (Statistical graph Co., Rockville, MD, USA) was used for statistical processing.

The individual effect of salinity, temperature, contact mode and contact time on EPS extraction was examined. Extraction tests were performed using NaCl solutions or distilled water at 30-50 ºC applying ultrasound (U) or vortex agitation (v) for 5 and 10 min. Significant differences between EPS extracts were determined by analysis of variance (ANOVA) using the general linear model procedure. An alpha level of 95% ($p < 0.05$) was used to determine significance.

In a second stage, the individual and combined effect of ultrasonication time ($t = x_1$), sodium chloride concentration ($C_{NaCl} = x_2$), and temperature ($T = x_3$) on EPS extraction was investigated. Fifteen ultrasonic-assisted extraction tests were performed using a Box-Behnken design (BBD) by combining three levels of each independent factor (x_i). The factor levels were coded as −1 (0 min of ultrasonication, 0 wt% NaCl, 30º C), 0 or central point (30 min of ultrasonication, 0.9 wt% NaCl, 40 ºC), and +1 (60 min of ultrasonication, 1.8 wt% NaCl, 50 ºC). The mass of P, PS, HS, and TOC extracted per unit of mass of sludge were selected as response. A non-linear regression method was employed to fit the second-order polynomial (Eq. 43) to the experimental data of each response and to identify the relevant model terms. Considering all the linear terms, square terms, and linear-by-linear interaction items, the quadratic response model can be expressed as [227]:

$$w = \beta_0 + \sum \beta_i x_i + \sum \beta_{ii} \cdot x_i^2 + \sum \beta_{ij} \cdot x_i \cdot x_j \quad (43)$$

where, β_o is the offset term, β_i is the linear effect, β_{ii} is the quadratic effect, β_{ij} is the linear by linear interaction effect between the independent factors x_i and x_j.

A kinetic study was also carried out under the optimal extraction conditions selected with BBD results in order to determine and compare the extraction rate of P, PS and HS. Samples of the EPS extract were taken every 10 min until reaching a constant concentration of P, PS and HS, from which the ultimate extracted mass per gram of sludge, w_∞, was calculated. The following m-order kinetic model was employed to fit the experimental kinetic data [228,229]:

$$\frac{dw}{dt} = h(w_\infty - w)^p \quad (44)$$

where w is the mass fraction of solute extracted at a given time t, p is the order of the equation and h is the extraction rate constant. The boundary conditions were from t=0 to t and from w_0 to w, and the value of w_0 being the mass of P, PS, and HS extracted at time 0, without application of ultrasonication.

The integrated form of Eq. 44 for p=0, 1 and 2 is shown in Eqs. 45, 46 and 47, respectively, which were used to estimate w for each solute during the extraction process.

$$w = w_0 + h \cdot t \quad (45)$$

$$w = w_\infty - (w_\infty - w_0) \cdot e^{-h \cdot t} \quad (46)$$

$$w = w_\infty - \frac{w_\infty - w_0}{1 + h \cdot t \cdot (w_\infty - w_0)} \quad (47)$$

Eqs. 48 and 49 show the linearized form of Eqs. 46 and 47, respectively.

$$ln(w_\infty - w) = ln(w_\infty - w_0) - h \cdot t \quad (48)$$

$$\frac{t}{w - w_0} = \frac{1}{h \cdot (w_\infty - w_0)^2} + \frac{1}{w_\infty - w_0} \cdot t \tag{49}$$

Eqs. 45, 48 and 49 were employed to fit the experimental kinetic data and h was calculated for each type of EPS. The average absolute relative deviation (AARD) calculations according to Eq. 50, the root-mean square error (RMSE) calculations according to Eq. 51 and R^2 were used to assess the goodness of fittings of those kinetic models.

$$AARD = \frac{100}{j} \cdot \sum_{i=1}^{j} \frac{\left|w_{exp} - w_{cal}\right|_i}{w_{exp}} \tag{50}$$

$$RMSE = \sqrt{\frac{\sum_{i=1}^{j} \left(w_{exp} - w_{cal}\right)_i^2}{j}} \tag{51}$$

where j is the number of experimental data, and w_{exp} and w_{cal} are the mass of solute obtained experimentally and estimated by the model, respectively. Eqs. 45, 46 and 48 were employed to determine the values of w_{cal}.

7.2.3 Ultrafiltration tests

The degree of retention (α), the specific resistance to filtration (SRF), and the compressibility index of the gel layer of EPS (n) were determined. For that purpose, two extracts were selected, the ones with the highest and lowest EPS concentration, with an additional test being carried out in which 1.8 wt% salt was added to the extract obtained with distilled water in order to assess the contribution of salinity to the fouling process.

Fouling capacity was determined using batch dead-end tests lasting 20 h with total recirculation of the permeate, using the experimental setup shown in Fig. 31 PVDF hollow-fibre ultrafiltration membrane (Micronet R, Porous Fibers) was used with a nominal pore size of 0.03 μm, a length of 0.92 m, a diameter of 2.4 mm and an effective filtration area of 6.94×10^{-3} m^2, rolled on a support 6 cm in diameter. The membrane was connected at each end to a variable-

speed reversible peristaltic pump (Watson Marlow 520U). The membrane was placed in a 1-litre hermetic stirred tank with 0.8 L of the studied extract. A permeate vessel was placed inside the tank to store the permeate required for backwashing. Transmembrane pressure (TMP) and temperature were monitored using electronic probes PN2069 (IFM Electronics) and TR2432 (IFM Electronics). The filtration flux was determined from the pump calibration, the speed of which was controlled by a PLC. After each filtration test, the membrane was rinsed with tap water, and a chemical cleaning was carried out using a 500 mg/L sodium hypochlorite solution for 2 h.

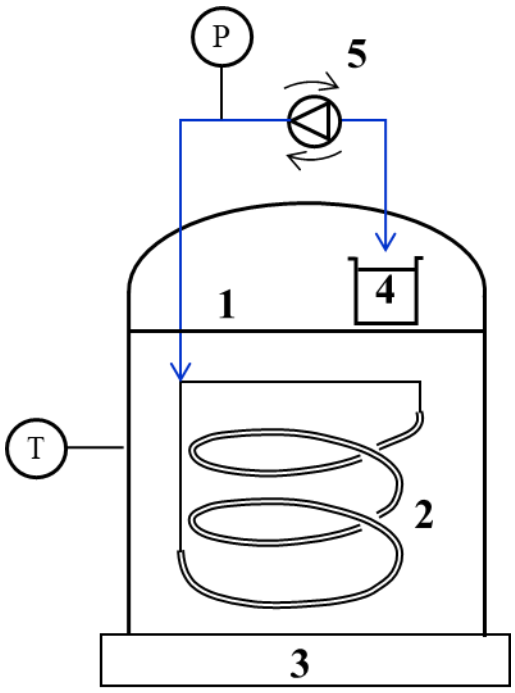

Fig. 31. Experimental set-up equipped with a 1 L stirred tank (1) with a single submerged hollow fiber membrane (2) supported by a magnetic stirrer with hot plate that supports the tank (3) and a reversible peristaltic pump (5) for filtration and backwash that is collected in a permeate vessel (4). P y T correspond to pressure and temperature sensors.

Given that the materials deposited on the membrane are highly deformable, resistance to filtration is affected by TMP and therefore by the flux. To correct that effect, resistance was determined at six different fluxes, J, and using filtration/backwashing cycles carried out on a continuous basis, as shown by Fig. 32. The flux series did not follow a rising or falling pattern, to avoid hysteresis effects. Filtration and backwash fluxes were initially set at 42, 52, 68, 84, 102, and 118 $L/m^2 \cdot h$, and were automatically reduced when TMP exceeded 250 mbar; which kept the

value of TMP between 50 mbar and 250 mbar. Thus, membrane filtered at least twice the volume of EPS solution contained in the tank at the end of each test, which represents a minimum of 231 L/m^2.

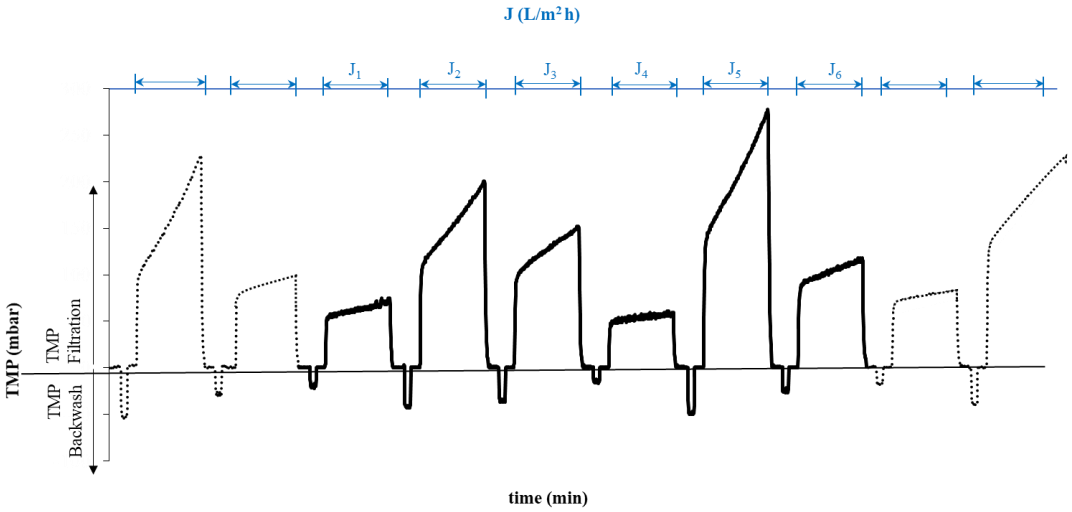

Fig. 32. Transmembranal pressure (TMP) during filtration and backwash with 6 different filtration flux.

Initial filtration resistance (R, m^{-1}) has been determined by the Darcy's law (Eq. 52) using the experimental TPM (Pa) at the beginning of the filtration stage for each flux J (Fig. 32).

$$R = \frac{TMP}{J \cdot m} \tag{52}$$

where μ is the permeate viscosity (Pa·s), which depends on the temperature, T (°C), in accordance with the equation:

$$\mu = \frac{0.479}{(T + 42.5)^{1.5}} \tag{53}$$

Logarithmic regression of R *vs* TMP was used to fit the resistance of the three preceding and succeeding filtration stages to the well-known power-law expression (Eq. 54) of the conventional filtration theory [230–232]. The results of n and the fitting parameter, κ, have been used to calculate the normalised resistance, R_n, at a reference pressure (TMP_{ref}) of 100 mbar:

$$R = \kappa(TMP)^n \quad (54)$$

$$R_n = R\left(\frac{TMP_{ref}}{TMP}\right)^n \quad (55)$$

Assuming that the SRF of the materials deposited on the membrane is constant at the reference pressure, and that α is independent of the membrane fouling level, the increase in resistance per unit of filtered volume will be proportional to the EPS concentration, C, of the filtered solution [232]:

$$\frac{dR_n}{dV} = \frac{SRF \cdot dm/A}{dV} = SRF \cdot \frac{\alpha \cdot C \cdot dV}{A \cdot dV} = \frac{SRF}{A}\alpha \cdot C \quad (56)$$

where V is the volume filtered over time, m is the mass of solute retained by the membrane and A is the membrane area, 6.94×10^{-3} m^2.

Moreover, the decrease in solute concentration in solution, -dC, can be expressed as:

$$-dC = \frac{dm}{V_t} = \frac{\alpha \cdot C \cdot dV}{V_t} \quad (57)$$

where V_t is the volume of solution in the filtration tank, 0.8 L.

Integrating Eq. 57, from the initial state, when concentration is C_0, and after filtering a volume V, the solute concentration is obtained as a function of the filtered volume, thus:

$$C = C_0 \cdot e^{\frac{-\alpha \cdot V}{V_t}} \quad (58)$$

Combining Eqs. 14 and 16 and integrating with boundary conditions from t=0 to t and from R_0 to R, the resistance is also expressed as a function of the filtered volume, thus:

$$R_n = R_0 + \frac{SRF \cdot V_t \cdot C_0}{A} \cdot \left(1 - e^{-\alpha \cdot V/V_t}\right) \quad (59)$$

where R_0 is the resistance at the beginning of the test, the unrecovered resistance after the chemical cleaning.

The product of SRF multiplied by the total mass of solute per unit of area, $V_t \cdot C_0/A$, represents the resistance due to total solute retention, R_S:

$$R_S = SRF \cdot \frac{V_t \cdot C_o}{A} \tag{60}$$

Finally, Eq. 61 shows the linearized form of Eq. 59, which was employed to obtain α and SRF from the variation of R_n with the filtered volume:

$$ln(R_0 + R_S - R_n) = ln\, R_S - \frac{\alpha}{V_t} \cdot V \tag{61}$$

7.3 Results and discussion

7.3.1 EPS extraction from AnMBR sludge

7.3.1.1 Effect of the extraction conditions

The experimental results of EPS extraction in units of mass extracted per unit of mass of total solids (w_{TOC} , w_P , w_{PS}, and w_{HS}), as a function of temperature, salinity, contact time and contact mode, are shown in Fig. 33 and Table 16.

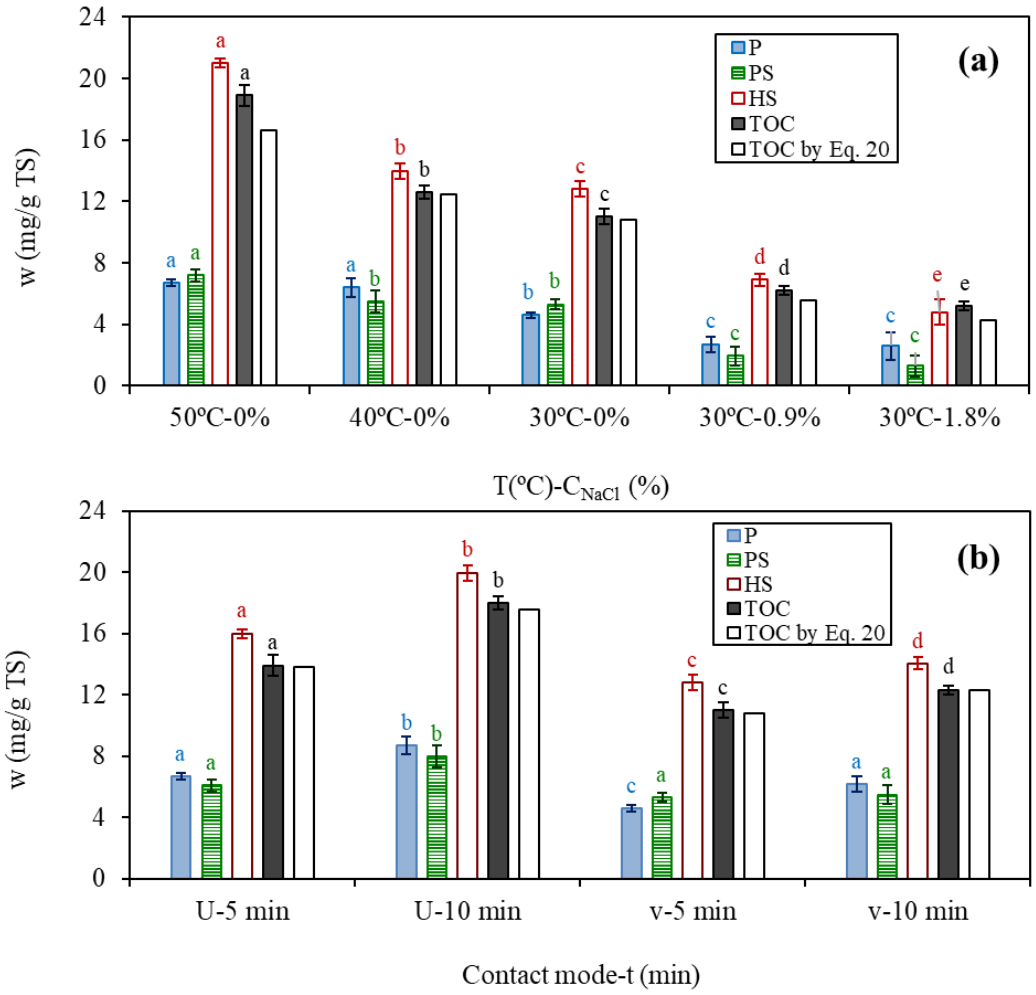

Fig. 33**.** Experimental mass extracted of HS, P, PS and TOC from AnMBR sludge (a) using vortex agitation for 5 min with water at 30-50 ºC or NaCl solutions at 30 ºC, and (b) using vortex agitation (v) and ultrasonication (U) for 5 or 10 min with water at 30 ºC. Different letters in the same solute indicate significant differences ($p<0.05$) in the mass extracted of this solute.

Table 16. Experimental values of the mass of P, PS, HS, and TOC per mass unit of sludge for the experimental-design test in ultrasonication-assisted extraction.

Run	$t=x_1$ (min)	$C_{NaCl}=x_2$ (wt%)	$T=x_3$ (ºC)	w_P (mg/g)	w_{PS} (mg/g)	w_{HS} (mg/g)	w_{TOC} (mg/g)
1	30	0.9	40	12.4±2.4	9.0±0.2	17.8±0.8	21.2±0.2
2	60	0.9	30	21.8±2.6	6.9±1.2	24.3±2.1	24.5±0.4
3	60	0.9	50	21.4±1.2	5.5±2.9	28.9±3.1	34.3±0.1
4	60	1.8	40	10.6±1.7	4.8±1.6	8.1±2.4	11.1±0.1
5	30	1.8	50	7.0±2.2	3.1±1.0	12.4±1.8	9.6±0.1
6	0	0.9	30	1.9±1.1	1.3±0.2	5.5±2.4	5.1±0.3
7	0	0	40	3.8±0.9	3.8±2.1	14.7±1.3	7.7±0.1
8	30	0.9	40	12.4±3.1	8.9±0.5	17.6±1.1	20.9±0.2
9	0	1.8	40	1.8±1.4	0.9±0.2	2.3±1.2	4.2±0.1
10	60	0	40	24.4±1.2	13.7±1.6	46.8±1.4	20.8±0.2
11	0	0.9	50	2.4±1.9	2.1±1.1	6.9±1.0	5.0±0.1
12	30	1.8	30	10.4±2.1	3.9±0.7	8.2±1.0	11.9±0.3
13	30	0	30	14.1±2.3	17.0±0.2	36.0±1.7	24.7±0.2
14	30	0	50	19.1±1.5	18.0±2.4	41.5±1.8	22.1±0.3
15	30	0.9	40	12.4±2.1	9.0±0.8	17.7±1.0	21.1±0.3

As can be seen from Fig. 33 (a), the overall extraction of organic matter increased using salt-free water as the solvent and 50 ºC. A significant increase in P, PS and HS extraction from about 2 to 7 mg/g TS for P and PS and from 4 to 21 mg/g TS for HS was obtained under the influence of an increase in temperature from 30 to 50 ºC and a reduction in salinity. It is interesting pointed that HS has resulted to be the major type of EPS released from the anaerobic sludge.

Effects of contact time and contact mode can be compared on the basis of the data given in Fig. 33 (b). It is observed that an ultrasonic contact has increased the rate of EPS diffusion during

extraction, obtaining extracts with higher amounts of P, PS and HS at both contact times. This means that the ultrasonic contact is more effective than the classical vortex contact [208,210,211], ensuring higher yields of EPS extraction at much shorter operating time. It is also observed that 10 min for vortex agitation only allows a partial extraction of the bound EPS, it being necessary to point out that longer contact times for vortex agitation.

Based on the empirical formulae of BSA ($C_{40}H_{62}O_{12}N_{10}$), D(+)-anhydrous glucose ($C_6H_{12}O_6$), and humic acid ($C_9H_9NO_6$) used as standards of the analysed compounds, the mass of organic carbon was determined per unit mass of each compound as 0.55 mg C/mg P, 0.40 mg C/mg PS, and 0.48 mg C/mg HS, and the total organic carbon associated with the three types of compounds, $w_{TOC-P,PS,HS,}$ was calculated as:

$$w_{TOC-P,PS,HS} = 0.55 \cdot w_P + 0.40 \cdot w_{PS} + 0.48 \cdot w_{HS} \quad (62)$$

The comparison of the theoretical TOC values by Eq. 62 with the experimental TOC results (Fig. 35), it can be concluded that the sum of the three groups of compounds analysed represents between 85% and 99% of the total organic matter extracted, depending on extraction conditions. The P concentration represent between 20% and 30% of the total organic matter, the PS values were the lowest, between 15% and 24%, and the HS were the most abundant EPS, between 54% and 60%. Dvořák et al. [233] also determined, using a sludge from a submerged MBR process, that the fraction of HS was slightly greater than P, PS, and DNA contents, 35% vs. 24%, 29% and 12% respectively. However, Chen et al. [234] using granular sludge from a submerged AnMBR, obtained a far lower proportion of HS, 22.2%. Many authors consider P and PS to be the more prevalent EPS [214,215], without taking into account of the HS values. Ding et al. [211] indicated that for sludge from a mesophilic submerged AnMBR, the P and PS content was 87.8% and 12.2%, respectively; Vincent et al. [235] reported a slightly lesser P content, 74%, in the sludge from a side-stream AnMBR, but Luna et al. [236] obtained that PS was the most prevalent EPS, 80.3%, in a submerged AnMBR.

The effects of temperature, salinity and contact time on EPS extraction for an ultrasonication-assisted extraction were examined using response surface methodology. The results of the experimental-design test in Table 16 show that PS was the least abundant EPS in all liquid extracts, representing between 10% and 25% of the overall polymeric substances extracted. Comparison of the experimental TOC results in Table 16 with the TOC values calculated by Eq. 62 shows that the sum of P, PS and HS accounts for more than 80% of the total organic matter extracted. which is in agreement with results depicted in Fig. 34. The statistical treatment of these experimental data from a BBD (Eq. 43) gave rise to the following second-order polynomials for an ultrasonication-assisted extraction:

$$w_P = 6.732 + 0.384 \cdot t - 2.020 \cdot C_{NaCl} - 0.072 \cdot t \cdot C_{NaCl} - 0.001 \cdot t^2 - 0.57 \cdot C_{NaCl}^2 \ (R^2=0.96) \quad (63)$$

$$w_{PS} = 8.452 + 0.403 \cdot t - 9.857 \cdot C_{NaCl} - 0.027 \cdot t \cdot C_{NaCl} - 0.005 \cdot t^2 + 2.629 \cdot C_{NaCl}^2 \ (R^2=0.94) \quad (64)$$

$$w_{HS} = 16.271 + 0.824 \cdot t - 16.590 \cdot C_{NaCl} - 0.244 \cdot t \cdot C_{NaCl} - 0.005 \cdot t^2 + 4.946 \cdot C_{NaCl}^2 \ (R^2=0.97) \quad (65)$$

$$w_{TOC} = 6.149 + 0.676 \cdot t + 7.991 \cdot C_{NaCl} - 0.057 \cdot t \cdot C_{NaCl} - 0.006 \cdot t^2 - 6.453 \cdot C_{NaCl}^2 \ (R^2=0.84) \quad (66)$$

R^2 coefficients were close to 0.9, in spite of the difficulty of the use of a heterogeneous material as this sludge. The EPS mass extracted from the sludge depends on the linear, quadratic, and combined effect of time and of solvent salinity. However, in Eqs. 63-66, the temperature effect does not appear, which means that the extraction with ultrasonic contact was not significantly affected by a temperature increase between 30 °C and 50 °C, as can also be seen in Fig. 34. This result can be due to the fact that the increase in temperature is in the order of the heterogeneous distribution of temperature in the liquid phase during sonication by the cavitation effect

The results of the analysis of variance in Fig. 34, and the parameters in Eqs. 63-66 show that, an increase in contact time and a decrease in salinity cause a positive effect on EPS extraction. From the HS linear terms, it can be observed that HS extraction is more negatively affected by the salt presence in the solvent. Finally, the effects t^2, $(t \cdot C_{NaCl})$, and C_{NaCl}^2 were also significant effects for HS extraction, as can be seen in Fig. 34.

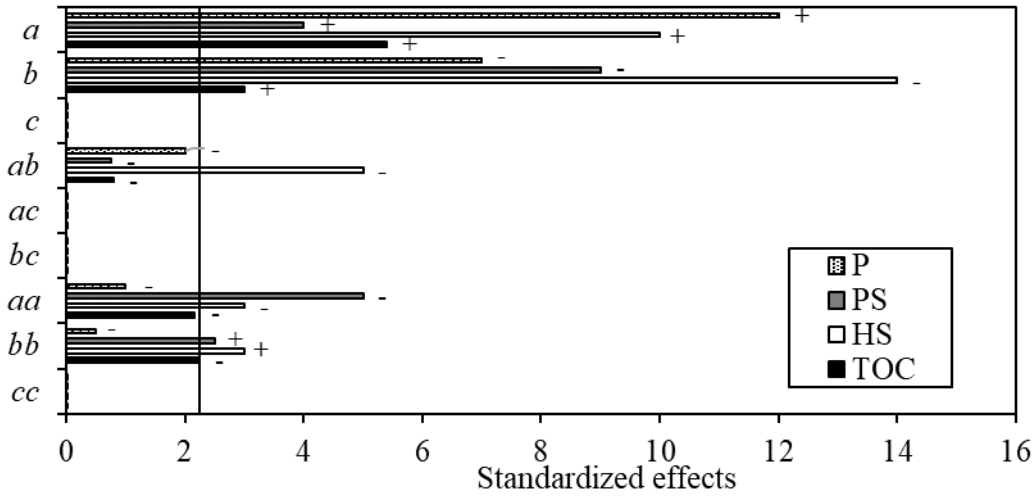

Fig. 34. Standardized effects of main factors and its interactions affecting EPS extraction where (a) is contact time, (b) is NaCl concentration and (c) is temperature.

Fig. 35 presents the experimental value compared with the predicted value from Eqs. 63-66. The fit between predicted values and experimental values was very close to the diagonal, with a slope of 1 for all compounds, and linear regression coefficients between 0.90 and 0.99, which confirms that quadratic models are a correct fit for the experimental results.

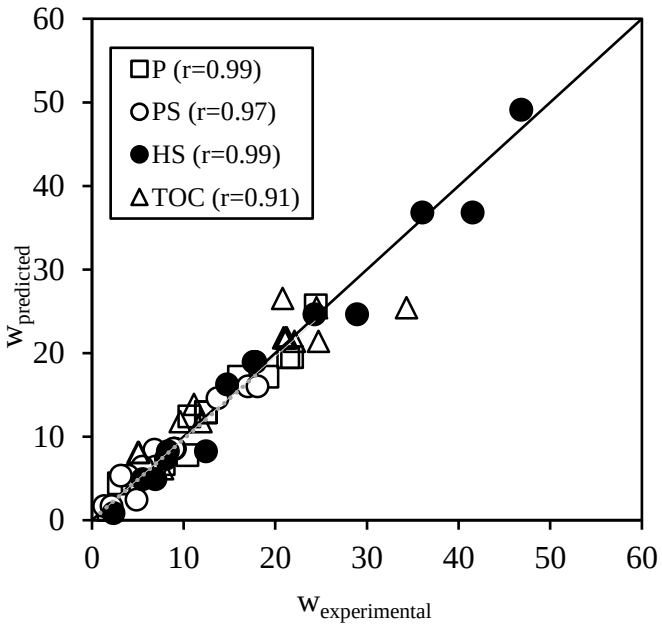

Fig. 35. The real experimental extraction value of P, PS, HS and TOC compared to the extraction value predicted by Eqs. 63-66.

Optimising the response of the experiment design for ultrasonication-assisted extraction shows that maximum extraction occurs when using salt-free water as the solvent, a temperature of 30 ºC

and a minimum contact time of 56 min (= t_∞), with a predicted ultimate value of w_∞=23±2 mg P/g TS, 19±5 mg PS/g ST, 54±3 mg HS/g TS and 33±5 mg TOC/g TS.

7.3.2 Kinetics of EPS extraction

Based on the optimum response from the experiment-design test, and to analyse the extraction rate of each type of polymeric substances, a kinetic study was performed by ultrasonication-assisted extraction, using water at 30 °C. To describe these extraction processes, zero-order (Eq. 45), first-order (Eq. 46 or Eq. 48) and second-order (Eq. 47 or Eq. 49) models were fitted the experimental data. The parameters for each model and statistical results are presented in

Table 17 and Fig. 36.

Fig. 36 (a) shows that initially, the mass extracted for each type of EPS increases nearly linearly with ultrasound time, reaching its ultimate value at about 60 min. This result of t_∞ is consistent with the optimal BBD response, which predicted a maximum contact time of 56 min. A value of w_∞ (

Table 17) close to 20 mg/g TS was obtained for P and PS, which was significantly lower than the value of 54 mg/g TS for HS, and all of them similar to those predicted by BBD. In addition,

Table 17 and Fig. 36 (a) also show the mass of P, PS, and HS extracted at t=0 min, without ultrasonication, which can be considered the loosely-bound EPS extracted from the outer layer of the flocs. This result indicates that the loosely-bound fraction was much larger for HS than for P and PS.

The model that best represented the experimental data of PS and HS extractions was the zero-order model, and consequently, its extraction rate (dw/dt=h) can be considered constant during ultrasonication contact. However, the models that best represented the experimental data of P extraction were the zero-order and the second-order models as shown Fig. 36(b) and

Table 17. The difference between both models was considered significant since their coefficients of determination were 0.989 and 0.996, and the absolute deviation (AARD) were 6.4% and 0.4% for the zero-order and the second-order models, respectively. A more detailed analysis of the results in Fig. 36 (b) shows the zero-order model described quite well the experimental data, except for a slight difference in w_0. However, the second-order model predicts a $w_\infty \approx 52$ mg P/g TS, a t_∞ of approximately 650 min and a protein extraction of 28.9 mg/g ST at 90 min, which is significantly higher than the experimental values. Based on this result, we can conclude that a zero-order model good describes the experimental kinetic data of the P, PS and HS extraction. This model is showing that the extraction rate (h) and the ultimate extraction (w_∞) were significant higher for HS than for P and PS compounds. Using Eq. 45 and w_∞ values, it was determined that the minimum ultrasonication time (t_∞) for the optimum extraction of each compound was ranged from 54 to 56 min and the final extract presented 95.5, 89 and 219.5 mg/L of P, PS and HS, respectively.

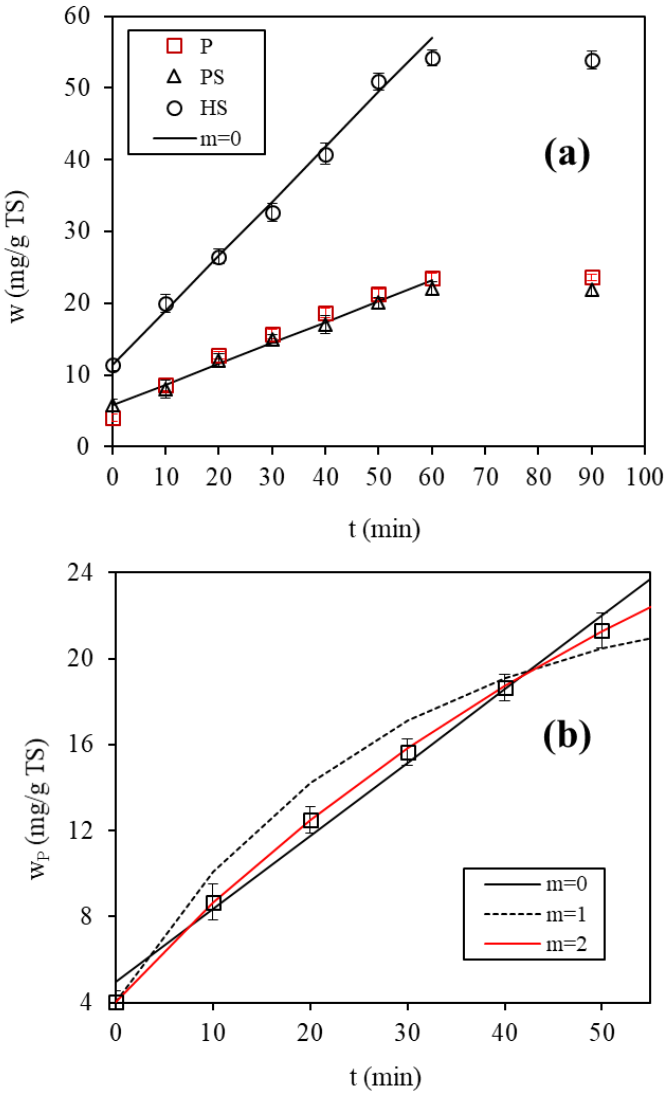

Fig. 36. (a) The effect of ultrasonication time on the mass extracted (w) of P, PS and HS extracted using water at 30 °C. (b) Experimental data (symbols) and the predicted data by Eq. 45 (line). Comparison of kinetic models for P extraction.

Table 17. Parameters of each kinetic model used to fit the extraction results shown in Fig. 36 and the values of the initial extracted mass at t=0 min (w_0) and of the ultimate extracted mass at $t \geq t_\infty$ (w_∞) for P, PS and HS. AARD and RMSE were calculated by Eqs. 50 and 51.

PARAMETERS	P	PS	HS
w_0 (mg/g TS)	4.0±0.5	5.8±0.6	11.4±0.7
w_∞ (mg/g TS)	23.6±0.4	22.0±0.2	54.2±0.2
h (by Eq. 45, mg/g ST○min)	0.34	0.29	0.76
w_0 (by Eq. 45, mg/g TS)	4.94	5.73	11.36
R^2 (Eq. 45)	0.989	0.993	0.994
AARD (Eq. 45)	6.38	3.23	2.59
RMSE (Eq. 45)	0.60	0.42	0.64
t_∞ by Eq. 45 (min)	54.5	56.1	56.3
h (by Eq. 48, min^{-1})	0.037	0.035	0.037
$(w_\infty - w_0)$ (by Eq. 48, mg/g TS)	19.50	16.20	42.80
R^2 (Eq. 48)	0.939	0.892	0.800
AARD (Eq. 46)	7.71	11.33	14.87
RMSE (Eq. 46)	1.15	1.53	5.08
h (kg ST/mg○min)	0.018	-	-
$(w_\infty - w_0)$ (by Eq. 49, mg/g TS)	55.6	-	-
R^2 (Eq.49)	0.996	0.267	0.154
AARD (Eq. 47)	0.42	-	-
RMSE (Eq. 47)	0.09	-	-

7.3.3 Filtration test of EPS solutions

7.3.3.1 Fouling rate, SRT and degree of retention

An assessment of the fouling capacity of a submerged hollow-fibre membrane with three solutions was made: (a) extract of the highest EPS concentration, 138.8 mg TOC/L, obtained with distilled water and 60 minutes' ultrasonication, (b) the same extract but with salt added, 138.8 mg TOC/L and 1.8 wt% salt, and (c) extract of lowest EPS concentration, 35.1 mg TOC/L, obtained with 1.8 wt% of salt without ultrasonication.

Fig. 37 (a) shows evolution of resistance versus the filtered volume of each solution. The more concentrated EPS solution with salt added fouled the membrane faster than the concentrated EPS solution without salt, which in turn fouled faster than the more diluted EPS solution despite its salt content. Filtering 1.6 L of the solutions with 138.8 TOC mg/L raised resistance to 1.11 and $1.88 \cdot 10^{12}$ m^{-1}, being greater for the salty solution, whereas filtering the same volume of the diluted EPS solution, 35.1 mg TOC/L, took resistance to just $0.57 \cdot 10^{12}$ m^{-1} (Table 4). An assessment of the contribution of salt on membrane fouling in the absence of EPS was made by using a solution of salt in water. For that purpose, the resistance to filtration of a clean membrane was determined with distilled water and water with a salt concentration of 1.8 wt%, with a small difference in resistance being observed of 0.29 and $0.45 \cdot 10^{12}$ m^{-1}, respectively. That small increase of only $0.16 \cdot 10^{12}$ m^{-1} is significantly less than that observed in filtering solutions with the highest EPS concentration, which confirms that the effect of salt on membrane fouling depends on the presence of EPS.

Other authors have studied the effect of salinity on the fouling of aerobic membrane bioreactors. Guo et al. [237] studied the behaviour of three MBR treating synthetic municipal wastewater without salt and with the addition of 0.75% and 1.5% of salt, observing that after 4 days of operation at 12.5 $L/m^2 \cdot h$, the TMP reached values of 70, 170, and 220 mbar, respectively. Jang et al. [238] determined that after 20 days of operation with a flux of 3.5 $L/m^2 \cdot h$,

the salinity reduced by half the time needed to reach a reference TMP of 270 mbar which decrease from 132 h using salt-free residual water to 60 h using residual water with 20 g/L of salt.

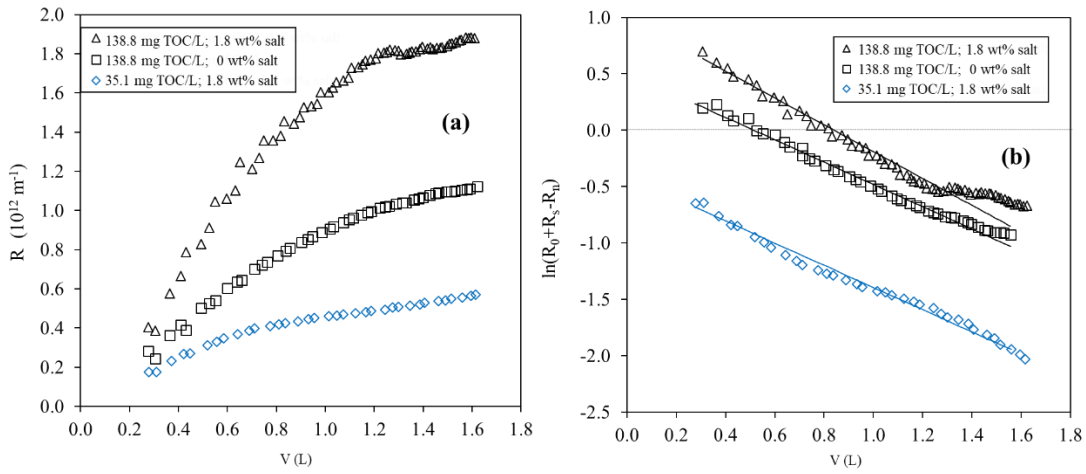

Fig. 37. Evolution of membrane fouling with different EPS extracts relative to the filtered volume, based on (a) resistances to filtration, and (b) based on the linearised fouling model (Eq. 61).

The resistance to backwashing of the diluted EPS solution with salt and the salt-free concentrated EPS solution increased slightly from $0.25\pm0.1\cdot10^{12}$ m^{-1} to $0.29\pm0.1\cdot10^{12}$ m^{-1}. However, in the case of the concentrated and salty EPS solution, resistance to backwashing increased appreciably until it reached a value of $0.38\cdot10^{12}$ m^{-1}, which means that the increase in internal resistance is produced by the combined effect of the EPS and salt.

The degree of retention, α, and specific resistance to filtration, SRF, were determined based on the model described in section 2.4. Fig. 37 (b) represents the experimental resistance results linearized with respect to filtered volume, in accordance with Eq. 61. To minimize bias, robust regressions were carried out using Huber's method, using 1.345 as tuning parameter to obtain the regression parameters with a confidence level of 95%.

The values for SRF and α are shown in

Table 18. It is worth highlighting that in spite of the resistance reached in the solution with low EPS concentration, $0.57\cdot10^{12}$ m^{-1}, is notably lower than the value for the concentrated solution of the same salinity, $1.88\cdot10^{12}$ m^{-1}; the specific resistance to filtration of both solutions was the

same, 161.1 and $169.4 \cdot 10^{12}$ m/kg TOC, respectively. Those values are of the same order as those obtained by Hong et al. [225], $193 \cdot 10^{12}$ m/kg in a dead-end stirred cell with a flat sheet membrane. However, it should be noted that they used a biomass suspension with a concentration of 4 g/L, which means that the SRF obtained in our work for the gel layer formed by the EPS is only slightly lower than the SRF of the cake of the above-mentioned work. Lin et al. [224] determined the cake resistance under the same conditions in a flat-sheet membrane submerged MBR, before and after replacing the supernatant by water, observing that cake resistance decreased from $6.0 \cdot 10^{12}$ m^{-1} to $0.85 \cdot 10^{12}$ m^{-1}, which means that the biopolymers retained by the cake contribute more to filtration resistance than the particulate matter. Hemmelman et al. [220] in an AnMBR treating saline wastewater determined an SRF of $270 \cdot 10^{12}$ m/kg, suggesting the formation of a dense and compact cake layer and single cell growth as the drawbacks of the filtration stage of AnMBR's in saline conditions. The experimental value of SRF of the concentrated EPS solution without salt was notably lower, $103.8 \cdot 10^{12}$ m/kg TOC. Zhang et al. [223] explained that although MF or UF membranes cannot reject inorganic salts, the negative electric charge of functional groups in EPS lead to a higher concentration of counter-ions in the cake matrix than in the permeate, resulting in an osmotic pressure difference that is the main contributor to filtration resistance.

With respect to the degree of retention, it was notably higher, 95%, for the solution with the higher EPS concentration and 1.8 wt% salt, than the other two solutions, 79%. Those results show that, as the filtration resistance, the degree of retention also increases as the result of a combined effect of the EPS concentration and the salt.

Table 18. Resistance, compressibility index and model parameters for the three EPS extracts.

C_{NaCl} (wt%)	TOC (mg/L)	R^a (10^{12} m^{-1})	n^a	SRF (10^{12} m/kgTOC)	α (%)
0	138.8	1.11	0.23	103.8	79
1.8	138.8	1.88	0.03	169.4	95
1.8	35.1	0.57	0.04	161.1	79

(a) Resistance to filtration and compressibility index after filtering 1.6 L of solution

7.3.4 Compressibility index

Fig. 38 shows the evolution of the compressibility index versus the filtered volume of the three solutions. The compressibility index of the gel layer generated in filtering the solution with higher concentration of organic matter, 138.8 mg TOC/L, salt-free, was greater than for the other two solutions, and decreased slowly from 0.29 to 0.23. Conversely, the compressibility index of the gel layer formed during the filtration of the solution with the same concentration of EPS but with 1.8 wt% of salt decreased notably during the filtration process, reaching a final value of 0.03, which, in practice, means that the gel layer was incompressible at the end of the test. Those results indicate that the compressibility index is not only dependent on the elasticity of the materials that form the cake, but also on the salinity that provides rigidity to the gel layer as a consequence of the increase in osmotic pressure that opposes interstitial water migration involved in cake compression [224]. Finally, the solution with lower EPS concentration, 35.1 mg TOC/L and 1.8 wt% of salt, showed a low compressibility index that remained relatively constant over time, 0.06±0.03, due to the formation of a thin gel layer on the membrane that was barely affected by the compression forces.

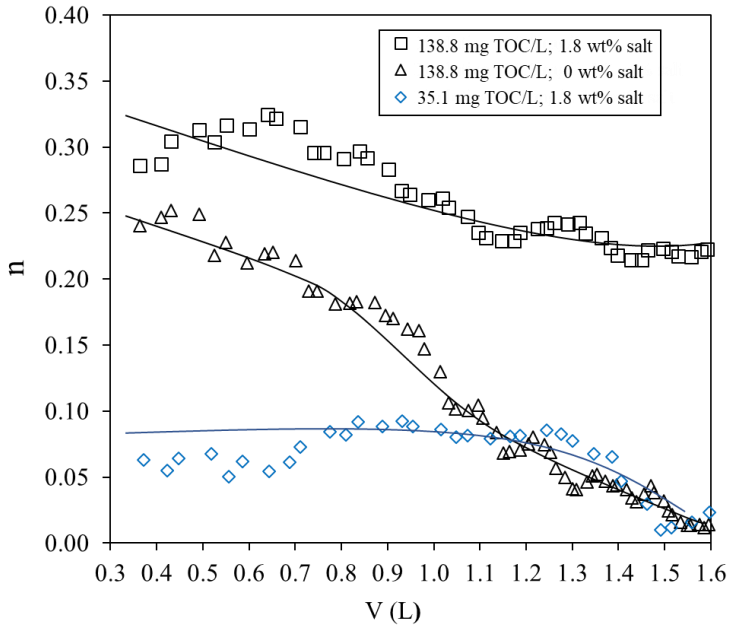

Fig. 38. Evolution of the compressibility index of the various solutions relative to the filtered volume.

7.4 Conclusion

The contact time needed for extracting EPS from the AnMBR sludge must be greater than the times normally used, being 50 minutes the required time for ultrasonication-assisted extraction. Temperatures between 30 °C and 50 °C do not significantly affect the EPS extraction process whilst contact time and the absence of salt from the solvent favour EPS recovery. Over 97% of the total organic matter extracted from the sludge of the side-stream AnMBR matches proteins, polysaccharides, and humic substances. Humic substances were the higher fraction of EPS extracted, between 50% and 58% of TOC, whereas the content of the compounds commonly considered as prevalent EPS, proteins and polysaccharides, was significantly lesser, 24-32% and 14-16%, respectively. A fouling model allowed to determine the degree of retention, the SRF and the compressibility index of the gel layer formed by EPS extracted from AnMBR sludge with and without salt. The degree of retention of EPS was higher than 79%, reaching 95% for the highest EPS and salt concentrations. The EPS extract with a concentration of 138.8 mg TOC/L and 1.8 wt% salt causes faster fouling than that due to EPS and to salt separately. 1.8 wt% salt

increases the SRF of EPS from $103.8 \cdot 10^{12}$ to $165.3 \cdot 10^{12}$ m/kg TOC, and provides rigidity to the EPS gel layer as a consequence of the increase in osmotic pressure that opposes the compression.

Capítulo 8: Conclusiones generales

La tecnología AnMBR aplicada al tratamiento de vertidos residuales es una alternativa eficaz frente a otros tratamientos convencionales. La calidad del efluente obtenida, la adaptación a distintos tipos de aguas residuales, su bajo consumo energético o su diseño compacto hacen que sea una tecnología atractiva a la hora de implementarla a gran escala. Sin embargo, el ensuciamiento de las membranas sigue siendo el principal cuello de botella al que se enfrenta el desarrollo de esta tecnología.

Esta tesis se ha centrado en el estudio del proceso de ensuciamiento de dos membranas de ultrafiltración de distinto tipo, operados en paralelo con los mismos fangos anaerobios mediante ensayos de aproximadamente 7 días de duración. Por otra parte, se ha estudiado la cinética y la eficacia de la extracción de EPS.

Se han empleado dos montajes experimentales, uno de ellos equipado con un módulo de membrana sumergida de fibras huecas y, el otro, con una membrana tubular externa operada con recirculación e inyección de gas, en modo *gas-lift*.

Se ha estudiado cómo el ensuciamiento se ve afectado por la configuración de la membrana. Mediante diseños de experimentos de Box-Behnken, se ha determinado cuales son los parámetros más influyentes tanto sobre el ensuciamiento reversible como sobre el ensuciamiento irreversible. Por otra parte, se ha estudiado el comportamiento del proceso de filtración de tres fangos anaerobios distintos ante las dos tecnologías de filtración.

En primer lugar, se ha demostrado que las condiciones de operación propias de cada tipo de membrana, afecta a la distribución del tamaño de partícula, a la concentración y retención de EPS, a la concentración del fango, a las velocidades de ensuciamiento reversible e irreversible y a la eficacia de las operaciones de limpieza química.

Se ha comprobado que, debido al estrés mecánico provocado por la recirculación de la membrana externa, la fracción de partículas menores de 10 µm aumentó de 25.1% a 34.6% en tan solo un día, en cambio la distribución de tamaño de las mismas partículas apenas se vio alterado en las condiciones de operación propias de la membrana sumergida. La concentración de sólidos

suspendidos volátiles descendió de 3.3 a 1.2 g VSS/L en 7 días en el sistema de filtración con membrana externa disminuyendo la actividad metanogénica total en un 40%, sin embargo, la actividad metanogénica específica se mantuvo constante.

También se observó que la concentración de proteína y polisacáridos solubles en el fango, tras 7 días de filtración en recirculación total, fueron un 20 y un 37% superiores en el equipo de filtración equipado con la membrana tubular externa que en el de la membrana sumergida de fibras huecas.

Con respecto a la concentración inicial de EPS en el fango, la capacidad de retención de la membrana sumergida fue ligeramente superior que la de la membrana externa tras 7 días de filtración. En cambio, con respecto a los EPS que permanecen en el fango tras 7 días de filtración, la retención de EPS, principalmente proteínas y sustancias húmicas, fue superior en la membrana externa.

La elevada capacidad de retención de proteínas en ambas membranas con los diferentes tipos de fangos, prueba que estas juegan un papel muy importante en el ensuciamiento de las membranas.

Respecto a la resistencia a la filtración, se emplearon ciclos de filtración de 15 minutos de duración, con el mismo flujo de gas en las dos membranas, 1.2 $Nm^3/m^2 \cdot h$, y una velocidad de recirculación en la membrana tubular de 0.51 m/s, y se observó que la resistencia total de la membrana tubular externa, con un flujo de 12 – 15 L/m^2h, alcanzó 9.3×10^{12} m^{-1} en 7 días. En cambio, la resistencia total de la membrana sumergida de fibras huecas no superó 1.1×10^{12} m^{-1} a pesar de operar con un flujo más elevado, entre 15 y 25 $L/m^2 \cdot h$, y durante un periodo de tiempo mayor, 12 días.

La efectividad del proceso de limpieza también fue diferente en ambas membranas. Mientras que un aclarado con agua seguido en un enjuague con 100 mg/L NaClO fue suficiente para que la membrana sumergida recuperase los valores iniciales de resistencia, la membrana tubular

necesitó una limpieza química con 500 mg/L de NaClO seguida de una limpieza ácida con 100 mg/L de $H_2C_2O_4$.

El diseño de experimentos de Box-Behnken ha resultado ser una herramienta de gran utilidad a la hora de determinar cuáles son los efectos individuales y combinados de las variables de operación que tienen mayor influencia sobre el ensuciamiento de las membranas. Se ha evaluado el efecto del flujo de filtración y contralavado, la duración de la filtración y el contralavado, el flujo de gas y en el caso de la membrana externa, la velocidad de recirculación, sobre el ensuciamiento reversible e irreversible de ambas membranas,

El ensuciamiento reversible se mantuvo por debajo de 0.55 mbar/min en la membrana externa empleando flujos de filtración comprendidos entre 11 y 13 L/m^{2}h. Sin embargo, el aumento irreversible de la resistencia, basado en la producción neta de permeado, osciló entre 0.43 y 7.2×10^{12} m^{-2}, dependiendo, principalmente, de la velocidad de recirculación. El ensuciamiento irreversible en la membrana sumergida fue mucho menor, entre 0.11 y 1.7×10^{12} m^{-2} a pesar de emplear flujos de filtración superiores, entre 18 y 22 L/m^{2}h, con los que el ensuciamiento reversible también fue mayor, hasta 2.1 mbar/min.

Se observó un incremento significativo de la velocidad de ensuciamiento reversible cuando aumentó la intensidad del contralavado en ambas membranas. Sin embargo, la intensidad del contralavado tuvo un menor efecto sobre la velocidad de ensuciamiento irreversible.

Además, se estudió el proceso de filtración de tres fangos anaerobios procedentes del tratamiento anaerobio de tres aguas residuales distintas seleccionadas por su composición química. Las aguas residuales procedían de una fábrica de snacks, por su alto contenido en aceites y grasas, agua residual de matadero por su alto contenido en proteínas y agua residual de cervecera por su alto contenido en carbohidratos. Durante 3 meses fangos anaerobios de una planta de gestión de biorresiduos se alimentaron con aguas residuales de cada fábrica.

Los fangos anteriores se sometieron a ensayos de filtración. Se empleó un flujo de 15 L/m^{2}h en la membrana tubular externa y un flujo de 20 L/m^{2}h en la membrana sumergida de fibras

huecas. Con cada uno de los fangos, cada 12 horas, se determinó el flujo crítico mediante el método *flux-step*, empleando 8 flujos de filtración comprendidos entre 12 y 18 L/m^{2}h en la membrana externa y entre 17 y 23 L/m^{2}h en la membrana sumergida.

Todos los parámetros de ensuciamiento estudiados indicaron que el fango que con el que la velocidad de ensuciamiento es mayor, tanto en la membrana externa como en la membrana sumergida, fue el fango procedente del agua residual de la fábrica de snack más que el de agua residual de matadero que a su vez muestra una mayor capacidad de ensuciamiento que el procedente de cervecera. Igualmente se observó que el ensuciamiento de la membrana externa fue siempre mayor que en el de la membrana sumergida. Las diferencias observadas en las primeras horas, en los que los valores de TMP iniciales fueron casi el doble en la membrana externa, pueden ser debidas a la ruptura de flóculos causado por el estrés mecánico del circuito de recirculación.

Al finalizar los ensayos se limpiaron las dos membranas hasta alcanzar sus resistencias originales. Mientras que para limpiar la membrana sumergida fue suficiente un enjuagado con agua seguido de dos limpiezas químicas de 100 y 500 mg/L de NaClO y una limpieza final de 100 mg/L de $H_2C_2O_4$, en el caso de la membrana externa, tras filtrar fango de agua residual de fábrica de snacks y fango de agua residual de matadero fue necesaria una limpieza extra con 150 mg/L de $H_2C_2O_4$.

Finalmente, se llevó a cabo un estudio sobre su caracterización bajo distintas condiciones de extracción y su efecto sobre el ensuciamiento de una membrana de fibra hueca. Se estudio de la influencia de la temperatura, concentración salina, tiempo de contacto y modo de contacto.

Se ha comprobado que proteínas, polisacáridos y sustancias húmicas componen entre el 80 y 99% de la materia orgánica total extraía del fango, siendo entre un 50 y un 64% sustancias húmicas.

La extracción asistida por ultrasonidos fue más eficaz que la extracción con agitación en vortex, asegurando mayores rendimientos de extracción de EPS en tiempos de contacto más cortos.

La extracción de proteínas, polisacáridos y sustancias húmicas mediante ultrasonidos apenas se vio afectada por el incremento de temperatura de 30 a 50ºC, sin embargo, el tiempo de contacto y salinidad si afectan significativamente al proceso de extracción de EPSs. El mayor rendimiento de extracción se obtuvo cuando la extracción se llevó a cabo con 30°C, en agua sin sal durante un tiempo de 50 min de contacto.

Se ha comprobado que en presencia de un 1.8 % de NaCl la resistencia específica de extractos de EPS a distintas velocidades de permeado aumentó de $103.8 \cdot 10^{12}$ m/kg TOC a $169.4 \cdot 10^{12}$ m/kg TOC. La presencia de sal proporcionó rigidez a la capa de EPS reduciendo enormemente el índice de compresibilidad de 0.23 a 0.03.

Referencias

[1] C. Ramos, A. García, V. Diez, Performance of an AnMBR pilot plant treating high-strength lipid wastewater: Biological and filtration processes, Water Res. 67 (2014) 203–215. https://doi.org/10.1016/j.watres.2014.09.021.

[2] F. Meng, S. Zhang, Y. Oh, Z. Zhou, H.S. Shin, S.R. Chae, Fouling in membrane bioreactors: An updated review, Water Res. 114 (2017) 151–180. https://doi.org/10.1016/j.watres.2017.02.006.

[3] E. Jeong, H.W. Kim, J.Y. Nam, Y.T. Ahn, H.S. Shin, Effects of the hydraulic retention time on the fouling characteristics of an anaerobic membrane bioreactor for treating acidifi ed wastewater, Desalin. Water Treat. 18 (2010) 251–256. https://doi.org/10.5004/dwt.2010.1781.

[4] D. Jeison, P. Telkamp, J.B. van Lier, Thermophilic Sidestream Anaerobic Membrane Bioreactors: The Shear Rate Dilemma, Water Environ. Res. 81 (2009) 2372–2380. https://doi.org/10.2175/106143009x426040.

[5] S.H. Roh, Y.N. Chun, J.W. Nah, H.J. Shin, S. Il Kim, Wastewater treatment by anaerobic digestion coupled with membrane processing, J. Ind. Eng. Chem. 12 (2006) 489–493.

[6] A. Spagni, S. Casu, N.A. Crispino, R. Farina, D. Mattioli, Filterability in a submerged anaerobic membrane bioreactor, Desalination. 250 (2010) 787–792. https://doi.org/10.1016/j.desal.2008.11.042.

[7] Z. Huang, S.L. Ong, H.Y. Ng, Feasibility of submerged anaerobic membrane bioreactor (SAMBR) for treatment of low-strength wastewater, Water Sci. Technol. 58 (2008) 1925–1931. https://doi.org/10.2166/wst.2008.749.

[8] K.C. Wijekoon, C. Visvanathan, A. Abeynayaka, Effect of organic loading rate on VFA production, organic matter removal and microbial activity of a two-stage thermophilic anaerobic membrane bioreactor, Bioresour. Technol. 102 (2011) 5353–5360. https://doi.org/10.1016/j.biortech.2010.12.081.

[9] P. Sui, X. Wen, X. Huang, Membrane fouling control by ultrasound in an anaerobic membrane bioreactor, Front. Environ. Sci. Eng. China. 1 (2007) 362–367. https://doi.org/10.1007/s11783-007-0062-9.

[10] A. Saddoud, I. Hassaïri, S. Sayadi, Anaerobic membrane reactor with phase separation for the treatment of cheese whey, Bioresour. Technol. 98 (2007) 2102–2108. https://doi.org/10.1016/j.biortech.2006.08.013.

[11] M.S. Kim, D.Y. Lee, D.H. Kim, Continuous hydrogen production from tofu processing waste using anaerobic mixed microflora under thermophilic conditions, in: Int. J. Hydrogen Energy, 2011: pp. 8712–8718. https://doi.org/10.1016/j.ijhydene.2010.06.040.

[12] A. Torres, A. Hemmelmann, C. Vergara, D. Jeison, Application of two-phase slug-flow regime to control flux reduction on anaerobic membrane bioreactors treating wastewaters with high suspended solids concentration, Sep. Purif. Technol. 79 (2011) 20–25. https://doi.org/10.1016/j.seppur.2011.03.006.

[13] K. Stamatelatou, A. Kopsahelis, P.S. Blika, C.A. Paraskeva, G. Lyberatos, Anaerobic digestion of olive mill wastewater in a periodic anaerobic baffled reactor (PABR) followed by further effluent purification via membrane separation technologies, J. Chem. Technol. Biotechnol. 84 (2009) 909–917. https://doi.org/10.1002/jctb.2170.

[14] A. Saddoud, S. Sayadi, Application of acidogenic fixed-bed reactor prior to anaerobic membrane bioreactor for sustainable slaughterhouse wastewater treatment, J. Hazard. Mater. 149 (2007) 700–706. https://doi.org/10.1016/J.JHAZMAT.2007.04.031.

[15] B.E.L. Baêta, R.L. Ramos, D.R.S. Lima, S.F. Aquino, Use of submerged anaerobic membrane bioreactor (SAMBR) containing powdered activated carbon (PAC) for the treatment of textile effluents, Water Sci. Technol. 65 (2012) 1540–1547. https://doi.org/10.2166/wst.2012.043.

[16] H. Lin, W. Peng, M. Zhang, J. Chen, H. Hong, Y. Zhang, A review on anaerobic membrane bioreactors: Applications, membrane fouling and future perspectives, Desalination. 314 (2013) 169–188. https://doi.org/10.1016/j.desal.2013.01.019.

[17] R.K. Dereli, M.E. Ersahin, H. Ozgun, I. Ozturk, D. Jeison, F. van der Zee, J.B. van Lier, Potentials of anaerobic membrane bioreactors to overcome treatment limitations induced by industrial wastewaters, Bioresour. Technol. 122 (2012) 160–170. https://doi.org/10.1016/j.biortech.2012.05.139.

[18] B.E. Rittmann, Aerobic biological treatment. Water treatment processes, Environ. Sci. Technol. 21 (1987) 128–136. https://doi.org/10.1021/es00156a002.

[19] C.W. Smith, D. Di Gregorio, R.M. Talcott, The use of ultrafiltration membrane for activated sludge separation, in: Proc. 24th Annu. Purdue Ind. Waste Conf., West Lafayette, 1969: pp. 1300–1310.

[20] I. Bemberis, P.J. Hubbard, F.B. Leonard, Membrane sewage treatment systems - potential for complete wastewater treatment, in: Am. Soc. Agric. Engneers, Chicago, Illinois, 1971: pp. 1–28.

[21] J.R. Bailey, I. Bemberis, P.J. Hubbard, F.B. Leonard, J.B. Presti, Phase I Final Report - Shipboard Sewage Treatment System, (1971).

[22] H.E. Grethlein, Anaerobic digestion and membrane separation of domestic wastewater, J. Water Pollut. Control Fed. 50 (1978) 754–763.

[23] K. Yamamoto, M. Hiasa, T. Mahmood, T. Matsuo, DIRECT SOLID-LIQUID SEPARATION USING HOLLOW FIBER MEMBRANE IN AN ACTIVATED SLUDGE AERATION TANK, in: Water Pollut. Res. Control Bright., Elsevier, 1988: pp. 43–54. https://doi.org/10.1016/B978-1-4832-8439-2.50009-2.

[24] S. Kimura, Japan's aqua renaissance '90 project, in: Water Sci. Technol., 1991: pp. 1573–1582. https://doi.org/10.2166/wst.1991.0611.

[25] K. Minami, K. Okamura, S. Ogawa, T. Naritomi, Continuous anaerobic treatment of wastewater from a kraft pulp mill, J. Ferment. Bioeng. 71 (1991) 270–274. https://doi.org/10.1016/0922-338X(91)90280-T.

[26] K. Minami, A trial of high performance anaerobic treatment on wastewater from a kraft pulp mill, Desalination. 98 (1994) 273–283. https://doi.org/10.1016/0011-9164(94)00152-9.

[27] S. Churchouse, D. Wildgoose, Membrane Bioreactors Hit the Big Time: - from Lab to Full Scale Application, in: Cranfield University, School of Water Sciences, Cranfield, 1999.

[28] P.M. Sutton, A. Li, R.R. Evans, S.R. Korchin, DORR-OLIVER'S FIXED-FILM, SUSPENDED-GROWTH ANAEROBIC SYSTEMS FOR INDUSTRIAL WASTEWATER TREATMENT AND ENERGY RECOVERY., in: Proc. Ind. Waste Conf., 1983: pp. 667–675.

[29] S. Judd, C. Judd, The membrane bioreactors site, (n.d.). www.thembrsite.com (accessed July 15, 2020).

[30] R. Marín Galvín, Tipología de los vertidos a los saneamientos públicos, Tecnoaqua. 30 (2018) 34–46.

[31] Metcalf and Eddy Inc., Ingeniería de aguas residuales: tratamiento, vertido y reutilización.,

McGraw-Hill, 1995.

[32] H. Lin, W. Peng, M. Zhang, J. Chen, H. Hong, Y. Zhang, A review on anaerobic membrane bioreactors: Applications, membrane fouling and future perspectives, Desalination. 314 (2013) 169–188. https://doi.org/10.1016/j.desal.2013.01.019.

[33] V. Diez, C. Ramos, J.L. Cabezas, Treating wastewater with high oil and grease content using an Anaerobic Membrane Bioreactor (AnMBR). Filtration and cleaning assays, Water Sci. Technol. 65 (2012) 1847–1853. https://doi.org/10.2166/wst.2012.852.

[34] P.D. Jensen, S.D. Yap, A. Boyle-Gotla, J. Janoschka, C. Carney, M. Pidou, D.J. Batstone, Anaerobic membrane bioreactors enable high rate treatment of slaughterhouse wastewater, Biochem. Eng. J. 97 (2015) 132–141. https://doi.org/10.1016/j.bej.2015.02.009.

[35] H. Chen, S. Chang, Q. Guo, Y. Hong, P. Wu, Brewery wastewater treatment using an anaerobic membrane bioreactor, Biochem. Eng. J. 105 (2016) 321–331. https://doi.org/10.1016/j.bej.2015.10.006.

[36] B.K. Ince, O. Ince, P.J. Sallis, G.K. Anderson, Inert COD production in a membrane anaerobic reactor treating brewery wastewater, Water Res. 34 (2000) 3943–3948. https://doi.org/10.1016/S0043-1354(00)00170-6.

[37] A. Tawfik, M. Sobhey, M. Badawy, Treatment of a combined dairy and domestic wastewater in an up-flow anaerobic sludge blanket (UASB) reactor followed by activated sludge (AS system), Desalination. 227 (2008) 167–177. https://doi.org/10.1016/j.desal.2007.06.023.

[38] J. Rajesh Banu, S. Anandan, S. Kaliappan, I.T. Yeom, Treatment of dairy wastewater using anaerobic and solar photocatalytic methods, Sol. Energy. 82 (2008) 812–819. https://doi.org/10.1016/j.solener.2008.02.015.

[39] B. Farizoglu, B. Keskinler, E. Yildiz, A. Nuhoglu, Cheese whey treatment performance of an aerobic jet loop membrane bioreactor, Process Biochem. 39 (2004) 2283–2291. https://doi.org/10.1016/j.procbio.2003.11.028.

[40] H.Q. Yu, Q.B. Zhao, Y. Tang, Anaerobic treatment of winery wastewater using laboratory-scale multi- and single-fed filters at ambient temperatures, Process Biochem. 41 (2006) 2477–2481. https://doi.org/10.1016/j.procbio.2006.06.011.

[41] R. Kurian, C. Acharya, G. Nakhla, A. Bassi, Conventional and thermophilic aerobic treatability of high strength oily pet food wastewater using membrane-coupled bioreactors, Water Res. 39 (2005) 4299–4308. https://doi.org/10.1016/j.watres.2005.08.030.

[42] P.C. Sridang, A. Pottier, C. Wisniewski, A. Grasmick, Performance and microbial surveying in submerged membrane bioreactor for seafood processing wastewater treatment, J. Memb. Sci. 317 (2008) 43–49. https://doi.org/10.1016/j.memsci.2007.11.011.

[43] P. Krzeminski, L. Leverette, S. Malamis, E. Katsou, Membrane bioreactors – A review on recent developments in energy reduction, fouling control, novel configurations, LCA and market prospects, J. Memb. Sci. 527 (2017) 207–227. https://doi.org/10.1016/j.memsci.2016.12.010.

[44] S.G. Pavlostathis, E. Giraldo-Gomez, Kinetics of anaerobic treatment: A critical review, Crit. Rev. Environ. Control. 21 (1991) 411–490. https://doi.org/10.1080/10643389109388424.

[45] C. Visvanathan, A. Abeynayaka, Developments and future potentials of anaerobic membrane bioreactors (AnMBRs), Membr. Water Treat. 3 (2012) 1–23. https://doi.org/10.12989/mwt.2012.3.1.001.

[46] M. Maaz, M. Yasin, M. Aslam, G. Kumar, A.E. Atabani, M. Idrees, F. Anjum, F. Jamil,

R. Ahmad, A.L. Khan, G. Lesage, M. Heran, J. Kim, Anaerobic membrane bioreactors for wastewater treatment: Novel configurations, fouling control and energy considerations, Bioresour. Technol. 283 (2019) 358–372. https://doi.org/10.1016/j.biortech.2019.03.061.

[47] B. Ketheesan, D.C. Stuckey, Effects of hydraulic/organic shock/transient loads in anaerobic wastewater treatment: A review, Crit. Rev. Environ. Sci. Technol. 45 (2015) 2693–2727. https://doi.org/10.1080/10643389.2015.1046771.

[48] Z. Xie, Z. Wang, Q. Wang, C. Zhu, Z. Wu, An anaerobic dynamic membrane bioreactor (AnDMBR) for landfill leachate treatment: Performance and microbial community identification, Bioresour. Technol. 161 (2014) 29–39. https://doi.org/10.1016/j.biortech.2014.03.014.

[49] M.A. Khan, H.H. Ngo, W.S. Guo, Y.W. Liu, J.L. Zhou, J. Zhang, S. Liang, B.J. Ni, X.B. Zhang, J. Wang, Comparing the value of bioproducts from different stages of anaerobic membrane bioreactors, Bioresour. Technol. 214 (2016) 816–825. https://doi.org/10.1016/j.biortech.2016.05.013.

[50] E. Baruth, Water treatment plant design, 4th ed., McGraw-Hill, New York, 2005.

[51] H. Ozgun, R.K. Dereli, M.E. Ersahin, C. Kinaci, H. Spanjers, J.B. Van Lier, A review of anaerobic membrane bioreactors for municipal wastewater treatment: Integration options, limitations and expectations, Sep. Purif. Technol. 118 (2013) 89–104. https://doi.org/10.1016/j.seppur.2013.06.036.

[52] M. Racar, D. Dolar, K. Karadakić, N. Čavarović, N. Glumac, D. Ašperger, K. Košutić, Challenges of municipal wastewater reclamation for irrigation by MBR and NF/RO: Physico-chemical and microbiological parameters, and emerging contaminants, Sci. Total Environ. 722 (2020) 137959. https://doi.org/10.1016/j.scitotenv.2020.137959.

[53] L. Dvořák, M. Gómez, J. Dolina, A. Černín, Anaerobic membrane bioreactors—a mini

review with emphasis on industrial wastewater treatment: applications, limitations and perspectives, Desalin. Water Treat. 57 (2016) 19062–19076. https://doi.org/10.1080/19443994.2015.1100879.

[54] Z. Wang, J. Ma, C.Y. Tang, K. Kimura, Q. Wang, X. Han, Membrane cleaning in membrane bioreactors: A review, J. Memb. Sci. 468 (2014) 276–307. https://doi.org/10.1016/j.memsci.2014.05.060.

[55] B.D. Cho, A.G. Fane, Fouling transients in nominally sub-critical flux operation of a membrane bioreactor, J. Memb. Sci. 209 (2002) 391–403. https://doi.org/10.1016/S0376-7388(02)00321-6.

[56] J. Zhang, H.C. Chua, J. Zhou, A.G. Fane, Factors affecting the membrane performance in submerged membrane bioreactors, J. Memb. Sci. 284 (2006) 54–66. https://doi.org/10.1016/j.memsci.2006.06.022.

[57] H. Lin, M. Zhang, F. Wang, F. Meng, B.Q. Liao, H. Hong, J. Chen, W. Gao, A critical review of extracellular polymeric substances (EPSs) in membrane bioreactors: Characteristics, roles in membrane fouling and control strategies, J. Memb. Sci. 460 (2014) 110–125. https://doi.org/10.1016/j.memsci.2014.02.034.

[58] S. Wang, G. Guillen, E.M.V. Hoek, Direct observation of microbial adhesion to membranes, Environ. Sci. Technol. 39 (2005) 6461–6469. https://doi.org/10.1021/es050188s.

[59] C.M. Pang, P. Hong, H. Guo, W.T. Liu, Biofilm formation characteristics of bacterial isolates retrieved from a reverse osmosis membrane, Environ. Sci. Technol. 39 (2005) 7541–7550. https://doi.org/10.1021/es050170h.

[60] A. Ramesh, D.J. Lee, J.Y. Lai, Membrane biofouling by extracellular polymeric substances or soluble microbial products from membrane bioreactor sludge, Appl.

Microbiol. Biotechnol. 74 (2007) 699–707. https://doi.org/10.1007/s00253-006-0706-x.

[61] B.Q. Liao, D.M. Bagley, H.E. Kraemer, G.G. Leppard, S.N. Liss, A Review of Biofouling and its Control in Membrane Separation Bioreactors, Water Environ. Res. 76 (2004) 425–436. https://doi.org/10.2175/106143004x151527.

[62] P. Le-Clech, V. Chen, T.A.G. Fane, Fouling in membrane bioreactors used in wastewater treatment, J. Memb. Sci. 284 (2006) 17–53. https://doi.org/10.1016/j.memsci.2006.08.019.

[63] F. Meng, Z. Zhou, B.J. Ni, X. Zheng, G. Huang, X. Jia, S. Li, Y. Xiong, M. Kraume, Characterization of the size-fractionated biomacromolecules: Tracking their role and fate in a membrane bioreactor, Water Res. 45 (2011) 4661–4671. https://doi.org/10.1016/j.watres.2011.06.026.

[64] D. Jermann, W. Pronk, S. Meylan, M. Boller, Interplay of different NOM fouling mechanisms during ultrafiltration for drinking water production, Water Res. 41 (2007) 1713–1722. https://doi.org/10.1016/j.watres.2006.12.030.

[65] T. Seviour, B.C. Donose, M. Pijuan, Z. Yuan, Purification and conformational analysis of a key exopolysaccharide component of mixed culture aerobic sludge granules, Environ. Sci. Technol. 44 (2010) 4729–4734. https://doi.org/10.1021/es100362b.

[66] Z. Wang, J. Cao, F. Meng, Interactions between protein-like and humic-like components in dissolved organic matter revealed by fluorescence quenching, Water Res. 68 (2015) 404–413. https://doi.org/10.1016/j.watres.2014.10.024.

[67] H.C. Flemming, J. Wingender, Relevance of microbial extracellular polymeric substances (EPSs) - Part I: Structural and ecological aspects, in: Water Sci. Technol., 2001: pp. 1–8. https://doi.org/10.2166/wst.2001.0328.

[68] P. Le-Clech, V. Chen, T.A.G. Fane, Fouling in membrane bioreactors used in wastewater treatment, J. Memb. Sci. 284 (2006) 17–53. https://doi.org/10.1016/j.memsci.2006.08.019.

[69] F. Meng, S.R. Chae, A. Drews, M. Kraume, H.S. Shin, F. Yang, Recent advances in membrane bioreactors (MBRs): Membrane fouling and membrane material, Water Res. 43 (2009) 1489–1512. https://doi.org/10.1016/j.watres.2008.12.044.

[70] A.Y. Hu, D.C. Stuckey, Activated carbon addition to a submerged anaerobic membrane bioreactor: Effect on performance, transmembrane pressure, and flux, J. Environ. Eng. 133 (2007) 73–80. https://doi.org/10.1061/(ASCE)0733-9372(2007)133:1(73).

[71] C.A. Ng, D. Sun, A.G. Fane, Operation of membrane bioreactor with powdered activated carbon addition, Sep. Sci. Technol. 41 (2006) 1447–1466. https://doi.org/10.1080/01496390600634632.

[72] Z. Wang, Z. Wu, X. Yin, L. Tian, Membrane fouling in a submerged membrane bioreactor (MBR) under sub-critical flux operation: Membrane foulant and gel layer characterization, J. Memb. Sci. 325 (2008) 238–244. https://doi.org/10.1016/j.memsci.2008.07.035.

[73] I.J. Kang, S.H. Yoon, C.H. Lee, Comparison of the filtration characteristics of organic and inorganic membranes in a membrane-coupled anaerobic bioreactor, Water Res. 36 (2002) 1803–1813. https://doi.org/10.1016/S0043-1354(01)00388-8.

[74] I.S. Kim, N. Jang, The effect of calcium on the membrane biofouling in the membrane bioreactor (MBR), Water Res. 40 (2006) 2756–2764. https://doi.org/10.1016/j.watres.2006.03.036.

[75] D.F. Ayala, V. Ferre, S.J. Judd, Membrane life estimation in full-scale immersed membrane bioreactors, J. Memb. Sci. 378 (2011) 95–100. https://doi.org/10.1016/j.memsci.2011.03.013.

[76] I.-S. Chang, P. Le Clech, B. Jefferson, S. Judd, Membrane Fouling in Membrane Bioreactors for Wastewater Treatment, J. Environ. Eng. 128 (2002) 1018–1029. https://doi.org/10.1061/(ASCE)0733-9372(2002)128:11(1018).

[77] G. Di Bella, D. Di Trapani, A brief review on the resistance-in-series model in membrane bioreactors (MBRs), Membranes (Basel). 9 (2019) 24. https://doi.org/10.3390/membranes9020024.

[78] Á. Robles, M.V. Ruano, A. Charfi, G. Lesage, M. Heran, J. Harmand, A. Seco, J.P. Steyer, D.J. Batstone, J. Kim, J. Ferrer, A review on anaerobic membrane bioreactors (AnMBRs) focused on modelling and control aspects, Bioresour. Technol. 270 (2018) 612–626. https://doi.org/10.1016/j.biortech.2018.09.049.

[79] W. Lee, S. Kang, H. Shin, Sludge characteristics and their contribution to microfiltration in submerged membrane bioreactors, J. Memb. Sci. 216 (2003) 217–227. https://doi.org/10.1016/S0376-7388(03)00073-5.

[80] F.G. Meng, H.M. Zhang, Y.S. Li, X.W. Zhang, F.L. Yang, J.N. Xiao, Cake layer morphology in microfiltration of activated sludge wastewater based on fractal analysis, Sep. Purif. Technol. 44 (2005) 250–257. https://doi.org/10.1016/j.seppur.2005.01.015.

[81] X. yan Li, X. mao Wang, Modelling of membrane fouling in a submerged membrane bioreactor, J. Memb. Sci. 278 (2006) 151–161. https://doi.org/10.1016/j.memsci.2005.10.051.

[82] H. Choi, K. Zhang, D.D. Dionysiou, D.B. Oerther, G.A. Sorial, Influence of cross-flow velocity on membrane performance during filtration of biological suspension, J. Memb. Sci. 248 (2005) 189–199. https://doi.org/10.1016/j.memsci.2004.08.027.

[83] J. Busch, A. Cruse, W. Marquardt, Modeling submerged hollow-fiber membrane filtration for wastewater treatment, J. Memb. Sci. 288 (2007) 94–111.

https://doi.org/10.1016/j.memsci.2006.11.008.

[84] H. Choi, K. Zhang, D.D. Dionysiou, D.B. Oerther, G.A. Sorial, Effect of permeate flux and tangential flow on membrane fouling for wastewater treatment, Sep. Purif. Technol. 45 (2005) 68–78. https://doi.org/10.1016/j.seppur.2005.02.010.

[85] V. Diez, D. Ezquerra, J.L. Cabezas, A. García, C. Ramos, A modified method for evaluation of critical flux, fouling rate and in situ determination of resistance and compressibility in MBR under different fouling conditions, J. Memb. Sci. 453 (2014) 1–11. https://doi.org/10.1016/j.memsci.2013.10.055.

[86] D.C. Stuckey, Recent developments in anaerobic membrane reactors, Bioresour. Technol. 122 (2012) 137–148. https://doi.org/10.1016/j.biortech.2012.05.138.

[87] N. Yamato, K. Kimura, T. Miyoshi, Y. Watanabe, Difference in membrane fouling in membrane bioreactors (MBRs) caused by membrane polymer materials, J. Memb. Sci. 280 (2006) 911–919. https://doi.org/10.1016/j.memsci.2006.03.009.

[88] G. Zhang, S. Ji, X. Gao, Z. Liu, Adsorptive fouling of extracellular polymeric substances with polymeric ultrafiltration membranes, J. Memb. Sci. 309 (2008) 28–35. https://doi.org/10.1016/j.memsci.2007.10.012.

[89] V. Kochkodan, N. Hilal, A comprehensive review on surface modified polymer membranes for biofouling mitigation, Desalination. 356 (2015) 187–207. https://doi.org/10.1016/j.desal.2014.09.015.

[90] L.H. de Andrade, F.D. dos S. Mendes, J.C. Espindola, M.C.S. Amaral, Internal versus external submerged membrane bioreactor configurations for dairy wastewater treatment, Desalin. Water Treat. 52 (2014) 2920–2932. https://doi.org/10.1080/19443994.2013.799048.

[91] P. Le-Clech, B. Jefferson, S.J. Judd, A comparison of submerged and sidestream tubular membrane bioreactor configurations, Desalination. 173 (2005) 113–122. https://doi.org/10.1016/j.desal.2004.08.029.

[92] C. Chen, W. Guo, H.H. Ngo, S.W. Chang, D. Duc Nguyen, P. Dan Nguyen, X.T. Bui, Y. Wu, Impact of reactor configurations on the performance of a granular anaerobic membrane bioreactor for municipal wastewater treatment, Int. Biodeterior. Biodegrad. 121 (2017) 131–138. https://doi.org/10.1016/j.ibiod.2017.03.021.

[93] J.P. Nywening, H. Zhou, Influence of filtration conditions on membrane fouling and scouring aeration effectiveness in submerged membrane bioreactors to treat municipal wastewater, Water Res. 43 (2009) 3548–3558. https://doi.org/10.1016/j.watres.2009.04.050.

[94] Z.F. Cui, S. Chang, A.G. Fane, The use of gas bubbling to enhance membrane processes, J. Memb. Sci. 221 (2003) 1–35. https://doi.org/10.1016/S0376-7388(03)00246-1.

[95] I.S. Chang, S.J. Judd, Air sparging of a submerged MBR for municipal wastewater treatment, Process Biochem. 37 (2002) 915–920. https://doi.org/10.1016/S0032-9592(01)00291-6.

[96] M. Aslam, A. Charfi, G. Lesage, M. Heran, J. Kim, Membrane bioreactors for wastewater treatment: A review of mechanical cleaning by scouring agents to control membrane fouling, Chem. Eng. J. 307 (2017) 897–913. https://doi.org/10.1016/j.cej.2016.08.144.

[97] M.A.H. Johir, R. Aryal, S. Vigneswaran, J. Kandasamy, A. Grasmick, Influence of supporting media in suspension on membrane fouling reduction in submerged membrane bioreactor (SMBR), J. Memb. Sci. 374 (2011) 121–128. https://doi.org/10.1016/j.memsci.2011.03.023.

[98] A. Kola, Y. Ye, P. Le-Clech, V. Chen, Transverse vibration as novel membrane fouling

mitigation strategy in anaerobic membrane bioreactor applications, J. Memb. Sci. 455 (2014) 320–329. https://doi.org/10.1016/j.memsci.2013.12.078.

[99] O. Díaz, E. González, L. Vera, J.J. Macías-Hernández, J. Rodríguez-Sevilla, Fouling analysis and mitigation in a tertiary MBR operated under restricted aeration, J. Memb. Sci. 525 (2017) 368–377. https://doi.org/10.1016/j.memsci.2016.12.014.

[100] P. van der Marel, A. Zwijnenburg, A. Kemperman, M. Wessling, H. Temmink, W. van der Meer, An improved flux-step method to determine the critical flux and the critical flux for irreversibility in a membrane bioreactor, J. Memb. Sci. 332 (2009) 24–29. https://doi.org/10.1016/j.memsci.2009.01.046.

[101] D. Navaratna, V. Jegatheesan, Implications of short and long term critical flux experiments for laboratory-scale MBR operations, Bioresour. Technol. 102 (2011) 5361–5369. https://doi.org/10.1016/j.biortech.2010.12.080.

[102] T. Zsirai, P. Buzatu, P. Aerts, S. Judd, Efficacy of relaxation, backflushing, chemical cleaning and clogging removal for an immersed hollow fibre membrane bioreactor, Water Res. 46 (2012) 4499–4507. https://doi.org/10.1016/j.watres.2012.05.004.

[103] M. Bagheri, S.A. Mirbagheri, Critical review of fouling mitigation strategies in membrane bioreactors treating water and wastewater, Bioresour. Technol. 258 (2018) 318–334. https://doi.org/10.1016/j.biortech.2018.03.026.

[104] S.J. Judd, C. Judd, The MBR Book: Principles and Applications of Membrane Bioreactors for Water and Wastewater Treatment, 2nd ed., 2011.

[105] M. Raffin, E. Germain, S. Judd, Optimisation of MF membrane cleaning protocol in an Indirect Potable Reuse (IPR) scheme, Sep. Purif. Technol. 80 (2011) 452–458. https://doi.org/10.1016/j.seppur.2011.05.027.

[106] G.E.P. Box, D.W. Behnken, Some New Three Level Designs for the Study of Quantitative Variables, Technometrics. 2 (1960) 455–475. https://doi.org/10.1080/00401706.1960.10489912.

[107] M. Raffin, E. Germain, S. Judd, Optimising operation of an integrated membrane system (IMS) - A Box-Behnken approach, Desalination. 273 (2011) 136–141. https://doi.org/10.1016/j.desal.2010.10.030.

[108] APHA-AWWA-WEF, Standard methods for the examination of water and wastewater, 21st ed., 2005.

[109] I. Angelidaki, M. Alves, D. Bolzonella, L. Borzacconi, J.L. Campos, A.J. Guwy, S. Kalyuzhnyi, P. Jenicek, J.B. Van Lier, Defining the biomethane potential (BMP) of solid organic wastes and energy crops: A proposed protocol for batch assays, Water Sci. Technol. 59 (2009) 927–934. https://doi.org/10.2166/wst.2009.040.

[110] U. Metzger, P. Le-Clech, R.M. Stuetz, F.H. Frimmel, V. Chen, Characterisation of polymeric fouling in membrane bioreactors and the effect of different filtration modes, J. Memb. Sci. 301 (2007) 180–189. https://doi.org/10.1016/j.memsci.2007.06.016.

[111] M. Dubois, K.A. Gilles, J.K. Hamilton, P.A. Rebers, F. Smith, Colorimetric Method for Determination of Sugars and Related Substances, Anal. Chem. 28 (1956) 350–356. https://doi.org/10.1021/ac60111a017.

[112] D.T. Sponza, Investigation of extracellular polymer substances (EPS) and physicochemical properties of different activated sludge flocs under steady-state conditions, Enzyme Microb. Technol. 32 (2003) 375–385. https://doi.org/10.1016/S0141-0229(02)00309-5.

[113] M.M. Bradford, A rapid and sensitive method for the quantitation of microgram quantities of protein utilizing the principle of protein-dye binding, Anal. Biochem. 72 (1976) 248–

254. https://doi.org/10.1016/0003-2697(76)90527-3.

[114] K. Grintzalis, C.D. Georgiou, Y.-J. Schneider, An accurate and sensitive Coomassie Brilliant Blue G-250-based assay for protein determination., Anal. Biochem. 480 (2015) 28–30. https://doi.org/10.1016/j.ab.2015.03.024.

[115] B. Frølund, R. Palmgren, K. Keiding, P.H. Nielsen, Extraction of extracellular polymers from activated sludge using a cation exchange resin, Water Res. 30 (1996) 1749–1758. https://doi.org/10.1016/0043-1354(95)00323-1.

[116] E. Poorasgari, T. Vistisen Bugge, M. Lykkegaard Christensen, M. Koustrup Jørgensen, Compressibility of fouling layers in membrane bioreactors, J. Memb. Sci. 475 (2015) 65–70. https://doi.org/10.1016/j.memsci.2014.09.056.

[117] B. Nielsen, H. Frolund, P. T. Griebe, Enzymatic activity in the activated-sludge floc matrix, Appl. Microbiol. Biotechnol. 43 (1995) 755–761.

[118] M. Pansu, J. Gautheyrou, Handbook of Soil Analysis, Springer Berlin Heidelberg, Berlin, Heidelberg, 2006. https://doi.org/10.1007/978-3-540-31211-6.

[119] I. Martin-Garcia, V. Monsalvo, M. Pidou, P. Le-Clech, S.J. Judd, E.J. McAdam, B. Jefferson, Impact of membrane configuration on fouling in anaerobic membrane bioreactors, J. Memb. Sci. 382 (2011) 41–49. https://doi.org/10.1016/j.memsci.2011.07.042.

[120] A.Y. Hu, D.C. Stuckey, Treatment of dilute wastewaters using a novel submerged Anaerobic Membrane Bioreactor, J. Environ. Eng. 132 (2006) 190–198. https://doi.org/10.1061/(asce)0733-9372(2006)132:2(190).

[121] A.L. Prieto, H. Futselaar, P.N.L. Lens, R. Bair, D.H. Yeh, Development and start up of a gas-lift anaerobic membrane bioreactor (Gl-AnMBR) for conversion of sewage to energy,

water and nutrients, J. Memb. Sci. 441 (2013) 158–167. https://doi.org/10.1016/j.memsci.2013.02.016.

[122] B.Q. Liao, J.T. Kraemer, D.M. Bagley, Anaerobic membrane bioreactors: Applications and research directions, 2006. https://doi.org/10.1080/10643380600678146.

[123] D. Jeison, J.B. van Lier, On-line cake-layer management by trans-membrane pressure steady state assessment in Anaerobic Membrane Bioreactors for wastewater treatment, Biochem. Eng. J. 29 (2006) 204–209. https://doi.org/10.1016/j.bej.2005.11.017.

[124] C. Wisniewski, A. Grasmick, Floc size distribution in a membrane bioreactor and consequences for membrane fouling, Colloids Surfaces A Physicochem. Eng. Asp. 138 (1998) 403–411. https://doi.org/10.1016/S0927-7757(96)03898-8.

[125] X. Du, Y. Wang, G. Leslie, G. Li, H. Liang, Shear stress in a pressure-driven membrane system and its impact on membrane fouling from a hydrodynamic condition perspective: a review, J. Chem. Technol. Biotechnol. 92 (2017) 463–478. https://doi.org/10.1002/jctb.5154.

[126] A. Hoque, K. Kimura, T. Miyoshi, N. Yamato, Y. Watanabe, Characteristics of foulants in air-sparged side-stream tubular membranes used in a municipal wastewater membrane bioreactor, Sep. Purif. Technol. 93 (2012) 83–91. https://doi.org/10.1016/j.seppur.2012.03.027.

[127] R. Campo, M. Capodici, G. Di Bella, M. Torregrossa, The role of EPS in the foaming and fouling for a MBR operated in intermittent aeration conditions, Biochem. Eng. J. 118 (2017) 41–52. https://doi.org/10.1016/j.bej.2016.11.012.

[128] C. Jacquin, B. Teychene, L. Lemee, G. Lesage, M. Heran, Characteristics and fouling behaviors of Dissolved Organic Matter fractions in a full-scale submerged membrane bioreactor for municipal wastewater treatment, Biochem. Eng. J. 132 (2018) 169–181.

https://doi.org/10.1016/j.bej.2017.12.016.

[129] S. Zhang, J. Xiong, X. Zuo, W. Liao, C. Ma, J. He, Z. Chen, Characteristics of the sludge filterability and microbial composition in PAC hybrid MBR: Effect of PAC replenishment ratio, Biochem. Eng. J. (2019) 10–17. https://doi.org/10.1016/j.bej.2019.02.001.

[130] M.E. Ersahin, Y. Tao, H. Ozgun, J.B. Gimenez, H. Spanjers, J.B. van Lier, Impact of anaerobic dynamic membrane bioreactor configuration on treatment and filterability performance, J. Memb. Sci. 526 (2017) 387–394. https://doi.org/10.1016/j.memsci.2016.12.057.

[131] W.R. Ghyoot, W.H. Verstraete, Coupling membrane filtration to anaerobic primary sludge digestion, Environ. Technol. (United Kingdom). 18 (1997) 569–580. https://doi.org/10.1080/09593331808616575.

[132] M. Brockmann, C.F. Seyfried, Sludge activity and cross-flow microfiltration - a non-beneficial relationship, Water Sci. Technol. 34 (1996) 205–213. https://doi.org/10.2166/wst.1996.0212.

[133] S. Buetehorn, M. Brannock, P. Le-Clech, G. Leslie, D. Volmering, K. Vossenkaul, T. Wintgens, M. Wessling, T. Melin, Limitations for transferring lab-scale microfiltration results to large-scale membrane bioreactor (MBR) processes, Sep. Purif. Technol. 95 (2012) 202–215. https://doi.org/10.1016/j.seppur.2012.05.001.

[134] K.Y.K. und R.E.C. Wazer, J. R. van, J. W. Lyons, Viscosity and flow measurement. A laboratory handbook of rheology, 1964. https://doi.org/10.1002/star.19640161109.

[135] C. Ramos, F. Zecchino, D. Ezquerra, V. Diez, Chemical cleaning of membranes from an anaerobic membrane bioreactor treating food industry wastewater, J. Memb. Sci. 458 (2014) 179–188. https://doi.org/10.1016/J.MEMSCI.2014.01.067.

[136] M.L. Salazar-Peláez, J.M. Morgan-Sagastume, A. Noyola, Influence of hydraulic retention time on fouling in a UASB coupled with an external ultrafiltration membrane treating synthetic municipal wastewater, Desalination. 277 (2011) 164–170. https://doi.org/10.1016/j.desal.2011.04.021.

[137] H.J. Lin, K. Xie, B. Mahendran, D.M. Bagley, K.T. Leung, S.N. Liss, B.Q. Liao, Sludge properties and their effects on membrane fouling in submerged anaerobic membrane bioreactors (SAnMBRs), Water Res. 43 (2009) 3827–3837. https://doi.org/10.1016/j.watres.2009.05.025.

[138] K.H. Choo, C.H. Lee, Membrane fouling mechanisms in the membrane-coupled anaerobic bioreactor, Water Res. 30 (1996) 1771–1780. https://doi.org/10.1016/0043-1354(96)00053-X.

[139] G. Belfort, R.H. Davis, A.L. Zydney, The behavior of suspensions and macromolecular solutions in crossflow microfiltration, J. Memb. Sci. 96 (1994) 1–58. https://doi.org/10.1016/0376-7388(94)00119-7.

[140] K.H. Choo, C.H. Lee, Hydrodynamic behavior of anaerobic biosolids during crossflow filtration in the membrane anaerobic bioreactor, Water Res. 32 (1998) 3387–3397. https://doi.org/10.1016/S0043-1354(98)00103-1.

[141] A. Massé, M. Spérandio, C. Cabassud, Comparison of sludge characteristics and performance of a submerged membrane bioreactor and an activated sludge process at high solids retention time, Water Res. 40 (2006) 2405–2415. https://doi.org/10.1016/j.watres.2006.04.015.

[142] D. Jeison, J.B. van Lier, Cake formation and consolidation: Main factors governing the applicable flux in anaerobic submerged membrane bioreactors (AnSMBR) treating acidified wastewaters, Sep. Purif. Technol. 56 (2007) 71–78.

https://doi.org/10.1016/j.seppur.2007.01.022.

[143] Z. Yu, Z. Song, X. Wen, X. Huang, Using polyaluminum chloride and polyacrylamide to control membrane fouling in a cross-flow anaerobic membrane bioreactor, J. Memb. Sci. 479 (2015) 20–27. https://doi.org/10.1016/j.memsci.2015.01.016.

[144] Y. Xiong, M. Harb, P.Y. Hong, Characterization of biofoulants illustrates different membrane fouling mechanisms for aerobic and anaerobic membrane bioreactors, Sep. Purif. Technol. 157 (2015) 192–202. https://doi.org/10.1016/j.seppur.2015.11.024.

[145] Y. Liu, H. Liu, L. Cui, K. Zhang, The ratio of food-to-microorganism (F/M) on membrane fouling of anaerobic membrane bioreactors treating low-strength wastewater, Desalination. 297 (2012) 97–103. https://doi.org/10.1016/j.desal.2012.04.026.

[146] M. Stricot, A. Filali, N. Lesage, M. Spérandio, C. Cabassud, Side-stream membrane bioreactors: Influence of stress generated by hydrodynamics on floc structure, supernatant quality and fouling propensity, Water Res. 44 (2010) 2113–2124. https://doi.org/10.1016/j.watres.2009.12.021.

[147] J. Liu, C. Tian, X. Jia, J. Xiong, S. Dong, L. Wang, L. Bo, The brewery wastewater treatment and membrane fouling mitigation strategies in anaerobic baffled anaerobic/aerobic membrane bioreactor, Biochem. Eng. J. 127 (2017) 53–59. https://doi.org/10.1016/j.bej.2017.07.009.

[148] H. Zhang, M. Sun, L. Song, J. Guo, L. Zhang, Fate of NaClO and membrane foulants during in-situ cleaning of membrane bioreactors: Combined effect on thermodynamic properties of sludge, Biochem. Eng. J. (2019) 146–152. https://doi.org/10.1016/j.bej.2019.04.016.

[149] A. Beaubien, M. Bâty, F. Jeannot, E. Francoeur, J. Manem, Design and operation of anaerobic membrane bioreactors: Development of a filtration testing strategy, J. Memb.

Sci. 109 (1996) 173–184. https://doi.org/10.1016/0376-7388(95)00199-9.

[150] O.T. Iorhemen, R.A. Hamza, J.H. Tay, Membrane bioreactor (Mbr) technology for wastewater treatment and reclamation: Membrane fouling, Membranes (Basel). 6 (2016) 13–16. https://doi.org/10.3390/membranes6020033.

[151] I.-S. Chang, P. Le Clech, B. Jefferson, S. Judd, Membrane Fouling in Membrane Bioreactors for Wastewater Treatment, J. Environ. Eng. 128 (2002) 1018–1029. https://doi.org/10.1061/(ASCE)0733-9372(2002)128:11(1018).

[152] W. Zhang, J. Luo, L. Ding, M.Y. Jaffrin, A review on flux decline control strategies in pressure-driven membrane processes, Ind. Eng. Chem. Res. 54 (2015) 2843–2861. https://doi.org/10.1021/ie504848m.

[153] H.Y. Ng, T.W. Tan, S.L. Ong, Membrane fouling of submerged membrane bioreactors: Impact of mean cell residence time and the contributing factors, Environ. Sci. Technol. 40 (2006) 2706–2713. https://doi.org/10.1021/es0516155.

[154] R. Martinez, M.O. Ruiz, C. Ramos, J.M. Cámara, V. Diez, Comparison of external and submerged membranes used in Anaerobic Membrane Bioreactors. Fouling related issues and biological activity, Biochem. Eng. J. (2020) 107558. https://doi.org/10.1016/j.bej.2020.107558.

[155] S. Judd, F. Turan, Sidestream vs immersed membrane bioreactors: A cost analysis, 91st Annu. Water Environ. Fed. Tech. Exhib. Conf. WEFTEC 2018. (2019) 3722–3733. https://doi.org/10.2175/193864718825136008.

[156] H. Monclús, M. Dalmau, S. Gabarrón, G. Ferrero, I. Rodríguez-Roda, J. Comas, Full-scale validation of an air scour control system for energy savings in membrane bioreactors, Water Res. 79 (2015) 1–9. https://doi.org/10.1016/j.watres.2015.03.032.

[157] R. Villarroel, S. Delgado, E. González, M. Morales, Physical cleaning initiation controlled by transmembrane pressure set-point in a submerged membrane bioreactor, Sep. Purif. Technol. 104 (2013) 55–63. https://doi.org/10.1016/j.seppur.2012.10.047.

[158] E. González, O. Díaz, E. Segredo-Morales, L.E. Rodríguez-Gómez, L. Vera, Enhancement of Peak Flux Capacity in Membrane Bioreactors for Wastewater Reuse by Controlling the Backwashing Strategy, Ind. Eng. Chem. Res. 58 (2019) 1373–1381. https://doi.org/10.1021/acs.iecr.8b05650.

[159] L. Vera, E. González, I. Ruigómez, J. Gómez, S. Delgado, Influence of Gas Sparging Intermittence on Ultrafiltration Performance of Anaerobic Suspensions, Ind. Eng. Chem. Res. 55 (2016) 4668–4675. https://doi.org/10.1021/acs.iecr.5b04529.

[160] E. Amini, M.R. Mehrnia, S.M. Mousavi, N. Mostoufi, Experimental study and computational fluid dynamics simulation of a full-scale membrane bioreactor for municipal wastewater treatment application, Ind. Eng. Chem. Res. 52 (2013) 9930–9939. https://doi.org/10.1021/ie400632y.

[161] M. Kim, B. Sankararao, S. Lee, C. Yoo, Prediction and identification of membrane fouling mechanism in a membrane bioreactor using a combined mechanistic model, Ind. Eng. Chem. Res. 52 (2013) 17198–17205. https://doi.org/10.1021/ie402056r.

[162] J. Wu, C. He, Y. Zhang, Modeling membrane fouling in a submerged membrane bioreactor by considering the role of solid, colloidal and soluble components, J. Memb. Sci. 397–398 (2012) 102–111. https://doi.org/10.1016/j.memsci.2012.01.026.

[163] X.S. Yi, W.X. Shi, S.L. Yu, X.H. Li, N. Sun, C. He, Factorial design applied to flux decline of anionic polyacrylamide removal from water by modified polyvinylidene fluoride ultrafiltration membranes, Desalination. 274 (2011) 7–12. https://doi.org/10.1016/j.desal.2010.10.019.

[164] P. Schoeberl, M. Brik, M. Bertoni, R. Braun, W. Fuchs, Optimization of operational parameters for a submerged membrane bioreactor treating dyehouse wastewater, Sep. Purif. Technol. 44 (2005) 61–68. https://doi.org/10.1016/j.seppur.2004.12.004.

[165] E. Akhondi, F. Wicaksana, A.G. Fane, Evaluation of fouling deposition, fouling reversibility and energy consumption of submerged hollow fiber membrane systems with periodic backwash, J. Memb. Sci. 452 (2014) 319–331. https://doi.org/10.1016/j.memsci.2013.10.031.

[166] W. Zhang, Z. Zhu, M.Y. Jaffrin, L. Ding, Effects of hydraulic conditions on effluent quality, flux behavior, and energy consumption in a shear-enhanced membrane filtration using Box-Behnken response surface methodology, Ind. Eng. Chem. Res. 53 (2014) 7176–7185. https://doi.org/10.1021/ie500117u.

[167] Y. Yang, A. Bogler, Z. Ronen, G. Oron, M. Herzberg, R. Bernstein, Initial Deposition and Pioneering Colonization on Polymeric Membranes of Anaerobes Isolated from an Anaerobic Membrane Bioreactor (AnMBR), Environ. Sci. Technol. 54 (2020) 5832–5842. https://doi.org/10.1021/acs.est.9b06763.

[168] T. Zsirai, P. Aerts, S. Judd, Reproducibility and applicability of the flux step test for a hollow fibre membrane bioreactor, Sep. Purif. Technol. 107 (2013) 144–149. https://doi.org/10.1016/j.seppur.2013.01.027.

[169] P.J. Huber, Robust regression: asymptotics, conjetures and Monte Carlo, Ann. Stat. 1 (1973) 799–821.

[170] A. Drews, Membrane fouling in membrane bioreactors-Characterisation, contradictions, cause and cures, J. Memb. Sci. 363 (2010) 1–28. https://doi.org/10.1016/j.memsci.2010.06.046.

[171] E. González, O. Díaz, L. Vera, L.E. Rodríguez-Gómez, J. Rodríguez-Sevilla, Feedback

control system for filtration optimisation based on a simple fouling model dynamically applied to membrane bioreactors, J. Memb. Sci. 552 (2018) 243–252. https://doi.org/10.1016/j.memsci.2018.02.007.

[172] M.L. Christensen, T.V. Bugge, B.H. Hede, M. Nierychlo, P. Larsen, M.K. Jørgensen, Effects of relaxation time on fouling propensity in membrane bioreactors, J. Memb. Sci. 504 (2016) 176–184. https://doi.org/10.1016/j.memsci.2016.01.006.

[173] G. Foley, A review of factors affecting filter cake properties in dead-end microfiltration of microbial suspensions, J. Memb. Sci. 274 (2006) 38–46. https://doi.org/10.1016/j.memsci.2005.12.008.

[174] A. Robles, M. V. Ruano, J. Ribes, A. Seco, J. Ferrer, Mathematical modelling of filtration in submerged anaerobic MBRs (SAnMBRs): Long-term validation, J. Memb. Sci. 446 (2013) 303–309. https://doi.org/10.1016/j.memsci.2013.07.001.

[175] J. Wu, P. Le-Clech, R.M. Stuetz, A.G. Fane, V. Chen, Effects of relaxation and backwashing conditions on fouling in membrane bioreactor, J. Memb. Sci. 324 (2008) 26–32. https://doi.org/10.1016/j.memsci.2008.06.057.

[176] M.A. Musa, S. Idrus, H.C. Man, N.N.N. Daud, Wastewater treatment and biogas recovery using anaerobic membrane bioreactors (AnMBRs): Strategies and achievements, Energies. 11 (2018). https://doi.org/10.3390/en11071675.

[177] W. Fuchs, H. Binder, G. Mavrias, R. Braun, Anaerobic treatment of wastewater with high organic content using a stirred tank reactor coupled with a membrane filtration unit, Water Res. 37 (2003) 902–908. https://doi.org/10.1016/S0043-1354(02)00246-4.

[178] M. Jain, Anaerobic Membrane Bioreactor as Highly Efficient and Reliable Technology for Wastewater Treatment—A Review, Adv. Chem. Eng. Sci. 08 (2018) 82–100. https://doi.org/10.4236/aces.2018.82006.

[179] M.A. Musa, S. Idrus, H.C. Man, N.N.N. Daud, Wastewater treatment and biogas recovery using anaerobic membrane bioreactors (AnMBRs): Strategies and achievements, Energies. 11 (2018) 1675. https://doi.org/10.3390/en11071675.

[180] X. Song, W. Luo, F.I. Hai, W.E. Price, W. Guo, H.H. Ngo, L.D. Nghiem, Resource recovery from wastewater by anaerobic membrane bioreactors: Opportunities and challenges, Bioresour. Technol. 270 (2018) 669–677. https://doi.org/10.1016/j.biortech.2018.09.001.

[181] L. Chen, P. Cheng, L. Ye, H. Chen, X. Xu, L. Zhu, Biological performance and fouling mitigation in the biochar-amended anaerobic membrane bioreactor (AnMBR) treating pharmaceutical wastewater, Bioresour. Technol. 302 (2020). https://doi.org/10.1016/j.biortech.2020.122805.

[182] M.T. Do, D.C. Stuckey, Fate and removal of Ciprofloxacin in an anaerobic membrane bioreactor (AnMBR), Bioresour. Technol. 289 (2019). https://doi.org/10.1016/j.biortech.2019.121683.

[183] D. Hu, T. Xiao, Z. Chen, H. Wang, J. Xu, X. Li, H. Su, Y. Zhang, Effect of the high cross flow velocity on performance of a pilot-scale anaerobic membrane bioreactor for treating antibiotic solvent wastewater, Bioresour. Technol. 243 (2017) 47–56. https://doi.org/10.1016/j.biortech.2017.06.030.

[184] M. Aslam, R. Ahmad, M. Yasin, A.L. Khan, M.K. Shahid, S. Hossain, Z. Khan, F. Jamil, S. Rafiq, M.R. Bilad, J. Kim, G. Kumar, Anaerobic membrane bioreactors for biohydrogen production: Recent developments, challenges and perspectives, Bioresour. Technol. 269 (2018) 452–464. https://doi.org/10.1016/j.biortech.2018.08.050.

[185] H. Cheng, Y. Hiro, T. Hojo, Y.Y. Li, Upgrading methane fermentation of food waste by using a hollow fiber type anaerobic membrane bioreactor, Bioresour. Technol. 267 (2018)

386–394. https://doi.org/10.1016/j.biortech.2018.07.045.

[186] X. Xiao, Z. Huang, W. Ruan, L. Yan, H. Miao, H. Ren, M. Zhao, Evaluation and characterization during the anaerobic digestion of high-strength kitchen waste slurry via a pilot-scale anaerobic membrane bioreactor, Bioresour. Technol. 193 (2015) 234–242. https://doi.org/10.1016/j.biortech.2015.06.065.

[187] L. Deng, W. Guo, H.H. Ngo, H. Zhang, J. Wang, J. Li, S. Xia, Y. Wu, Biofouling and control approaches in membrane bioreactors, Bioresour. Technol. 221 (2016) 656–665. https://doi.org/10.1016/j.biortech.2016.09.105.

[188] R. Van den Broeck, P. Krzeminski, J. Van Dierdonck, G. Gins, M. Lousada-Ferreira, J.F.M. Van Impe, J.H.J.M. van der Graaf, I.Y. Smets, J.B. van Lier, Activated sludge characteristics affecting sludge filterability in municipal and industrial MBRs: Unraveling correlations using multi-component regression analysis, J. Memb. Sci. 378 (2011) 330–338. https://doi.org/10.1016/j.memsci.2011.05.010.

[189] R.K. Dereli, B. Heffernan, A. Grelot, F.P. Van Der Zee, J.B. Van Lier, Influence of high lipid containing wastewater on filtration performance and fouling in AnMBRs operated at different solids retention times, Sep. Purif. Technol. 139 (2015) 43–52. https://doi.org/10.1016/j.seppur.2014.10.029.

[190] M. Yao, K. Zhang, L. Cui, Characterization of protein-polysaccharide ratios on membrane fouling, Desalination. 259 (2010) 11–16. https://doi.org/10.1016/j.desal.2010.04.049.

[191] S. Arabi, G. Nakhla, Impact of protein/carbohydrate ratio in the feed wastewater on the membrane fouling in membrane bioreactors, J. Memb. Sci. 324 (2008) 142–150. https://doi.org/10.1016/j.memsci.2008.07.026.

[192] J. Liu, C. Tian, X. Jia, J. Xiong, S. Dong, L. Wang, L. Bo, The brewery wastewater treatment and membrane fouling mitigation strategies in anaerobic baffled

anaerobic/aerobic membrane bioreactor, Biochem. Eng. J. 127 (2017) 53–59. https://doi.org/10.1016/J.BEJ.2017.07.009.

[193] Q. Zhang, G.H. Victor Tan, D.C. Stuckey, Optimal biogas sparging strategy, and the correlation between sludge and fouling layer properties in a submerged anaerobic membrane bioreactor (SAnMBR), Chem. Eng. J. 319 (2017) 248–257. https://doi.org/10.1016/j.cej.2017.02.146.

[194] V. Diez, A. Iglesias, J.M. Cámara, M.O. Ruiz, C. Ramos, A novel anaerobic filter membrane bioreactor: Prototype start-up and filtration assays, Water Sci. Technol. 78 (2018) 1833–1842. https://doi.org/10.2166/wst.2018.309.

[195] P. Le Clech, B. Jefferson, I.S. Chang, S.J. Judd, Critical flux determination by the flux-step method in a submerged membrane bioreactor, J. Memb. Sci. 227 (2003) 81–93. https://doi.org/10.1016/j.memsci.2003.07.021.

[196] H. Evenblij, J.H.J.M. van der Graaf, Occurrence of EPS in activated sludge from a membrane bioreactor treating municipal wastewater., Water Sci. Technol. 50 (2004) 293–300. http://www.ncbi.nlm.nih.gov/pubmed/15686034 (accessed February 26, 2020).

[197] M. Dubois, K.A. Gilles, J.K. Hamilton, P.A. Rebers, F. Smith, Colorimetric Method for Determination of Sugars and Related Substances, Anal. Chem. 28 (1956) 350–356. https://doi.org/10.1021/ac60111a017.

[198] L. Qin, G. Zhang, Q. Meng, H. Zhang, L. Xu, B. Lv, Enhanced submerged membrane bioreactor combined with biosurfactant rhamnolipids: Performance for frying oil degradation and membrane fouling reduction, in: Bioresour. Technol., Elsevier Ltd, 2012: pp. 314–320. https://doi.org/10.1016/j.biortech.2012.08.103.

[199] N. Ozaki, K. Yamamoto, Hydraulic effects on sludge accumulation on membrane surface in crossflow filtration, Water Res. 35 (2001) 3137–3146. https://doi.org/10.1016/S0043-

1354(01)00046-X.

[200] S. Ognier, C. Wisniewski, A. Grasmick, Membrane bioreactor fouling in sub-critical filtration conditions: A local critical flux concept, J. Memb. Sci. 229 (2004) 171–177. https://doi.org/10.1016/j.memsci.2003.10.026.

[201] P. van der Marel, A. Zwijnenburg, A. Kemperman, M. Wessling, H. Temmink, W. van der Meer, Influence of membrane properties on fouling in submerged membrane bioreactors, J. Memb. Sci. 348 (2010) 66–74. https://doi.org/10.1016/j.memsci.2009.10.054.

[202] B.G. Choi, J. Cho, K.G. Song, S.K. Maeng, Correlation between effluent organic matter characteristics and membrane fouling in a membrane bioreactor using advanced organic matter characterization tools, Desalination. 309 (2013) 74–83. https://doi.org/10.1016/j.desal.2012.09.018.

[203] B. Teychene, C. Guigui, C. Cabassud, G. Amy, Toward a better identification of foulant species in MBR processes, Desalination. 231 (2008) 27–34. https://doi.org/10.1016/j.desal.2007.12.006.

[204] K. Kimura, N. Yamato, H. Yamamura, Y. Watanabe, Membrane fouling in pilot-scale membrane bioreactors (MBRs) treating municipal wastewater, Environ. Sci. Technol. 39 (2005) 6293–6299. https://doi.org/10.1021/es0502425.

[205] K. Calderón, B. Rodelas, N. Cabirol, J. González-López, A. Noyola, Analysis of microbial communities developed on the fouling layers of a membrane-coupled anaerobic bioreactor applied to wastewater treatment, Bioresour. Technol. 102 (2011) 4618–4627. https://doi.org/10.1016/j.biortech.2011.01.007.

[206] R. Liikanen, J. Yli-Kuivila, R. Laukkanen, Efficiency of various chemical cleanings for nanofiltration membrane fouled by conventionally-treated surface water, J. Memb. Sci.

195 (2002) 265–276. https://doi.org/10.1016/S0376-7388(01)00569-5.

[207] X. Shi, G. Tal, N.P. Hankins, V. Gitis, Fouling and cleaning of ultrafiltration membranes: A review, J. Water Process Eng. 1 (2014) 121–138. https://doi.org/10.1016/j.jwpe.2014.04.003.

[208] A. Cosenza, G. Di Bella, G. Mannina, M. Torregrossa, The role of EPS in fouling and foaming phenomena for a membrane bioreactor, Bioresour. Technol. 147 (2013) 184–192. https://doi.org/10.1016/j.biortech.2013.08.026.

[209] X. Han, Z. Wang, C. Zhu, Z. Wu, Effect of ultrasonic power density on extracting loosely bound and tightly bound extracellular polymeric substances, Desalination. 329 (2013) 35–40. https://doi.org/10.1016/j.desal.2013.09.002.

[210] X.Y. Li, S.F. Yang, Influence of loosely bound extracellular polymeric substances (EPS) on the flocculation, sedimentation and dewaterability of activated sludge, Water Res. 41 (2007) 1022–1030. https://doi.org/10.1016/j.watres.2006.06.037.

[211] Y. Ding, Y. Tian, Z. Li, W. Zuo, J. Zhang, A comprehensive study into fouling properties of extracellular polymeric substance (EPS) extracted from bulk sludge and cake sludge in a mesophilic anaerobic membrane bioreactor, Bioresour. Technol. 192 (2015) 105–114. https://doi.org/10.1016/j.biortech.2015.05.067.

[212] H. Liu, H.H.P. Fang, Extraction of extracellular polymeric substances (EPS) of sludges, J. Biotechnol. 95 (2002) 249–256. https://doi.org/10.1016/S0168-1656(02)00025-1.

[213] J.W. Morgan, C.F. Forster, L. Evison, A comparative study of the nature of biopolymers extracted from anaerobic and activated sludges, Water Res. 24 (1990) 743–750. https://doi.org/10.1016/0043-1354(90)90030-A.

[214] A.G. Geyik, F. Çeçen, Production of protein- and carbohydrate-EPS in activated sludge

reactors operated at different carbon to nitrogen ratios, J. Chem. Technol. Biotechnol. 91 (2016) 522–531. https://doi.org/10.1002/jctb.4608.

[215] H. Wang, H. Deng, L. Ma, L. Ge, The effect of carbon source on extracellular polymeric substances production and its influence on sludge floc properties, J. Chem. Technol. Biotechnol. 89 (2014) 516–521. https://doi.org/10.1002/jctb.4147.

[216] A. Sweity, W. Ying, M.S. Ali-Shtayeh, F. Yang, A. Bick, G. Oron, M. Herzberg, Relation between EPS adherence, viscoelastic properties, and MBR operation: Biofouling study with QCM-D, Water Res. 45 (2011) 6430–6440. https://doi.org/10.1016/j.watres.2011.09.038.

[217] L. Sun, L. Chen, W.Z. Guo, T. Ye, Y. Yang, Extraction of extracellular polymeric substances in activated sludge using sequential extraction, J. Chem. Technol. Biotechnol. 90 (2015) 1448–1454. https://doi.org/10.1002/jctb.4449.

[218] P. D'Abzac, F. Bordas, E. Van Hullebusch, P.N.L. Lens, G. Guibaud, Extraction of extracellular polymeric substances (EPS) from anaerobic granular sludges: Comparison of chemical and physical extraction protocols, Appl. Microbiol. Biotechnol. 85 (2010) 1589–1599. https://doi.org/10.1007/s00253-009-2288-x.

[219] J. Wingender, T.R. Neu, H.-C. Flemming, What are Bacterial Extracellular Polymeric Substances?, in: Microb. Extracell. Polym. Subst., Springer Berlin Heidelberg, 1999: pp. 1–19. https://doi.org/10.1007/978-3-642-60147-7_1.

[220] A. Hemmelmann, A. Torres, C. Vergara, L. Azocar, D. Jeison, Application of anaerobic membrane bioreactors for the treatment of protein-containing wastewaters under saline conditions, J. Chem. Technol. Biotechnol. 88 (2013) 658–663. https://doi.org/10.1002/jctb.3882.

[221] E. Reid, X. Liu, S.J. Judd, Effect of high salinity on activated sludge characteristics and

membrane permeability in an immersed membrane bioreactor, J. Memb. Sci. 283 (2006) 164–171. https://doi.org/10.1016/j.memsci.2006.06.021.

[222] J. Chen, M. Zhang, A. Wang, H. Lin, H. Hong, X. Lu, Osmotic pressure effect on membrane fouling in a submerged anaerobic membrane bioreactor and its experimental verification, Bioresour. Technol. 125 (2012) 97–101. https://doi.org/10.1016/j.biortech.2012.08.038.

[223] M. Zhang, W. Peng, J. Chen, Y. He, L. Ding, A. Wang, H. Lin, H. Hong, Y. Zhang, H. Yu, A new insight into membrane fouling mechanism in submerged membrane bioreactor: Osmotic pressure during cake layer filtration, Water Res. 47 (2013) 2777–2786. https://doi.org/10.1016/j.watres.2013.02.041.

[224] H. Lin, M. Zhang, F. Wang, Y. He, J. Chen, H. Hong, A. Wang, H. Yu, Experimental evidence for osmotic pressure-induced fouling in a membrane bioreactor, Bioresour. Technol. 158 (2014) 119–126. https://doi.org/10.1016/j.biortech.2014.02.018.

[225] H. Hong, M. Zhang, Y. He, J. Chen, H. Lin, Fouling mechanisms of gel layer in a submerged membrane bioreactor, Bioresour. Technol. 166 (2014) 295–302. https://doi.org/10.1016/j.biortech.2014.05.063.

[226] B. Fr/olund, T. Griebe, P.H. Nielsen, Enzymatic activity in the activated-sludge floc matrix, Appl. Microbiol. Biotechnol. 43 (1995) 755–761. https://doi.org/10.1007/BF00164784.

[227] D.C. Montgomery, Design and Analysis of Experiments, 5th ed., 2017.

[228] D.T. Veličković, D.M. Milenović, M.S. Ristić, V.B. Veljković, Kinetics of ultrasonic extraction of extractive substances from garden (Salvia officinalis L.) and glutinous (Salvia glutinosa L.) sage, Ultrason. Sonochem. 13 (2006) 150–156. https://doi.org/10.1016/j.ultsonch.2005.02.002.

[229] J.L.A. Dagostin, D. Carpiné, M.L. Corazza, Extraction of soybean oil using ethanol and mixtures with alkyl esters (biodiesel) as co-solvent: Kinetics and thermodynamics, Ind. Crops Prod. 74 (2015) 69–75. https://doi.org/10.1016/j.indcrop.2015.04.054.

[230] G.T. Vladisavljević, S.K. Milonjić, V.L.J. Pavasović, Flux decline and gel resistance in unstirred ultrafiltration of aluminium hydrous oxide sols, J. Colloid Interface Sci. 176 (1995) 491–494. https://doi.org/10.1006/jcis.1995.9941.

[231] Y. Lee, M.M. Clark, Modeling of flux decline during crossflow ultrafiltration of colloidal suspensions, J. Memb. Sci. 149 (1998) 181–202. https://doi.org/10.1016/S0376-7388(98)00177-X.

[232] R.S. Juang, H.L. Chen, Y.S. Chen, Membrane fouling and resistance analysis in dead-end ultrafiltration of Bacillus subtilis fermentation broths, Sep. Purif. Technol. 63 (2008) 531–538. https://doi.org/10.1016/j.seppur.2008.06.011.

[233] L. Dvořák, M. Gómez, M. Dvořáková, I. Růžičková, J. Wanner, The impact of different operating conditions on membrane fouling and EPS production, Bioresour. Technol. 102 (2011) 6870–6875. https://doi.org/10.1016/j.biortech.2011.04.061.

[234] C. Chen, W. Guo, H.H. Ngo, S.W. Chang, D. Duc Nguyen, P. Dan Nguyen, X.T. Bui, Y. Wu, Impact of reactor configurations on the performance of a granular anaerobic membrane bioreactor for municipal wastewater treatment, Int. Biodeterior. Biodegrad. 121 (2017) 131–138. https://doi.org/10.1016/j.ibiod.2017.03.021.

[235] N. Martin Vincent, J. Tong, D. Yu, J. Zhang, Y. Wei, Membrane Fouling Characteristics of a Side-Stream Tubular Anaerobic Membrane Bioreactor (AnMBR) Treating Domestic Wastewater, Processes. 6 (2018) 50. https://doi.org/10.3390/pr6050050.

[236] H.J. Luna, B.E.L. Baêta, S.F. Aquino, M.S.R. Susa, EPS and SMP dynamics at different heights of a submerged anaerobic membrane bioreactor (SAMBR), Process Biochem. 49

(2014) 2241–2248. https://doi.org/10.1016/j.procbio.2014.09.013.

[237] X. Guo, Y. Miao, B. Wu, L. Ye, H. Yu, S. Liu, X. xiang Zhang, Correlation between microbial community structure and biofouling as determined by analysis of microbial community dynamics, Bioresour. Technol. 197 (2015) 99–105. https://doi.org/10.1016/j.biortech.2015.08.049.

[238] D. Jang, Y. Hwang, H. Shin, W. Lee, Effects of salinity on the characteristics of biomass and membrane fouling in membrane bioreactors, Bioresour. Technol. 141 (2013) 50–56. https://doi.org/10.1016/j.biortech.2013.02.062.